Sukkur IBA University

Sukkur IBA Journal of Emerging Technologies

Recognized in HEC Pakistan "Y" Category

P-ISSN: 2616-7069 E-ISSN: 2617-3115

Volume: 5 | No.: 1 | Jan- June | 2022

Sukkur IBA Journal of Emerging Technologies (SJET) is a bi-annual research journal published by **Sukkur IBA University**, Pakistan. **SJET** is dedicated to serve as a key resource to provide applied engineering research associated with the Electrical, Electronics, and innovations in Energy at the global scale. This Journal publishes manuscripts that are well written by highlighting development in emerging technologies. This journal covers all branches of Engineering, Science & Emerging Technologies.

Disclaimer: The research material expressed in the **Sukkur IBA Journal of Emerging Technologies (SJET)** is the sole contribution of the authors. The research contribution of the authors does not reflect the management, advisory board, the editorial board, **Sukkur IBA University** press, and the organization to which the authors are affiliated. Manuscripts published in **SJET** shall be processed through double-blind peer-reviewed by the two experts of the field. The identities of the experts/reviewers shall remain anonymous to the authors. The Journal shall be published two issues in a year. Neither the **Sukkur IBA University** nor the **SJET** shall be responsible for errors or any consequences highlighted by the reader. The errors and deficiencies in terms of research in the manuscript can directly be reported to the authors.

==========

Publisher: **Sukkur IBA Journal of Emerging Technologies (SJET)**
Office of Research, Innovation & Commercialization – ORIC
Sukkur IBA University - Airport Road Sukkur-65200, Sindh Pakistan
Tel: (09271) 5644233 -37 Fax: (092 71) 5804425 Email: sjet@iba-suk.edu.pk URL: sjet.iba-suk.edu.pk

==========

Mission Statement

The mission of **Sukkur IBA Journal of Emerging Technologies (SJET)** is to provide a premier interdisciplinary platform to researchers, scientists, and practitioners from the field of engineering in particular, electrical, electronics, renewable, and emerging engineering fields for the dissemination of their finding and to contribute in the knowledge domain.

Aims & Objectives

Sukkur IBA Journal of Emerging Technologies (SJET) will publish and encourage the submission of critically reviewed manuscripts on cutting-edge research in the field of emerging engineering technologies.

The objectives of **SJET** are:

1. To bring new engineering ideas, research, and findings on a single platform.
2. To integrate interdisciplinary research for a technological sustainable solution.
3. To provide a scholarly platform to connect academia and industries for socio-economic development.

Research Themes

The research focused on but not limited to the following core thematic areas:

Renewable Energy Sources and Storage:

- Solar energy system fabrication and construction of advanced fuel cell technology
- Designing and analyzing smart hydro and wind energy systems
- Developing systems for biomass and bio-fuels
- Energy management and storage
- Energy devices and materials
- Energy harvesting for wireless and body sensor networks
- Energy efficiency and policies
- Energy devices and materials

Power Systems and Smart Grids:

- Power Quality Issues and solutions
- Microgrid systems and their Integration Problems
- Design control and management
- Energy management and Environmental issues
- Hybrid power system
- Distributed and co-generation systems
- Power market and power system economics

Electrical Machines and Adjustable Speed Drives:

- AC and DC machines and drives
- Sensor-less control
- Piezo and electrostatic actuators
- Machine design and equipment training
- Maintenance and fault diagnosis
- Bearing less driving technologies

==========

Publisher: **Sukkur IBA Journal of Emerging Technologies (SJET)**
Office of Research, Innovation & Commercialization – ORIC
Sukkur IBA University - Airport Road Sukkur-65200, Sindh Pakistan
Tel: (09271) 5644233 -37 Fax: (092 71) 5804425 Email: sjet@iba-suk.edu.pk URL: sjet.iba-suk.edu.pk

==========

Power Electronics and its Application:

- Hard-switching and soft-switching static converters
- Multi-level and matrix converters
- Emerging topologies
- Simulation and control power converters
- Power factor correctors
- Active filters and total harmonics distortions analysis
- Optoelectronics and photonic devices
- Power semiconductors, passive components, and packaging technologies
- Switch-mode power supplies and automotive
- Applications of power electronics in-home appliance

High Voltage Engineering and Insulation Technology:

- Micro-electromechanical system (MEMS)
- Power Integrated circuits (PIC)
- Power Engineering related Technologies
- Power system stability and control
- Power system transient modeling, simulation, and analysis
- Electromagnetic transient programs (EMTP)
- HVDC and FACTS applications

Nanomaterials/Nanotechnology:

- Sensors and Actuators
- Electronic Thin Films
- Nanogenerators
- Nanomaterials
- Nanotechnology optoelectronic sensors
- magnetic sensors
- thermal sensors
- mechanical sensors

Communication and Signal Processing:

- Communication & signal processing
- Radio frequency systems, microwave, and antenna design
- Analog and mixed-signal circuits
- Filter designing
- Satellite communication, mobile communication
- Cognitive and software design radio
- Analog and Mixed-Signal Circuits

Biomedical Electronics:

- Energy-efficient wireless body sensor networks
- Wireless power/energy transfer in e-health applications
- Green and battery-friendly wireless medical networks
- Renewable energy and energy harvesting for wireless and body sensor networks
- Telemedicine and medical IoT
- Medical video transmission
- Energy management for medical health applications
- Role of 5G in medical health applications

Thermal and complex fluid dynamics:

- Active and passive techniques for fluid flow manipulation

==========
Publisher: **Sukkur IBA Journal of Emerging Technologies (SJET)**
Office of Research, Innovation & Commercialization – ORIC
Sukkur IBA University - Airport Road Sukkur-65200, Sindh Pakistan
Tel: (09271) 5644233 -37 Fax: (092 71) 5804425 Email: sjet@iba-suk.edu.pk URL: sjet.iba-suk.edu.pk
==========

- Fluid flow process for industrial equipment's
- Modeling of working fluids
- Experimental fluid dynamics
- Multifunctional heat exchangers/chemical reactors
- Energy-efficient combustion
- Environmental fluid flows

Materials and their processing

- Piezoelectric materials
- Polymers, metal oxides
- III, V and II, VI semiconductors
- Thick and thin films
- Optical glass fibers
- Amorphous
- Polycrystalline monocrystalline silicon, nanomaterials
- Synthesis of nanomaterials, composite materials
- Functional material
- Electronic thin films and integrated devices
- Engineering materials
- Solid and structural mechanics

==========
Publisher: **Sukkur IBA Journal of Emerging Technologies (SJET)**
Office of Research, Innovation & Commercialization – ORIC
Sukkur IBA University - Airport Road Sukkur-65200, Sindh Pakistan
Tel: (09271) 5644233 -37 Fax: (092 71) 5804425 Email: sjet@iba-suk.edu.pk URL: sjet.iba-suk.edu.pk
==========

Patron's Message

Sukkur IBA University has been imparting education with its core values of merit, quality, and excellence since its inception. Sukkur IBA University has achieved numerous milestones in a very short span of time that hardly any other university has achieved in the history of Pakistan. The institute continuously being ranked as one of the best Institute in Pakistan by the Higher Education Commission (HEC). The distinct service of Sukkur IBA University is to serve rural areas of Sindh and also underprivileged areas of other provinces of Pakistan. Sukkur IBA University is committed to serve the targeted youth of Pakistan who is suffering from poverty and deprived of equal opportunity to seek quality education. Sukkur IBA University is successfully undertaking its mission and objectives that lead Pakistan towards socio-economic prosperity.

In continuation of endeavors to touch new horizons in the field of Engineering and Emerging Technologies, Sukkur IBA University publishes an international referred journal. Sukkur IBA University believes that research is an integral part of modern learnings ad development. **Sukkur IBA Journal of Emerging Technologies (SJET)** is the modest effort to contribute and promote the research environment within the university and Pakistan as a whole. SJET is a peer-reviewed and multidisciplinary research journal to publish findings and results of the latest and innovative research in the field. Following the tradition of Sukkur IBA University, SJET is also aimed at achieving international recognition and high impact research publication in the near future.

Prof. Dr. Syed Mir Muhammad Shah
Vice-Chancellor
Sukkur IBA University
Patron **SJET**

==========
Publisher: **Sukkur IBA Journal of Emerging Technologies (SJET)**
Office of Research, Innovation & Commercialization – ORIC
Sukkur IBA University - Airport Road Sukkur-65200, Sindh Pakistan
Tel: (09271) 5644233 -37 Fax: (092 71) 5804425 Email: sjet@iba-suk.edu.pk URL: sjet.iba-suk.edu.pk
==========

Editorial

Dear Readers,

It is immense pleasure to present you the latest issue of the Sukkur IBA Journal of Emerging Technologies (SJET). Sukkur IBA University firmly believes in the research environment and has provided a platform for the intellectuals and researchers to share knowledge and new findings on emerging trends in various research areas to solve the difficult technical problems related to the technological advancements in response to the demands of the times. The SJET provided an interdisciplinary platform to the researchers' community to collaborate, co-innovate, and instigate efforts to break the technological barriers. This journal provides the opportunity to gain and present authentic and insightful scientific & technological information on the latest advances in the field of emerging technologies.

The SJET provides an invaluable source of information and enables the interested researchers to access the original information they are seeking. The manuscripts submitted in SJET have been followed by a double-blind peer-review process, which addresses key issues in the field of emerging engineering technologies. The SJET has endorsed high standards which are prerequisite for publishing high-quality research work. This journal manifests into an eco-system for the academician and engineers work together in the pursuit of excellence & innovation, that is why the editorial board of SJET is comprised of academic and industrial researchers from various advanced countries. The journal has been recognized by the higher education commission (HEC) of Pakistan under "Y" category. It has adopted an Open access policy without charging any publication fees that will certainly increase the readership by providing free access to a wider audience.

On behalf of the SJET, I welcome the submissions for the upcoming issue and looking forward to receiving your valuable feedback.

I hope this journal will make a difference in our perspective and choice of research.

Sincerely,

Dr. Saeed Ahmed Khan
Chief Editor
SJET

==========
Publisher: **Sukkur IBA Journal of Emerging Technologies (SJET)**
Office of Research, Innovation & Commercialization – ORIC
Sukkur IBA University - Airport Road Sukkur-65200, Sindh Pakistan
Tel: (09271) 5644233 -37 Fax: (092 71) 5804425 Email: sjet@iba-suk.edu.pk URL: sjet.iba-suk.edu.pk
==========

==========
Publisher: **Sukkur IBA Journal of Emerging Technologies (SJET)**
Office of Research, Innovation & Commercialization – ORIC
Sukkur IBA University - Airport Road Sukkur-65200, Sindh Pakistan
Tel: (09271) 5644233 -37 Fax: (092 71) 5804425 Email: sjet@iba-suk.edu.pk URL: sjet.iba-suk.edu.pk
==========

==========

Publisher: **Sukkur IBA Journal of Emerging Technologies (SJET)**
Office of Research, Innovation & Commercialization – ORIC
Sukkur IBA University - Airport Road Sukkur-65200, Sindh Pakistan
Tel: (09271) 5644233 -37 Fax: (092 71) 5804425 Email: sjet@iba-suk.edu.pk URL: sjet.iba-suk.edu.pk

==========

Vol. 5, No. 1 | January – June 2022

Investigation on High Reliability Wireless Communication of Underwater Sensor Networks for Submerged Acoustic Correspondence

Atif Ishtiaq[1]*, Sheeraz Ahmed[1] Asif Nawaz[2], Muhammad Adil[1], Zeeshan Najam[3], Shahid Latif[4], Malik Taimur Ali[1], Mohsin Tahir[4]

Abstract:

Underwater Sensor Networks (UWSNs) has been the hot area of communication and research in the recent years and is finding its applications in a wide range of Acoustic correspondences. Notwithstanding, contrasted and the earthly condition, the marine condition is intricate and inconsistent, so correspondence in this condition is extremely troublesome. This article has directed a top to bottom conversation and survey of submerged specialized techniques and organization advances, (for example, submerged acoustic correspondence, submerged optical correspondence, and steering conventions and media access control, and submarine multimodal transport organizations. This article additionally talks about the accomplishments of high-unwavering quality submerged correspondence innovation, and there are not many difficulties in managing submarine organizations. No such detailed work exists in literature which has addressed the concept of submerged acoustic communication.

Keywords: *Underwater wireless sensor networks, Multimodal communication, Acoustic communication, Optical communication, Underwater routing protocol, Underwater MAC protocol.*

The 21st century is the hundred years of the sea, and sea nations critically need to investigate and secure the sea. Marine topographical investigation, oil extraction, and ecological observing require stable submerged organizations. Simultaneously, the early admonition framework for characteristic marine fiascos and marine asset multiplication likewise advanced the improvement of marine computerization. The reason for an exceptionally solid marine organization is the highlight point submarine A correspondence framework with fast, low piece mistake rate (BER), long correspondence range, and low force utilization can be figured it out. Different strategies for correspondence in a submerged situation have been proposed: submerged acoustic correspondence (UAC), submerged optical correspondence (UOC), electromagnetic correspondence, gravity wave correspondence, quantum correspondence, and attractive field correspondence. Be that as it may, truth be told, just UOC and UAC can be utilized in submerged situations [1] [2], also, other specialized strategies are still in the research center check stage. UAC is presently the most adult specialized technique utilized in submerged situations. The speed of sound sent

[1]Department of Computer Science, Iqra National University, Peshawar, Pakistan.
[2]Faculty of Engineering Higher College of Technology Dubai, UAE
[3]Department of Electrical Engineering, MNS University of Engineering & Technology, Multan, Pakistan
[4]Department of Electrical Engineering, Iqra National University, Peshawar, Pakistan
Corresponding Author: sheerazahmed306@gmail.com

submerged can arrive at 1500 m/s. The constriction is incredibly low, and the sound lessening coefficient between 1 Hz and 50 kHz is around 104 dB/m to 102 dB/m. The correspondence speed of under 1000 m can arrive at a few m/s [3]. Sound waves can travel a great many kilometers Low recurrence and high forces are the main approaches to accomplish significant distance submerged correspondence. Notwithstanding, in spite of the fact that UAC has the upside of permitting significant distance correspondences, it likewise has numerous disadvantages. For instance, its proliferation delay is long, in light of the fact that the spread speed of submerged sound is five significant degrees Lower than radio recurrence (RF) speed. The State Maritime Organization necessitates that when a torrent cautioning happens, the sea perception organization ought to send the notice data inside 3 seconds, else it will Inconsequential. Clearly, UAC can't meet this prerequisite. Another significant imperfection of UAC is inadequate data transfer capacity assets. In correspondence, the most significant issue is transfer speed. The immediate advantage of more prominent data transfer capacity is that it can enormously speed up. Moreover, the commotion created Because of the adaptability and unpredictability of the submerged condition, it extraordinarily meddles with UAC, and the versatility of submerged hubs causes the Doppler impact. The seabed limit, water limit and diverse geographic conditions in the sea cause multipath impacts, which represent a significant test to excellent amphibian correspondence. UOC is viewed as an enhancement to UAC. The speed of optical correspondence can arrive at several m/s.

Be that as it may, since the light in the water rots quickly, the spread separation of the light in the submerged condition Just a couple hundred meters. Bluecom submerged optical correspondence framework can arrive at 20Mbps. The submerged transmission speed is under 200 m [4]. The Ambalux framework can arrive at a transmission speed of 10 Mbps. The most extreme submerged separation is 400 m [1] [5]. With single-photon torrential slide diodes, UOC can accomplish transmission In a moderately perfect water condition, a separation of 500 m submerged [6]. Despite the fact that this permits fast submerged Through information transmission, UOC advances exacting prerequisites on the earth and the water nature of the two hubs Acknowledge highlight point correspondence. The main condition is that the two correspondence hubs are inverse stable. During this time, the transmitter and collector must be unequivocally adjusted; something else, information transmission will be influenced Dangerous demolition.

The water quality in the earth incredibly influences optical correspondence on the grounds that, In sloppy water, the recipient can't get constant light signals. At the end of the day, information about water quality Condition is an essential for deciding if UOC is relevant. Submerged RF correspondence has been considered for submerged correspondence. Since water retains electromagnetic waves, RF waves can just infiltrate a profundity of around 7 m [7]. As the frequency builds, the infiltration capacity of electromagnetic waves in water expands, arriving at 200 m. In any case, in super low recurrence RF correspondence, the transmission speed is decreased. It takes about 30 minutes to communicate the message, and the framework can just spat simplex mode. Because of the enormous frequency, the reception apparatus of the transmitter must be several kilometers in length. This is clearly outlandish in the organization. We won't examine the submerged uses of RF correspondence in this article.

These correspondence advancements essentially decide the strength and unwavering quality of submerged sensor organizations. Obviously, there are different elements that influence the dependability of submerged sensor organizations, for example, steering conventions and Macintosh conventions on the organization layer. We will examine these procedures in detail in the accompanying sections. Our primary commitments are as follow: -

- Elements influencing the unwavering quality of submarine organizations, including

correspondence advancements and organizations Innovation, exploration and investigation.

- We have directed a thorough report on the most recent condition of submerged interchanges and its improvement of the presentation favorable circumstances of the submarine multimodal transport organization and proposals for the future advancement of submarines Organization presentation. The AI used to send submerged information is additionally examined.

- We examined the information transmission network helped by AUV in a creative manner. As an exceptional submerged information transmission Structure, we dissect its favorable circumstances and issues in the organization.

- We talked about the difficulties and uncertain issues confronting the future advancement of submerged information transmission, including correspondences and networks, and propose arrangements that we believe are achievable.

The remainder of this article is composed as follows. In the subsequent part, we talked about submerged correspondence innovations, including UAC and UOC. In the third segment, we considered the organization in the submerged condition. The fourth area presents a few difficulties and remarkable issues. At long last, the fifth part advances a few ends and assessments about future examination.

This part examines UAC and UOC in detail, and uncovers a few factors that influence information transmission at various occasions Correspondence innovation is applied to submerged arrangements.

2.1 Underwater Acoustic Communication

Toward the finish of the nineteenth century, submerged acoustic frameworks were first broadly utilized by the military [15]. In 1945, the U.S. Naval force's Submerged Acoustics Research center planned a down to earth submerged telephone. Because of specialized restrictions around then, the single-sideband adjustment innovation of the simple balance framework utilized in submerged phones utilizes a transporter recurrence of 8.33 KHz, and its correspondence separation may arrive at a few kilometers. Thusly, the submerged telephone utilizing recurrence tweak innovation has a transporter recurrence the kHz has been effectively evolved. Since the simple adjustment framework can't lessen the blurring and sign twisting brought about by the exceptional intricacy of the submerged sound channel, the presentation of the framework is extremely restricted. In the next decades, with the fast advancement of sign preparing innovation and with the continuous improvement of balance innovation, computerized balance innovation has been applied to UAC. At present, the advancement of UAC is restricted by adjustment innovation. Old advanced simple regulation Sound handling (DSP) and current symmetrical recurrence division multiplexing (OFDM) balance innovation both are gotten from earthbound correspondence frameworks. These advances can hypothetically be utilized in submerged correspondence frameworks. Experience and reasonable application have additionally demonstrated this point. In 2008, Milica and Baosheng [8, 9] examined the use of OFDM innovation in UAC framework, discovery. Accordingly, Darn et al. [10] OFDM entwined various access proposition (OFDM-IDMA) Correspondence through submerged acoustic channels makes UAC adjustment innovation more differentiated. With the advancement of submerged correspondence adjustment innovation, UAC has gotten more dependable. Be that as it may, the submerged acoustic channel is viewed as one of the most firm channel conditions, and its intricacy and inconstancy present impossible difficulties for solid data transmission.

2.1.1 Channel model

The usage of the channel model incredibly benefits the hypothetical examination of UAC and legitimately influences its quality. The submerged acoustic channel changes and changes after some time, and the direct examples in various oceanic conditions are additionally extraordinary. We have recorded some submerged acoustic channel models and clarified them in more detail. [11] proposed a straightforward numerical model for channel commotion, multipath impacts, and constriction. Table 1 highlights the features of various channel models available in literature.

Path attenuation model: -

$$A(l,f) = \frac{l^k}{l_r} \propto (f)^{l-l_r} \quad (1)$$

where f is the sign recurrence and l is the transmission separation regarding some l_r. The way misfortune example models the spreading misfortune and its standard qualities are between two targets.

Noise model: -

$$SNR\ (l,f) = \frac{S_l(f)}{A(l,f)N(f)} \quad (2)$$

where $S_l(f)$ is the power spectral density of the transmitted signal.

Multipath model:-

$$H_p(f) = \frac{\tau_p}{\sqrt{A(l_p,f)}} \quad (3)$$

speaks to the recurrence reaction of the p-th way. proposed a numerical model of an acoustic direct situated in a shallow water seaside condition. In the model, submerged acoustic weakening, mathematical dissemination, assimilation, signal base, and surface bob are thought of Geometric diffusion attenuation model: -

$$TL_{geo} = k \times \log l \quad (4)$$

where k is a consistent coefficient. In this model, dissemination can be isolated into roundabout dispersion and circular dissemination, and the k esteem is then 10 and 20, separately. l is the separation between the beneficiary and the transmitter. Infrared vitality is created when the transmitter performs acoustic regulation. At the point when the vitality transmits outward, the sound wave is constricted. The model is

$$TL_{abs} = \alpha \times l' \times 10^{-3} \quad (5)$$

where

$$\propto = \frac{A_1 P_1 f^2}{f^2+f_1^2} + \frac{A_2 P_2 f^2}{f^2+f_2^2} + A_3 P_3 f^2 \quad (6)$$

where α is the weakening coefficient. The model thinks about the pH, temperature, and saltiness in the submerged condition as boundaries.

TABLE I. FEATURES OF CHANNEL MODELS

Models	EF	PH	T	S	OC	HP	Description
Path Attenuation [11]	√	√	√	√			Focuses on the signal attenuation between the input and output; also studies the factors affecting signal attenuation, improving the accuracy of the model

Noise [11]	√						A general model of noise used to measure the effect of noise on data transmission
Multipath [10]	√				√		Measure the effect of different paths under multipath effect on communication
Doppler Power Spectrum [12]	√				√		Analyze the intersymbol interference caused by the Doppler shift
BELLHOP [13]						√	Used to calculate the propagation loss of a certain sound line

EF: Empirical formula, S: Salinity, OC: Ocean current, HP: Hydraulic Pressure

The above submerged acoustic channel model incorporates a few significant models: sound way weakening, commotion, multipath, and Doppler. The lessening of the UAC way is influenced by numerous elements, for example, recurrence, seawater temperature, saltiness, profundity and pH, infrared dissipating, and multipath dispersing. The constriction model proposed in [11] utilizes lessening coefficients to fit the inexact useful connection between submarines. The sound sign imparted and the sign got. Because of the fitting capacity, the channel model shows a major contrast from the real channel. Notwithstanding, the moderation model has more extensive materialness than the alleviation model proposed by Milica. For the most part, the clamor in UAC establishes added substance commotion. The least complex and best approach to portray the commotion is the sign to-clamor proportion (SNR) [11]. The model summed up above is through investigation The movement condition of the submarine hub. In spite of the fact that multipath and Doppler impact models can be developed, it is as yet hard to settle the high BER of UAC. By depending on balance innovation, the counter channel and hostile to commotion weakening innovation can be incredibly improved. Notwithstanding, for the Doppler impact and multipath impact, the strategy or calculation notwithstanding the adjustment, different advancements are expected to improve correspondence execution, for example, spread range innovation, evening out innovation, and synchronization innovation. In the following part, we will investigate research on multipath and Doppler impacts.

2.1.2 Multipath effect, Doppler effect, and orthogonal frequency-division multiplexing technology research

The multipath impact that exists in practically all ground and submerged correspondence advancements is a significant factor prompting fast sign constriction. Since the signs from various ways show up at the recipient at various occasions, on account of stage mistakes, the superposition of the signs will cause critical twisting or constriction of the got signal, which may prompt piece blunders. Genuinely influence the solid transmission of information. . There are numerous strategies to forestall the impacts of multipath on the earth, for example, those that can improve the exactness of collector telemetry and time-space balance, and those that utilization OFDM adjustment. So as to improve separation exactness and time-area evening out, situating and time synchronization innovations are required. However, dynamic the geography of the

submarine organization makes it hard to acquire exact situating and time synchronization for this situation condition [12]. OFDM balance is the best method to acknowledge multipath opposition submerged and can improve the submerged information transmission rate. The ideal submerged acoustic organization can be accomplished in the accompanying manners consolidates media access control (Macintosh) and security instruments [13].

In spite of the fact that OFDM shows incredible presentation regarding multipath impedance, it will be seriously influenced by the Doppler impact. The Doppler impact in submerged correspondence is brought about by the recurrence balance brought about by the sporadic development of submerged hubs or vehicles. Doppler move uncovers that when the recipient is before the sound source when the (hub) moves in a particular bearing, the frequency of the got signal is packed comparative with the frequency of the transmitter, and the recurrence is higher, and the other way around. As the hubs move quicker, the Doppler impact increments significantly. In extreme cases, this can cause bit mistakes and correspondence interferences. OFDM is as yet the best correspondence tweak method that adjusts the attributes of the channel and the submerged condition. the investigation. The work to improve the productivity of OFDM innovation in submerged correspondence is still in progress. Mahdi et al. The presentation of various info (MIMO) OFMD frameworks dependent on Quick Fourier Change (FFT) and Partial Fourier Change (FRFT) is looked at and examined [14]. Despite the fact that the intricacy of FRFT and FFT is Comparably, in all multipath submerged conditions, the exhibition of the previous is superior to the last mentioned, while in a level blurring condition, their presentation is the equivalent. Accordingly, the FRFT-based MIMO-OFDM framework is a serious framework. Because of the lackluster showing of OFMD frameworks that are not coded in blurring channels, [15]. The submerged exhibition of OFDM convolutional coding framework is considered. Coded modem appeared in recreation.

Better than the underlying MATLAB library, the coding increases of added substance white Gaussian commotion (AWGN) and Rayleigh channel are 0.635 dB and 1.45 dB (when BER is 10-1). Trials have indicated that under helpless equipment conditions, convolutional coding (CC) OFDM can deliver better execution. Coordinated channel (MF), zero power (ZF) and least mean square mistake (MMSE) equalizers can be utilized for channel evening out. Nonetheless, every one of these equalizers has inconveniences that influence the correspondence execution of the framework: in MIMO settings, the presentation of MF will be undermined, and the ZF equalizer will experience the ill effects of clamor upgrade and The MMSE equalizer must gauge the SNR to work appropriately. Khaled et al. Gives a joint Low-intricacy regularized ZF equalizer and transporter recurrence balance remuneration framework. The proposed balance calculation utilizes consistent regularization boundaries to improve the commotion upgrade issue and framework intricacy. OFDM is touchy to Doppler impact. The recurrence remuneration of numerous OFDM frameworks is An overall strategy to kill the Doppler impact by applying down-examining and leftover transporter recurrence counterbalance pay. Shingo, etc. A strategy for extending the testing extent and re-inspecting by estimating the Doppler standard deviation is proposed. The conventional strategy accept that there is a consistent Doppler recurrence move in the correspondence information outline, however in a genuine situation, the general speed between the sending and getting unit will change, and the Doppler move will likewise vary. This strategy can adequately tackle this issue and improve the framework Execution, or BER. Multi-transporter adjustment is a noteworthy component of the OFDM framework, and the symmetry between the transporters is an essential to guarantee great execution of the OFDM framework. At times, symmetry between sub-transporters on a period shifting channel is lost, coming about in between transporter obstruction (ICI). Post-

FFT and pre-FFT are two arrangement strategies to manage this issue. The post-FFT technique incorporates block adjustment or sequential leveling of the sign created between ICI subsequent to demodulating the sign [15].

Pre-FFT technique 5 applies recurrence balance pay to the sign before demodulating the sign to kill non-symmetry between sub-transporters [16]. A joined weight figuring calculation dependent on include disintegration is proposed. Contrasted and existing versatile techniques, this calculation can forestall mistake spread and take out the prerequisite for boundary modification. This strategy ensures the general optimality under the supposition of narrowband Doppler. The ideal weight vector for neighborhood FFT demodulation is acquired through the eigenvector related with the littlest eigenvalue of the pilot recognition mistake lattice. The calculation can likewise be legitimately stretched out to sub-band computations to make up for wideband Doppler impacts. In the above examination, it is discovered that UAC is the most experienced and the most well-known innovation is OFDM. This is fundamentally in light of the fact that OFDM can accomplish fast information transmission and can oppose multipath normally at low acoustic wave proliferation rates. Despite the fact that the OFDM framework is delicate to the Doppler impact, the adjustment innovation. As of late, it has been proposed to cure this deformity. The consequences of OFDM coding exploration and demodulation execution investigation ICI, FRFT, and FFT help make the OFDM submarine correspondence framework more like an ideal framework and improve the dependability of information transmission

3.1 Underwater routing

Submerged information transmission can't simply utilize basic highlight point information transmission. So as to acknowledge information transmission, brilliant correspondence innovation ought to be utilized to set up a solid submarine organization in the assigned ocean region. The directing convention is the fundamental convention of the correspondence organization, which is significant for the acknowledgment of the organization information bundle transfer measure. Broad examination has been led on submarine directing conventions, and many submarine steering convention calculations exist. Since the development and utilization of submarine organizations are still in their earliest stages, there are still not many submarine organizations that can be concentrated through analyses. Since it is hard to lead directing examination in a real situation, just a couple steering conventions have been tried in this condition. The excessive cost of submarine organization hubs is another motivation behind why the organization comprises of just a couple of hubs [17]. The plan of submarine steering conventions is more convoluted than that of earthbound directing conventions. The geography of the earthly organization is a two-dimensional plane, while the geography of the submarine organization is a three-dimensional [18]. Moreover, submarine directing is consistently powerful, and submarine steering is consistently static. Along these lines, it isn't suitable to completely recreate the ground steering convention to the submarine organization. Likewise, submarine steering faces hub development, power utilization, and different difficulties [19]. Specifically, submarine directing experiences similar weakness issues as land steering, and it is more hard to explain in submarine organizations [17] . In the accompanying segment, we will survey and sum up as of late created steering conventions so peruses can comprehend the current advancement status of submarine directing conventions. Figure 1 shows the model of the submerged sensor organization.

3.1.1 Location-based routing protocols

In the early examination on submarine directing, the presence or nonattendance of hub area data in the organization is viewed as the principle highlight those partitions submarine steering conventions into two sorts. The ordinary portrayal of area-based steering is the vector-based vehicle convention (VBF) [16], and the average portrayal of non-area based directing is the profundity based

directing convention (DBR) [17]. Reason for the VBF Understanding It includes utilizing the known area data of every hub to build up a powerful information interface from the source hub to the accepting hub. The fundamental thought is to set up a barrel shaped virtual line between the source hub and the collector hub. The hubs between the source hub and the sink hub in the pipeline are applicant hand-off hubs for sending parcels. The size of the virtual line built up by the convention is a key factor influencing the organization. In the event that the pipeline extend is excessively huge, the quantity of jumps and force utilization will increment unnecessarily, while too short a range will cause correspondence interference and parcel misfortune. Despite the fact that the convention is profoundly versatile in unique 3D submarine organizations, there are as yet significant issues to consider: hub power utilization and meager organizations. So as to take care of these two issues. Proposed the VBF jump by-bounce (HH) convention in [18]. The Engaged Shaft Directing (FBR) convention was proposed [19]. HH-VBF tackles the exhibition issue of VBF in scanty organizations. This strategy utilizes a jump by-bounce virtual line

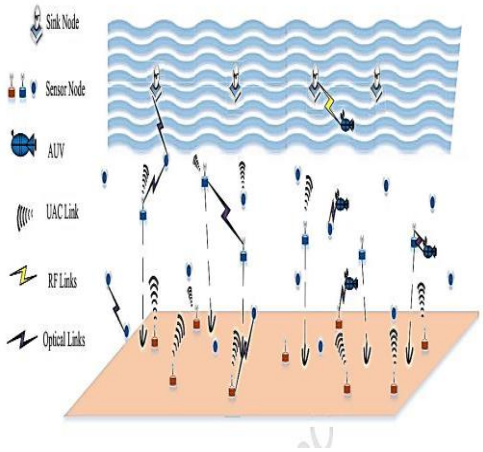

Fig. 1. Model of Underwater Sensor Network

Figure 1 shows the model of an environment of UWSNs. The source hub passes the information to the In its virtual pipeline, the source hub doesn't partake in ensuing information transmission. The following bounce hub is set up its own free channel shows up at the accepting hub until the information bundle is effectively sent to the following jump hub. FBR is a directing convention dependent on power inclusion, which utilizes various degrees of communicate power during transmission. In the directing cycle, the sending hub sends an information parcel demand with a particular communicate power level to its neighbors. In the event that the sending hub gets a transmission approval parcel (CTS) from the neighbor, it will be sent to the neighbor hub with a CTS reaction; in any case, if the CTS isn't gotten, the communicate power level is expanded to the following force level. Rehash this cycle until the CTS parcel is effectively gotten. Be that as it may, the consistent trade of solicitation to send (RTS)/CTS bundles will cause delays. Likewise, FBR additionally has situating issues.

3.1.2 Non-location-based routing protocols

In submarine organizations, it is here and there hard to decide the area data of hubs. Directing conventions dependent on the spot data are profoundly subject to subsea situating calculations, which represents a considerable test in subsea networks. In this way, steering conventions dependent on non-area data have useful worth. The first non-area data based steering convention proposed by Yan et al. for submerged conditions is DBR [17]. This convention just thinks about one boundary in information transmission, specifically the profundity of the hub. In the organization model, the well hubs are situated on the water surface, and the seabed hubs are dispersed at various profundities haphazardly apportioned. After the information bundle is produced, the hub sends the information parcel upward as per the profundity, and ceaselessly figures the profundity contrast between the hub and the nearby hub during the estimation. The

transmission cycle guarantees that information bundles must be communicated upwards. Since the convention just uses profundity as a norm for information transmission, hubs with shallower profundities will take an interest a lot in information transmission, and in this manner expend more power and neglect to run quicker. Moreover, the DBR convention doesn't give a more viable next-bounce hub choice. The H2-DBR convention [20] and the EEDBR (Vitality Productivity DBR) convention proposed later tackled the above issues and significantly improved the exhibition of the DBR convention. In 2014, Wahid et al. the DBR convention was created to actualize a dependable and vitality sparing directing convention dependent on physical separation and leftover vitality (R-ERP2R). This subsea directing convention is normally founded on physical separation [21]. It replaces the profundity figuring in the DBR convention with the count of the physical separation between the source hub and contiguous hubs. Such a calculation is more appropriate for submerged grouping sensor organizations. It considers the force utilization of submarine hubs on a worldwide scale. Thusly, the exhibition of this convention is better than EEDBR as far as organization information transmission and organization life. Its Hello Packet formation is shown in figure 2.

Fig. 2. Hello Packet

3.1.3 Energy-based routings

In 2018, Majid and Ahmad proposed a solid and vitality sparing weight based directing convention (RE-PBR) [21] and an improved VBF convention [22]. The RE-PBR convention presents a few boundaries, for example, Remaining vitality, connect quality record (LQI), and SNR esteem. To start with, the connection quality worth is added to the transfer steering choice calculation. Reenactment tests show that contrasted and EEDBR and DBR, the start to finish deferral and organization lifetime have been fundamentally improved. Contrasted and the first VBF In the arrangement, Ahmed's upgraded VBF convention thought about the rest of the vitality, and he inventively proposed a unique virtual line technique to improve VBF execution. The convention utilizes data, for example, remaining vitality and hub position changes as boundaries to powerfully decide the virtual line sweep of the source hub to adjust to the precarious submerged condition. So as to additionally improve the endurance season of the submarine organization. An improved DBR-based vitality recuperation DBR convention (EH-DBR) [23] is proposed, which utilizes the accompanying information bundles to gather vitality in the acoustic correspondence recurrence band to stack hub information. In principle, the life expectancy of the submarine organization can be broadened inconclusively. Numerous examinations have contemplated the force utilization of submarine hubs, which likewise shows that in the field of submarine correspondence organizations, the force utilization of hubs is an essential issue. As of late, numerous explores on the force utilization of correspondence organizations or hubs have been accounted for in the writing, just as many steering conventions [24] recommendations and upgrades.

3.1.4 VH-based routing protocols

The data vacuum (VH) issue is a significant issue in the presentation of submarine organizations, and it likewise represents a significant test to the designers of steering conventions. Among the numerous articles audited, just a couple of considered the issue of submerged VH. By and large, most steering conventions can settle on one of the accompanying two choices while experiencing VH: The first is to dispose of information parcels after numerous programmed recurrent solicitation (ARQ) conventions have fizzled. There is no reaction, and the second is to build the organization over-burden to sidestep the data weakness. These strategies can't impeccably tackle the VH issue, yet can adequately lessen the unpredictability of the

steering calculation. Lately, many examination results on data weaknesses have been accounted for. In [25], the principal complete stateless shrewd directing convention (SORP) was proposed. It utilizes a detached cooperation technique and locally identifies weaknesses and hubs caught in various regions of the organization geography during the steering cycle. It likewise receives another plan to accomplish a versatile transmission region that can be balanced and supplanted by the nearby thickness and the area of applicant transmission hubs, in this way improving vitality proficiency and dependability. Nadeem et al. Two conventions for preparing VH are proposed: impedance delicate directing convention (Intar) and solid obstruction touchy steering convention (REIntar). There are just a couple of contrasts between the two conventions. This understanding sets up a two-venture information interface. In the initial step, the source hub communicates a Welcome message to discover all the ways that can arrive at the getting hub and store them. The Welcome bundle incorporates ID, NumNequart, Timestamp, DistNeighbors, and HopSink. Subsequent to refreshing the accessible information authoritative, the source hub decides the following jump hub by ascertaining the estimation of the cost work (CF):

$$CF(j) = \frac{Dist\,(i,j)}{Hop\,(j) \times Neighbor\,(j)} \qquad (7)$$

where Hop(j) is the quantity of skips of the j-th potential sending center point (PFN) from the sink, Neighbor (j) is the quantity of neighbors of the j-th PFN, and Dist(i, j) is the partition between the j-th PFN and source center point I. The difference between the RE-Intar show and the Intar show is that significance information is added to the past HOLLE. The show can sufficiently deal with the information opening issue and shows a particular improvement in network execution.

3.1.5 Routing protocols based on machine learning

AI is a hotly debated issue of flow exploration, and learning calculations are viable with submerged correspondence organizations. Applying AI techniques to submarine organizations has become a significant method to tackle its key issues. Since the conventional ground convention can't adjust to the submerged condition, the presentation of the non-wise steering convention in the submerged organization is as yet not acceptable.

A proficient and adjusted Q-learning vitality utilization information assortment directing convention QLEEBDG [26] is proposed. The convention depends on fortification learning and plans to adjust the force utilization of certain accumulated hubs in the organization with the goal that one hub won't cause network interference or diminish power utilization for an enormous scope. Organization inclusion rapidly kicked the bucket because of extreme use. There is a genuine defect in fortification realizing, which is known as a dimensional emergency. Fortification adapting needs information for preparing. The dynamic cycle is the way toward learning nature. The Q esteem table is utilized to store current natural data. At the point when the condition of nature has just one measurement, the worth table Q just needs one line and N segments to record all the data. At the point when nature state is two-dimensional, a N*N table is expected to record data. When there are three measurements, a three-dimensional block cluster is expected to store the information. Shouldn't something be said about the four measurements? Support learning is hard to oversee. Nonetheless, the submerged condition is exceptionally unpredictable, the quantity of states can arrive at thousands, and the quantity of measurements can arrive at many measurements. all directing calculation dependent on fortification learning. Every hub is permitted to record the Q benefit of neighboring hubs dependent on the prize capacity, which significantly decreases the data put away in the Q esteem table. The

organization is upgraded locally, not around the world. In view of the previously mentioned issues brought about by support learning, Su et al. Proposed a steering convention dependent on Q-learning (DQN), DQELR vitality, and dormancy affectability [27]. The convention utilizes the base force utilization and the briefest postponement as the objective capacity of the organization so the organization keeps up a brief pause under powerful geography conditions and augments its administration life. Profound Fortification learning is a mix of support learning and profound neural organizations. Profound neural organizations can separate high-dimensional data includes, and can consummately conquer the dimensionality emergency of fortification learning. The info state and activity in the DQELR convention is around 1300 tuples, and Figure 3 shows a detailed map of various underwater routing protocols till date. The neural organization utilizes a five-dimensional model (counting the predisposition term b1) and three concealed layers of a completely associated network. This convention can generally inexact the best arrangement, and the test results are marginally improved contrasted and the vitality proficient and effective life-cycle Q-getting the hang of steering convention (QELAR) and VBF [27] [16]. The examination in the writing likewise called attention to an issue: on the grounds that the neural organization requires a ton of information for preparing, the convention requires a support learning calculation to become familiar with nature progressively, and the learning cycle has a long postponement, which may take a few hours or more It requires some investment to arrive at the neural organization The condition of combination. To dodge this issue, the DQELR convention utilizes a blend of disconnected and web based preparing; before the proper use of the convention, disconnected preparing can extraordinarily accelerate the calculation's combination speed. The submarine organization model given in [27] [16] is a unique organization hub model. The proposed directing convention must have the option to completely ensure the dependable information transmission of the organization with high flexibility.

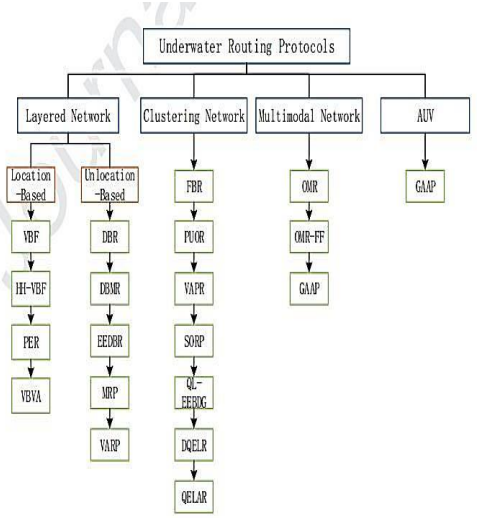

Fig. 3. Routing Protocol for UWSNs [27]

At the point when the organization geography changes progressively. Furthermore, Nadeem et al. Fortification learning is additionally used to dodge the utilization of neighboring hub innovation QLEEBDG-AND [22] in the directing convention of void hubs. Apply AI techniques to subsea directing, which furnishes each hub in the organization with certain canny dynamic capacity, it is a compelling answer for submerged courses and a hot examination subject. At last, we give a characterization outline of directing conventions and sum up the points of interest and weaknesses of the classifications depicted in Table 2.

TABLE II. ADVANTAGES AND DISADVANTAGES OF UNDERWATER NETWORK TYPES

CAT	Description
Layered Network	AD: Low complexity, easy to implement, low demand for network toplogy. DA: Difficult to control energy

	consumption and deal with voids
Clustering Network	AD: Strong scalability, Balanced energy consumption. DA: Algorithm complexity higher, and the netwok performance is affected by protocols
Multimodal Network	AD: Effectively improve network performance. DA: Higher requirements on network topology and required better resource allocation algorithm
AUV	AD: An effective method for big data transmission. DA: High network latency

3.2 Medium-Access Control Protocols

The media access control (MAC) convention is a key innovation for network access. In this manner, as an exemplary issue in wired and remote organizations, broad exploration has been directed for a long time. There have been valuable explores on the Macintosh convention of submerged acoustic recognition organizations. These examinations can be isolated by the channel access technique they talk about: asset assignment, asset rivalry, or blending.

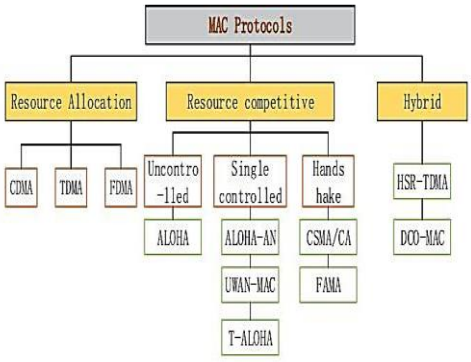

Fig. 4. MAC Routing Protocols for UWSNs [25]

Resource allocation type MAC protocol is divided into three main types: Frequency Division Multiple Access (FDMA), Time Division Multiple Access (TDMA) and Code Division Multiple Access (CDMA). FDMA realizes frequency division multiple access, orthogonal FDMA (OFDMA) protocol uses orthogonal frequency division; highlighted in figure 4.

As innovation for advancing channel portion, CDMA convention actualizes various access by spreading code distribution, while TDMA convention executes different access by isolating time allotments, along these lines diminishing bundle dispute [23]. The focal thought of the asset serious Macintosh convention is to seriously acquire remote channels for hubs that need to communicate information. They can be additionally partitioned into uncontrolled parcel conventions, single controlled bundle conventions, and handshake conventions. The principle thought of Macintosh Unchecked Parcel Convention is "send is yours", however it is anything but difficult to cause information bundle crash. Salud [24] is a regular uncontrolled parcel convention. Its all-encompassing convention decreases clashes by consolidating channel checking [25], inferring the working status of neighboring hubs [25], isolating time allotments [26], and utilizing a handshake convention [27]. The focal thought of the single control information parcel Macintosh convention is to utilize a solitary control information bundle to advise the adjoining channel that it is occupied. These conventions incorporate Salud with notification ahead of time (Salaam A) [28], Submerged Acoustic Organization Macintosh (UWAN-Macintosh) [19], and T-Lohi convention [10]. In view of the T-Lohi convention, by utilizing offbeat channel simultaneousness and straightforwardly partitioning the time allotment into the unit of the dispute time frame, the time division of the information parcel can be additionally diminished [11]. The handshake convention utilizes channel interference to trade two-way data and decreases the pace of bundle crashes by lessening the quantity of occupied channels. The most ordinary handshake

Macintosh convention is CSMA/CA [12]. In the submerged acoustic sensor organization, the issue of terminal introduction or covering up is intense. In this manner, a ton of exploration has been done on the handshake Macintosh convention in submerged acoustic sensor organizations. When there is a concealed terminal issue, if a channel is distinguished to be idle, it doesn't really imply that the channel is accessible; comparatively, when there is an uncovered terminal issue, if a channel is identified to be occupied, it doesn't really imply that channel inaccessible.

For the force utilization brought about via transporter detecting, a few conventions no longer use transporter detecting innovation. Impact Evasion Different Access (MACA) [23] is the primary handshake convention that doesn't utilize the transporter course; channel arrangement is brought out straightforwardly through three-party exchange. In view of this, in the writing research [24], the steadiness methodology is utilized to additionally improve the convention execution. In the handshake convention, because of concealed terminal issues, parcel impacts generally happen at the collector level. Thusly, so as to tackle the issue of shrouded terminals, a few conventions broaden the transmission season of control parcels and guarantee that all influenced neighbor hubs can get related control data before sending information bundles. FAMA convention [25] is the principal convention to decrease bundle impacts by utilizing postpone control parcels. In view of this, a few techniques have been grown, for example, time allotment division [66], sending caution information parcels [27], and planning information transmission start time and end time [28]. Used to additionally take care of the issue of concealed terminals. A hub doesn't comprehend the information transmission necessities of different hubs, yet indiscriminately sends information as indicated by its own needs. In related examinations, Spatio-fleeting irregularity has been utilized to improve channel usage and accomplish equal information transmission between numerous sets of hubs through the accompanying or comparative techniques: transmission settings of information bundles and control parcels [19], foundation and arrival of hub work Schedule [20], two-way relative information transmission [21], (various) and multi-bunch transmissions [22], postponed reaction to RTS order parcel and saved the following information transmission ahead of time [24].

3.3 Underwater Multimodal Network

As per research on submarine organizations, it is difficult to develop a fast and solid submarine organization utilizing just a single specialized technique. The multi-mode submarine organization (MDUN) in light of various specialized techniques is the most probable organization structure later on. It tends to be seen from Figure 1 that the three correspondence modes exist together in the whole organization. The accepting hub is situated on the water surface, the base station of the stage is the focal point of information assembly, and the RF utilized for correspondence between the recipient and the base station is additionally utilized between the beneficiary and the collector. sink. The sink center point talks with the submarine center point and the submarine-helped self-administering lowered vehicle (AUV) through different repeat gatherings. Right hand AUV and lowered center points impart data in short partitions through UOC. The momentum meaning of submerged polymorphic organizations is muddled. At the point when a framework contains a lot of innovations that don't meddle with one another, it is characterized as a multi-mode [27]. Roee proposed the routing protocol Based on MDUN [27]. The MDUN discussed in this article is a submarine network using three different frequency bands. It is assumed that the three UAC frequencies do not interfere with each other. Table 3 shows the advantages and disadvantages of underwater resources.

High, medium and low-recurrence UAC structure a six-hub organization. High and medium recurrence hydrophones can communicate information at short and medium paces. Low-recurrence submerged sounds can travel a significant distance.

Everything hubs can be furnished with different UAC modulators of various recurrence groups, and there can be numerous connections between two contiguous hubs in the organization. Another MDUN model was proposed in [20]. The model uses three specialized strategies: UOC, UAC, and electromagnetic waves. The general structure of the organization incorporates a getting hub, a subsea information source hub, and an assistant information offloading AUV.

TABLE III. ADVANTAGES AND DISADVANTAGES OF UNDERWATER NETWORK RESOURCES

CAT	Description
Resource Allocation	AD: Reducing packet conflict, easy to sleep, no hidden terminal issues, suitable for low power networks. DA: cannot adapt to network topology flexibly
Resource Competitive	AD: No complex time synchronization or control scheduling algorithms required, adapt to the changes of network topology. DA: Conflict retransmission
Hybrid	Can effectively balance the advantages and disadvantages of the above two types

The great hub is situated on the water surface and gathers information submerged. The submerged hub is fixed in the submerged recognition territory by a grapple chain to produce video data. Information bundles are produced at a speed of 5 M/min, and the AUV is utilized to empty submerged information. AUV and submarine hubs have both UAC and UOC capacities, and AUV additionally has remote electromagnetic wave correspondence capacities. The submarine node sends control information to the AUV through the UAC to determine its path to the node. When visiting a node, the AUV unloads the node data packet through the UOC, and then the AUV surface and send the data packet to the receiving node through electromagnetic wave communication. The over two organization models speak to two common multi-top submarine organizations: AUV doesn't help and AUV helps polymorphic organizations. We accept that the submerged acoustic organization proposed by Roee et al. Is certainly not A genuine MDUN. Submarine organizations that utilization different media correspondence advancements are more assorted. Its organization structure is delegate, rapid and short-separation, and a multi-mode network that consolidates significant distance and low-speed correspondence innovation can improve delay, throughput, power, and so on. Contrasted and a solitary mode organization, the organization can guarantee solid information transmission. The prevalence of organization engineering can once in a while significantly improve network execution. For sea organizations, an unadulterated submerged acoustic wave organization can give adequate inclusion, however it can't guarantee the transmission of enormous information. An unadulterated UOC organization can send enormous information, however it can't ensure adequate sea inclusion. As of now, sea information is developing exponentially, and multi-mode submarine organization or heterogeneous submarine organization is a more great organization model.

In the past segment, we referenced a multi-state network model that utilizes AUV to help offload information. AUV gets to information source hubs by offloading data to the organization as per a specific calculation and performs information transmission of video data [21]. The AUV access way calculation under this organization has become a key factor in network execution. Adding AUV to the submerged sensor organization will without a doubt improve the unwavering quality of its information transmission. At the point when the organization contains AUVs, their number, way, and force utilization will influence network information transmission. At present, there are not many investigations on the submarine organization helped by submerged vehicles. In [22], AUV way

arranging in a polymorphic organization condition is evaluated, and a heuristic choice calculation is proposed, to be specific Versatile Covetous AUV Way Search (GAAP). GAAP empowers AUV to boost the data estimation of the arrange and adjust to crises that happen in the organization. The calculation in this article permits AUV to communicate network information at a speed surpassing 80% of the hypothetical greatest. GAAP performs well in arranging a solitary AUV way, however as the quantity of AUVs in the organization expands, the issue of rehashed admittance to hubs will influence the calculation, which enormously influences execution. The web. Examination on submerged AUV direction arranging shows that the direction choice strategy for submerged AUV is a significant aspect of things to come submarine organization. AUV-helped specialized technique has unrivaled points of interest of huge scope information transmission Through customary specialized strategies. In AUV-based submarine, multi-state organizations, or heterogeneous organizations, a few AUV way choice calculations, AUV power streamlining, and clever way calculations actually should be fathomed. The issue of AUV way arranging is basically a directing issue. In any case, it is unique in relation to steering. The directing calculation has not been applied to the way choice of AUV, which makes this issue another examination theme. Later on, submarine organizations will unavoidably incorporate AUVs. AUV way search examination can improve the unwavering quality of submarine organization information transmission. Later on, the AUV way choice convention in the submarine organization convention stack will turn out to be significant.

In the marine environment, achieving solid information transmission is a troublesome test. In the following sections, we will discuss theories and methods used to transmit underwater data. Figure 5 shows and summarizes the challenges and outstanding issues based on the current research phase.

5.1.1 Underwater acoustic ommunication issues and challenges

The benefit of UAC in submerged correspondence is that it can understand significant distance correspondence, and the correspondence separation can arrive at several kilometers, yet there are not kidding abandons in the transmission rate, postponement, and BER. Factors, for example, channel blurring and multipath impacts are significant issues influencing UAC. In the flow research on UAC, the issue of channel blurring can be successfully illuminated by applying adjustment innovation, however a solid channel model should be built up. So as to adapt to the multipath impact, OFDM innovation shows better execution yet requires assistant evening out innovation to address the Doppler move. So as to adapt to the low correspondence rate, MIMO-OFDM innovation is utilized to improve data transfer capacity use, and multi-radio wire innovation is utilized to expand the correspondence rate. Huge advancement has been made lately It was fruitful in UAC, however there are as yet numerous difficulties. Above all else, the assorted variety and unpredictability of the submerged condition make it troublesome and unrealistic to display submerged acoustic channels, which requires solid submarines. Acoustic channel assessment calculation. Second, the high inactivity of UAC is the most troublesome issue to tackle. fathom. At present, there is no powerful strategy to decrease UAC delay, and no exploration identified with this issue has been directed. Third, the security of UAC is a central point of interest for the future utilization of submerged acoustic organizations. Secure personality check system, solid coding innovation, and exact situating innovation will influence the security and the dependability of UAC.

5.1.2 Optical communication problems and challenges

Compared with UAC, the two principle favorable circumstances of UOC are very high transmission rate and millisecond delay. Notwithstanding, the short correspondence separation permitted by UOC is the principle

obstruction to its turn of events. Right now, the longest transmission separation that can be accomplished in a quiet submerged condition is just 500 m, Meet the necessities of the canny sea organization. Because of the utilization of light as a correspondence medium, UOC hubs are anything but difficult to uncover the area of the handset, which makes military security It is hard to accomplish mystery correspondence. What's more, the highlight point UOC framework requires high exactness Alignment innovation, yet correspondence hubs regularly can only with significant effort keep up a steady situation in submerged environmental factors. On the off chance that the force framework is utilized to look after soundness, the vitality utilization of hubs will increment.

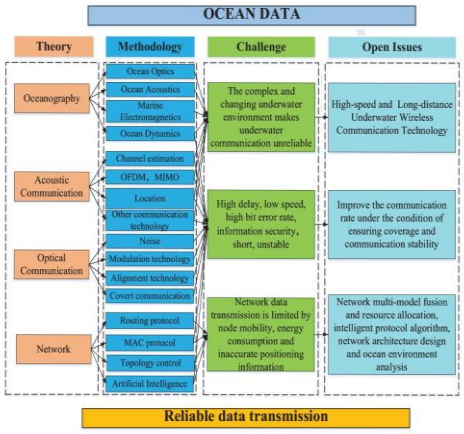

Fig. 5. Challenges and Issues of Ocean Data

This will abbreviate its administration life and truly influence the effectiveness and soundness of information transmission. distributed. The specialized technique depends on a laser discharging unit, which devours a ton of vitality and expends a great deal of vitality. Relies upon the water nature of the earth. To tackle this issue, the submerged correspondence framework. The utilization of diffuse light sources will be supplanted. However, the light intensity of the scattered light source is scattered [Fig 5.].

This will cause data transmission distance, channel noise, throughput and BER to decline, so it cannot replace the application of point-to-point communication systems under certain circumstances. Therefore, UOC systems should also be diversified. The complete use and networking of multiple UOC systems may be an important future theme.

5.2 Networking

The acknowledgment of submarine organizations is a definitive objective of submarine correspondence innovation applications, and the significance of building sea networks is self-evident. At the organization level, submarine directing is a significant issue in submarine organizations. As of late, there has been more examination on submarine steering than some other perspective. Compared with traditional land-based routing, submarine routing presents more problems and challenges. Generally, the topology of the terrestrial network does not cause height problems. In such an organization, directing calculations must be thought of and planned distinctly on a two-dimensional plane, and the associations between network hubs are steady. Nonetheless, in the submerged condition, the geography of the organization comprises a three-dimensional structure. To start with, it enormously expands the intricacy of the organization steering calculation, and second, the area of the hub is influenced by the sea and has gone through colossal changes. The flimsiness of the correspondence association among hubs and the vitality impediment of the hubs are significant difficulties in the plan of directing calculations.

As of late, with the fame of AI, numerous scientists have proposed submerged steering calculations, submerged channel assessment strategies, and leveling calculations dependent on AI. Calculations dependent on AI can successfully deal with the versatility of submarine hubs, data VH and hub power utilization. The impact of these calculations on voracious calculations will prompt more solid execution. Keen calculations ordinarily require a great deal of information preparing and ground-breaking figuring power, which will without a doubt prompt all the more overhead on the organization. UAC system can achieve higher coverage, but the

communication rate is very low, while UOC system can achieve higher communication rate, but the coverage is smaller. The MUDN form integrates UOC and UAC to provide coverage and achieve high-speed local data transmission, but there are bottlenecks Factors that affect latency and throughput still exist in the network. Applying underwater AUV to the transmission of auxiliary data in underwater networks can greatly alleviate these bottlenecks. Although changing the network structure will improve performance, it will also bring about some problems, such as AUV path planning and underwater acoustic and optical system resource allocation problems.

According to underwater communication technology and network research, it can be concluded that after using reasonable deployment topology technology, the future of ocean data transmission will involve the multi-mode and heterogeneous characteristics of different communication technologies. The resources of network nodes and different areas of the network are different. In addition, there will be significant differences in the speed and quality of regional communication. In marine correspondence, there is no correspondence advancement, network structure, or show that can totally change in accordance with all application circumstances, so conventional assortment will transform into a sign of future correspondence associations. Notwithstanding the sea, customary non-canny calculations additionally show evident deformities in the continually changing marine condition. Man-made consciousness based organization convention calculations will assume a significant function later on sea organization.

In this overview, we originally checked the current review records and foundation. We have examined submerged correspondence innovations, including UAC and UOC, just as directing conventions and Macintosh conventions. Investigated and broke down the components influencing the dependability of submarine organizations, including correspondence innovation and organization innovation. Next, we dissected the momentum research progress, submarine multi-mode UWSN, and AUV helped UWSN. At long last, we zeroed in on the issues and moves that should be defeated in improving submerged information transmission later on. We trust this survey will support analysts and designers comprehend the possibilities and flow status of submerged information transmission, just as the difficulties it faces.

REFERENCES

[1] Z. Zeng, S. Fu, H. Zhang, Y. Dong, J. Cheng, A survey of underwater optical wireless communications, IEEE Communications Surveys and Tutorials 19 (1) (2017) 204-238.

[2] S. Jiang, On reliable data transfer in underwater acoustic networks: a survey from networking perspective, IEEE Communications Surveys and Tutorials 20 (2) (2018) 1036-1055.

[3] G. Tuna, V. Gungor, A survey on deployment techniques, localization algorithms, and research challenges for underwater acoustic sensor networks, International Journal of Communication Systems 30 (17).

[4] C.-Y. Li, H. Lu, W. Tsai, Z. Wang, C. Hung, C. Su, Y. Lu, A 5m/25Gbps underwater wireless optical communication system, IEEE Photonics Journal 10 (3).

[5] M. A. Khalighi, M. Uysal, Survey on free space optical communication: a communication theory perspective, IEEE Communications Surveys and Tutorials 16 (4) (2014) 2231-2258.

[6] J. Shen, J. Wang, C. Yu, X. Chen, J. Wu, M. Zhao, F. Qu, Z. Xu, J. Han, J. Xu, Single LED-based 46-m underwater wireless optical communication enabled by a multi-pixel photon counter with digital output, Optics Communications 438 (2019) 78-82.

[7] U. M. Qureshi, F. K. Shaikh, Z. Aziz, S. M. Z. S. Shah, A. A. Sheikh, E. Felemban, S. B. Qaisar, RF path and absorption loss estimation for underwater wireless sensor networks in different water environments, SENSORS 16 (6).

[8] M. Stojanovic, OFDM for underwater acoustic communications: Adaptive synchronization and sparse channelestimation, in: Proceedings of 33rd IEEE International Conference on Acoustics, Speech and Signal Processing, Las Vegas, NV, 2008, pp. 5288-5291.

[9] B. Li, S. Zhou, J. Huang, P. Willett, Scalable OFDM design for underwater acoustic communications, in: Proceedings 33rd IEEE International Conference on Acoustics, Speech and Signal Processing, 2008, pp. 5304-5307.

[10] J. Aparicio, F. J. Alvarez, J. Urena, A. Jimenez, C. Diego, E. Garcia, Swell effect in shallow underwater acoustic communications, in: Proceedings of 15th IEEE International Conference on Emerging Technologies and Factory Automation, Univ Basque Country, Fac Engn, Bilbao, SPAIN, 2010.

[11] S. Milica, J. Preisig, Underwater acoustic communication channels: Propagation models and statistical characterization, IEEE Communica¬tions Magazine 47 (1) (2009) 84-89.

[12] D. V. Ha, V. D. Nguyen, Q. K. Nguyen, Modeling of doppler power spectrum for underwater acoustic channels, Journal of Communications and Networks 19 (3) (2017) 270-281.

[13] M. B. Porter, L. Jolla, The bellhop manual and user's guide: Preliminary draft.

[14] K. M. Awan, P. A. Shah, K. Iqbal, S. Gillani, Underwater wireless sensor networks: A review of recent issues and challenges, Wireless Communications and Mobile Computing.

[15] C. Chen, H. Zhu, M. Li, S. You, A review of visual-inertial simultaneous localization and mapping from filtering-based and optimization- based perspectives, ROBOTICS 7 (3).

[16] S. Jiang, State-of-the-art medium access control (mac) protocols for underwater acoustic networks: a survey based on a mac reference mode, IEEE Communications Surveys and Tutorials 21 (1) (2018) 96-131.

[17] S. Jiang, On securing underwater acoustic networks:a survey, IEEE Communications Surveys and Tutorials 21 (1) (2019) 729-752.

[18] H. Esmaiel, D. Jiang, Spectrum and energy efficient ofdm multicarrier modulation for an underwater acoustic channel, Wireless Personal Communications 96 (1) (2017) 1577-1593.

[19] A. Abdelkareem, B. Sharif, C. Tsimenidis, Adaptive time varying doppler shift compensation algorithm for of dm-based underwater acoustic communication systems, Ad Hoc Networks 45 (2016) 104—119.

[20] M. Wen, X. Cheng, L. Yang, Y. Li, X. Cheng, F. Ji, Index modulated ofdm for underwater acoustic communications, IEEE Communications Magazine 54 (5) (2016) 132-137.

[21] M. Nassiri, G. Baghersalimi, Comparative performance assessment between fft-based and frft-based mimo-ofdm systems in underwater acoustic communications, IET Communications 12 (6) (2018) 719-726.

[22] K. Ramadan, M. I. Dessouky, M. Elkordy, S. Elagooz, F. E. A. El-Samie, Joint low-complexity equalization and carrier frequency offset compensation for underwater acoustic ofdm communication systems with banded-matrix approximation at different channel conditions, International Journal of Communication Systems 31 (17).

[23] S. Yoshizawa, T. Saito, Y. Mabuchi, T. Tsukui, S. Sawada, Parallel resampling of OFDM signals for fluctuating doppler shifts in underwater acoustic communication, Journal of Electrical and Computer Engineering 2018 (2).

[24] J. Han, L. Zhang, Q. Zhang, G. Leus, Eigen decomposition-based partial FFT demodulation for differential OFDM in underwater acoustic communications, IEEE Transactions on Vehicular Technology 67 (7) (2018) 6706-6710.

[25] C.-F. Lin, H.-H. Lai, S.-H. Chang, MIMO GS OVSF/OFDM based underwater acoustic multimedia communication scheme, Wireless Per¬sonal Communications 101 (2) (2018) 601-617.

[26] J. Wu, Iterative compressive sensing for the cancellation of clipping noise in underwater acoustic OFDM system, Wireless Personal Commu¬nications 103 (3) (2018) 2093-2107.

[27] R. Diamant, P. Casari, F. Campagnaro, Fair and throughput-optimal routing in multi-modal underwater networks, Transactions on Wireless Communications 17 (3) (2018) 1738-1754.

[28] T. Qiu, J. Liu, W. Si, D. O. Wu, Robustness optimization scheme with multi-population co-evolution for scale-free wireless sensor.

Vol. 5, No. 1 | January – June 202

Design and Development of GUI for the Mitigation of Chromatic Dispersion: A New Approach

Bhagwan Das[1], Nawaz Ali Zardari[2], Farah Deeba[3], Dileep Kumar Ramnani[4]

Abstract:

Chromatic Dispersion (CD) is the important effect that is considering for optical communication system design as it broadens the pulse during the propagation along channel resulting in pulse overlapping and ultimately bit errors raises. The increment in bit error, in result reduce the performance of optical system. Therefore, mitigation CD is necessary in order to improve the performance of optical communication system. There are several techniques of mitigating CD have been proposed and all based on coding based and this will create issues for the communication design engineer that every time the parameters need to be revised. In order to avoid this issue, the ease for the system design engineer has been created in designing the Graphical User Interface (GUI). In this work, GUI is designed and developed that will request the parameters need to be select for the optical system and it will describe the all process for mitigating it from the system. In the first, the communication system designer have to select the Transmission along with modulation and after that transmission at distance is asked in terms of km. The CD is mitigated uses least mean square technique and Fast Fourier Transform method. The further smoothing of signal is improved by Pulse shaping via using the raised cosine filter. In the end, the original signal and the compensated signal are defined. The BER is also calculated to show whether the reduction through DSP is performed. The GUI is developed in MATLAB and every button backhand the strong coding is used in C++ for developing the system. The proposed design of GUI for the reduction in Chromatic Dispersion has successfully attained the reduction of CD as 40%. In addition to that BER of 10-3 has been attained using the proposed system. The system was designed and developed for the QAM modulation schemes. The designed system has been tested for the 10 Gb/s data rate. The designed and developed system offers the ease of use for the communication engineer, in which on one platform the user can observer well the optical system instead of programming.

Keywords: *Chromatic Dispersion, Digital Signal Processing, Graphical User Interface, MS VISIO.*

[1]Department of Electronic Engineering, Quaid-e-Awam University of Engineering, Science and Technology, Nawabshah, Sindh, Pakistan.
[2]Department of Telecommunication Engineering, Quaid-e-Awam University of Engineering, Science and Technology, Nawabshah, Sindh, Pakistan.
[3]Faculty of Engineering and science Technology, Department of Computing, Hamdard university Karachi Pakistan
[4]Department of Electronic Engineering, Dawood University of Engineering & Technology, Karachi.
Corresponding Author: engr.bhagwandas@hotmail.com

Optical communication is now widely used for high speed communication systems [1]. During the transmission, several transmission impairments effect the performance of systems such as linear and nonlinear parameters. Chromatic dispersion is one of them. Many techniques have already been utilized for the CD reduction [2].

When the signal propagates along fiber optic due to refractive index the pulse broadening effects occur and after some distance signal is lost. The main aim is that to design a platform for CD reduction which should be user friendly even we can execute it without programming [3]. Many researchers has developed the system related chromatic dispersion as discussed in. However, each system has its own advantages and disadvantages [4]. In this research, the CD is reduced in the electrical domain via Graphical User Interface that will help in designing the future communication system in order to solve chromatic issues. In the next section, the problem related to optical system designing for mitigation of chromatic dispersion is discussed and also the proposed work details are descripted in comparison to the work that have been carried out in the past.

The different researchers have worked on reduction of chromatic dispersion. Each work has its own significant in terms of application and results attained. In this paper, the research paper that are only related to development of GUI or similar software tool are discussed in order to demonstrate the need of efficient GUI design and development for the Chromatic dispersion for the various application of optical communication.

In this work, author Amiri in [5] focused the chromatic dispersion compensation is performed numerically for 250 km fiber and BER achieved was 10-2 for optical wireless channel. However, the system designed only based on numerical design and simulation was carried out using the ordinary programming no convenient way of demonstrating the simulation was proposed.

The author Neumann in [6] demonstrated the chromatic dispersion using discrete-time filtering strategy the system was designed using the programming no simulator to GUI was designed for the convenient of optical designer was considered. The system was tested on QPSK modulation with some reduction of complexity in existing circuits.

The author Wu in [7] has focused the equalization of Chromatic dispersion equalization for optical communication using PSO algorithm the proposed system was designed using the programming no simulator or GUI was created in order to facilitate the design for future perspective. The system was tested for QAM modulation and reduction of chromatic dispersion with 25% was attained using the proposed system. The filter also discussed the complex design issues.

The author Udayakumar in [8] designed the chromatic dispersion compensation system using FBG fiber Bragg grating. The worked was carried out using the optisystem software. The link is limited to few Gb/s and BER was not so much fascinating as per requirements of optical wireless channel. It is important to note that optisystem is an expansive simulation tool for developing optical related system and it increase the cost of design system using analysis.

The author Mustafa in [9] worked on compensation of chromatic dispersion in order to maximize transmission bit rate. The work is carried out using soliton transmission technique. It is important to discuss that work was carried using expansive software. Beside that the optical soliton wave technique is utilized and system was designed for the 1.9932.

The author Galvis-Velandia in [10] presented the analysis of dispersion compensation using self-phase modulation using modulator scheme for 50 km fiber link. The system was designed and analyzed for spectral separation of the transmitted channels for 0.2 nm the system has some harmonics alter the spectral density waveform. The system was designed using the programming no simulator or GUI was

designed to help the researcher and optical designer to modify the system characteristics for future design aspects.

Chromatic Dispersion (CD) is key parameter that is considered well when designing the optical communication [11]. The more CD in the signal will increase the Inter Symbol Interference (ISI) that will cause increase in error in transmissions [12]. In result, more bit are corrupted and system performance is highly degraded. Because of that mitigation of CD is important in designing the high performance optical communication [13]. In the past, various CD mitigation have been proposed via signal processing and through programing [14]. There are several issues are encountered when mitigating the CD via programming and signal processing [15]. One is every time, when system designer changes the other parameters the programmer needs to write the all code again and have to check the response of each parameter again and again this will consume lots of time in just checking the system [16]. Furthermore, the signal processing are limited in terms of smoothing the corrupted signal. In comparison to past, the proposed work designed and developed a convenient GUI for the communication system designer that will just ask the programmer to insert values and at back hand the programming for GUI is executing all the variation that is carried out for changing the system. One more advantages of the proposed system is that it will show instant outcome of the developed changes for CD means every time like in the past, the system designed don't need to write and execute the code. The proposed system need all the values of parameters selection. In the next section, the system designing is discussed in detail.

The design and development of GUI for CD mitigation is carried out in different step as shown in Fig. 1. The design steps are shown in flow chart.

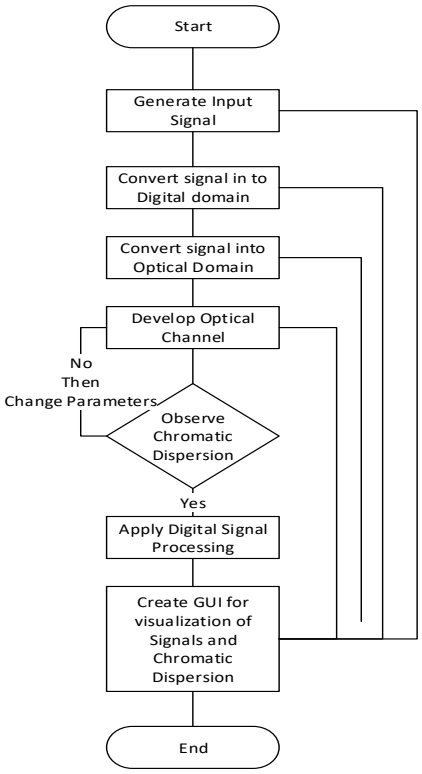

Fig. 1. Flow chart of Designed and Developed System

In Fig. 1, the proposed work research flow chart is depicted. It states that in the first design step need to generate an analog signal and its output can be seen in GUI after that this analog signal is converted in digital signal via analog-to-digital conversion. Here, the outcome of digital signal can be viewed at GUI as well as shown in flow chart Fig. 1. After that using modulation, the signal is converted in optical signal as discussed in [17]. The details of the techniques are shown in methodology section.

This optical signal can be seen in GUI. After that this signal propagated at optical channel and where the effect of chromatic dispersion is observed this can be seen on GUI. If the Chromatic dispersion is observed the digital signal processing techniques are applied in order to mitigate the CD. If there is no CD is observed than the parameters of optical fiber channel are varied [18]. Here,

both signal can be observed on GUI. Before Chromatic dispersion and after Chromatic Dispersion as shown in Fig. 1.

In the next section, the detailed methodology of the work is discussed including the analytical work done in order to design and develop the system that mitigates the CD and also the design of GUI and its outcome is discussed in detail.

In this work, the development of chromatic dispersion mitigation is performed analytically and after that system is programmed in MATLAB and in the last design of GUI is executed as shown in Fig. 2.

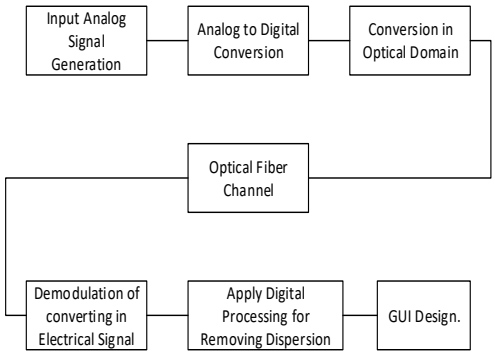

Fig. 2. Methodology for Development of Chromatic Dispersion and Design of GUI

The methodology of developing the chromatic dispersion reduction is shown in Fig. 2. In the first, the chromatic dispersion reduction is discussed and after that design of GUI is discussed.

A. Development of Mitigation of Chromatic dispersion

The input signal is generated using MATLAB, the analog signal is generated of 50 MHz with normalized amplitude values. The signal conditioning of input signal (digitlization) via analog to digital conversion is carried. The generated analog test signal is converted into digital with the frame Size of length 128 bits. The digital signal has 128 number of bits and cyclic prefix that reduce the ISI during the transmission and conversion from digital processing techniques [19] For converting in digital domain, the 1 to 256 subcarrier having index from [-128 to 128] and [0 to 256] is considered. The following commanded are programed:

Channel_Spacing = [0 256];

F= 50MHz;

Samples space= 10;

[y, t] = a2d (channel, F, Samples space)

The above code converting the signal in digital domain and after that second stage is modulating the signal in optical domain. This action is performed using the modulation. The modulations are well known process to changing the characteristic of the signal [20]. There are many modulation schemes are there. They characterized based on amplitude, Phase, and Frequency.

In this work, the 256 length of signal taken above is converted in optical signal via QAM modulation the amplitude of carrier is modulated by 90º. The response of QAM signal is shown in Fig. 3.

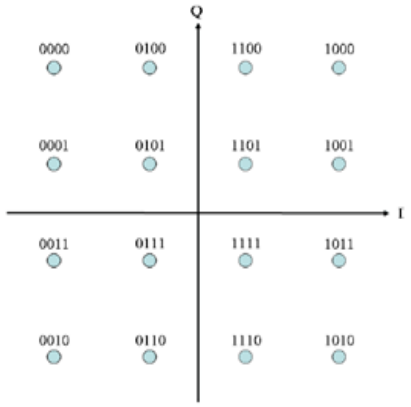

Fig. 3. The constellation diagram

The constellation diagram states that complex digital signal are converted in set in the optical symbols, bits are arranged in unique manner of direct modulation. The QAM modulator is developed in MATLAB Simulink. The model is sown in Fig. 4.

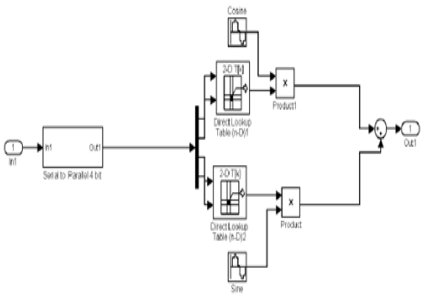

Fig. 4. Design of QAM Modulator

From the design of QAM modulator as shown in Fig. 4. The signal is modulated in stream of bits formed by log2P, where P defines the no. of symbols. 16-QAM modulations is performed in following way [21]:

```
P = 256;
I = log2(P);
nSamp = 10;
```

The signal that is modulated in converted above code converting the signal in digital domain and after that signal is converted in optical via direct modulation. This optical signal is ready to launch over optical fiber to be transmitted at different distances [22]. The signal propagation on optical fiber channel is performed using Non-Leaner Schrödinger Equation (NLSE). This NLSE is used to detonate all the basic parameters related to optical fiber transmission. This include losses in optical fiber, Phase and Group Velocity, Single Phase Modulation, nonlinear and linear effects in single mode fiber as shown (1) [21]:

$$\frac{\partial A}{\partial z} + \frac{i}{2}\beta_2 \frac{\partial^2 A}{\partial t^2} = i\gamma|A|^2 A - \frac{\alpha}{2}A \quad (1)$$

Equation 1 defines the propagation of signal that is carried out from QAM modulation over optical fiber. The channel is characterized based on Single Mode Fiber (SMF). The parameters that are characterized for designing the optical propagation are defined as A defies the power of optical field, α defines the disturbance in the signal, and the β is the one of the crucial parameters over which all the work is performed is chromatic dispersion. However, in this work, the second derivation of chromatic dispersion is taken in order to analyze the chromatic dispersion well in terms of spectrum. Γ defines the nonlinear effect that defines the phase variation, z defines the dimension propagation and also the t defines the interval at which optical signal will prorogate inside the optical fiber [3].

The NLSE is transform in MATLAB via Split Step Fourier Method (SSFM) this model is used as propagation model for transferring the signal over optical fiber [IV]. The simulation is carried for 20 km distance via SSFM. The model developed in MATLAB is used to program input signal, fiber loss db/km, and width of pulse in order to measure the chromatic dispersion. This include different measurement of optical amplitude, and step size for Fourier transform, chirp factor for dispersion [11].

After launching the signal over optical fiber modulation is carried out in converting signal from optical to electrical signal for that demodulation is used as shown in Fig. 5.

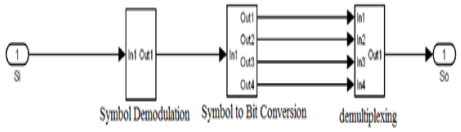

Fig. 5. Demodulation of the Signal

The reason why the demodulation is performed is because before propagation signal was changes in nature. The demodulation is carried out in terns phase and amplitude of detected signal the signal is converted based on MATLAB model as shown in Fig. 5. After that this transmitted signal over fiber optic is converted signal in electrical and onwards the electrical signal is used for chromatic dispersion mitigation using Digital Signal Processing (DSP) techniques. Chromatic dispersion widen the pulse width during the transmission at optical fiber. This produces losses in the signal and performance is further degraded. In this work,

the chromatic dispersion is mitigated in the electric way, which is far better compare to existing techniques [12] for low dispersion system. The chromatic dispersion is taken in account from (1) and it is defined that chromatic dispersion is calculated as in (2) by abandoning the nonlinear effects from the transmission because no pump signal is used and there was no spikes in the signal recorded [13]:

$$\frac{\partial A}{\partial z} = -\frac{i}{2}\beta_2 \frac{\partial^2 A}{\partial t^2} \qquad (2)$$

It was discussed earlier that second order of dispersion is taken for this work. The advantages are coming here because of time delay and different spectrum. The chromatic dispersion is calculated as in (3) [13]:

$$D = -\frac{2\Pi c}{\lambda^2}\beta_2 \qquad (3)$$

Where in (4)

$$\lambda = -\frac{2\Pi c}{\omega} \qquad (4)$$

This has the wavelength for dispersion at which pulse is broaden and wavelength interval. It is measured in terms of ps/nm/km. Solving (2) in time domain yields the solution in (5) [15]:

$$\frac{\partial A(z,t)}{\partial z} = j\frac{D\lambda^2}{4\Pi c}\frac{\partial^2 A(z,t)}{\partial t^2} \qquad (5)$$

The solution of (5) is not possible in time so the signal is converted in frequency domain for measuring the field pattern as in (6) [16]:

$$A(z,\omega) = A(0,\omega)e^{-j\frac{D\lambda^2}{4\Pi c}\omega^2 z} \qquad (6)$$

By further solving for z = 0 at instantaneous value for frequency will generate the transfer function as in (7):

$$H(z,\omega) = e^{-j\frac{d\lambda^2}{4\Pi c}\omega^2 z} \qquad (7)$$

After that signal having transfer function of chromatic dispersion in (7), the inverse FFT is taken in order to show the signal in time domain via (8):

$$h(z,t) = \sqrt{\frac{c}{jD\lambda^2 z}}e^{j\frac{\Pi c}{D\lambda^2 z}t^2} \qquad (8)$$

Further, signal is given to FIR filter to mitigate the chromatic dispersion in time domain as in (9) [18]:

$$z(n) = a_0 w(n) + a_1 w(n-1) + \overline{\qquad\qquad}\rightarrow a_N w(n-N) \qquad (9)$$

where in (9) input signal with filter weights are shown for filter length to generate output as in z. I this work, Least Mean Square (LMS) is used to mitigate the chromatic dispersion to maintain the accuracy and relevancy. LMS is used to maintain the filter weight. Tap weights should be initialized except the central one that is set to unity corresponding to no filtering to mitigate chromatic dispersion [22].,The filter signal still have some noises. For that smoothing of signal is required. In this work, the Raised Cosine Filter improves the shape of pulse. The filter is designed and constructed via (10) [12]:

$$G(\omega) = \begin{cases} T & for \quad |\omega| \le (1-\alpha)\frac{\omega_s}{2} \\ \frac{T}{2}\left\{1 - sin\left[\frac{T}{2\alpha}(|\omega| - \frac{\omega_s}{2})\right]\right\} & for \quad (1+\alpha)\frac{\omega_s}{2} \le |\omega| \le (1+\alpha)\frac{\omega_s}{2} \\ 0 & elsewhere \end{cases} \qquad (10)$$

The signal received from filter is observed in response and it was defined that phase has edges and tracking needs to be remove for that phase tracking is used to remove error at

the edges by mitigating the chromatic dispersion. The signal is chucked in smaller window and errors at the edges at specific frequencies are removed via Kaiser Window as shown in (11) [13]:

$$w[n] = \begin{cases} \dfrac{I_0\left[\beta\sqrt{1-\left(\dfrac{n-M/2}{M/2}\right)^2}\right]}{I_0(\beta)} & 0 \le n \le M \\ 0 & else \end{cases} \quad (11)$$

This is improving the detected stream from long stream of bits by changing the center lobe width and sided lobe. After that Bit Error Rate is calculated to check that chromatic dispersion is mitigated? BER is number of errors occurring over a time at which signal is received. The error rate depends on signal to noise ratio determined by Q factor. BER was calculated via (12) [13]:

$$BER = \left(\frac{1}{\sqrt{2\pi}}\right)\left(\frac{e^{-\frac{Q^2}{2}}}{Q}\right) \quad (12)$$

As the Q or Quality factor is increased BER decreased and it is defined that by mitigating the chromatic dispersion, the Q-factor is increased and BER Furthermore, the performance is setup via Eye diagram. It gives visual of signal in the shape of an eye to asses maximum transmission rate of a system, it is related to BER as the chromatic dispersion is more the eye will be close and if chromatic dispersion mitigation is archived the eye will be open [27-28].

In the next section, the Design of GUI of carried for finalizing the work step of mitigating the chromatic dispersions.

Graphical User Interface (GUI) is developed in order to mitigate the chromatic dispersion for its better visualization. It was discussed before that before designing of the system programming was required. GUI helps in recalling the signals and after that their respective output responses are shown in the results section. The GUI setup is shown in Fig. 6, the process involves in reducing the chromatic dispersion are shown. The GUI is characterized in a different section.

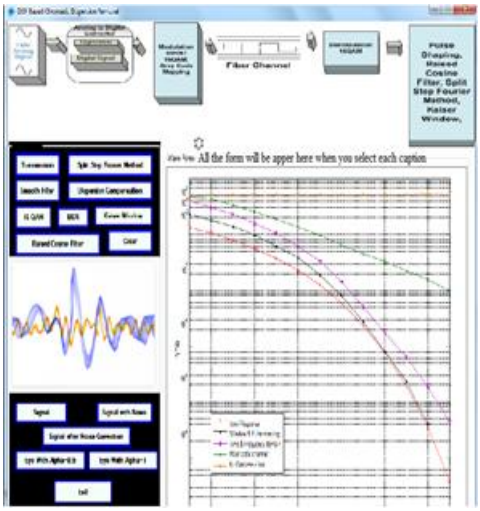

Fig. 6. GUI setup for designing the Mitigation of Chromatic Dispersion

Firstly, the system design via (1) - (12) by using the programming is transformed in GUI. The system designer can insert the value for generating the input signal of any frequency and after that from just signal click the signal will be converted in digital domain [29-30]. The next tag is used for converting optical signal from electrical one via modulation. After that fiber length is choose in order to select the length of fiber. The signal shows the propagation in GUI. The GUI measure the dispersion calculated from (6). After that DPS technique of having raised cosine filter and Kaiser Window is used in order to mitigate the dispersion. This GUI can show the repose of the signal before removing the dispersion and after applying the DSP techniques the response of chromatic dispersion can be shown in GUI as shown in Fig. 6.

Not only this, the GUI also gives the information about BER that was calculated via (12) along with eye diagram. These all measurements defines that signal has the chromatic dispersion during the transmission and via developing the GUI it easily describe the response of all optical communication under one system. The designer don't have to go anywhere else program for displaying the response of developed optical system. Furthermore, the parameters and system can be changed easily without any program efforts. In the next section, results for GUI designed and response of designing the mitigation of chromatic dispersion is show step by step.

In this work, the mitigation of chromatic dispersion is carried in MATLAB. The chromatic dispersion is removed by using the DSP technique in which raised cosine filter method and Kaiser window method are used. The response are recorded based on Bit Error Rate and Eye Diagram. The chromatic dispersion mitigation is carried out analytically and response are observed on GUI.

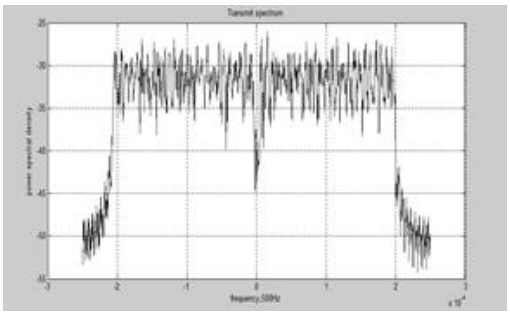

Fig. 7. The spectrum of the Input signal transmitted at a channel

The GUI generates the response of signal spectrum of input transmitted signal which is converted analog to digital is appeared in Right most box where star is mentioned as shown Fig. 7.

The response of modulation for QAM-16 is display via GUI as shown in Fig. 8.

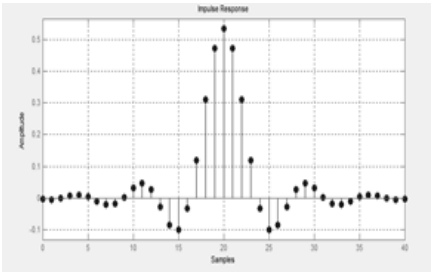

Fig. 8. The response of GUI for modulation (16 QAM)

It can be analyzed from Fig. 8 that the modulation of 16 QAM modulation scheme is used for the GUI. The 16-Qam scheme is widely used scheme for optical communication system due to less effect of noise during the transmission.

It was discussed that Split Step Fourier Method is used to design the optical fiber model. The response of optical fiber model is shown in Fig. 9 that is generated using the designed GUI.

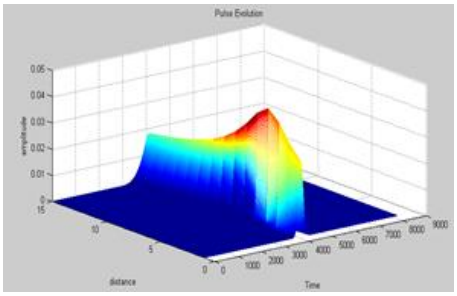

Fig. 9. Response of GUI for Pulse Model fiber Optic

The response of optical fiber model is developed from GUI modeling and depicted in Fig. 9. The optical model is designed using the NLSE equation. The response is characterized using different parameters such as; amplitude of pulse, distance and time for pulse incurred in optical fiber.

The output of chromatic dispersion is performed through raised cosine and Kaiser Window in time domain. The GUI is modeled to generate the response of mitigation of Chromatic Dispersion as shown in Fig. 10.

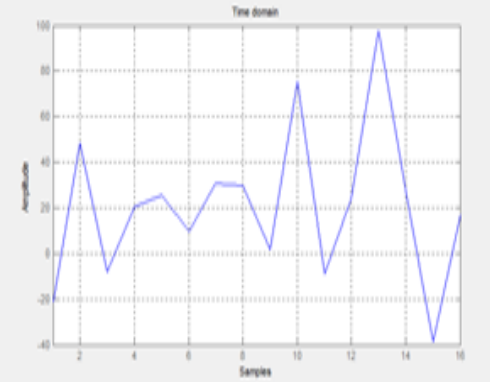

Fig. 10. Response of GUI for showing mitigation of Chromatic dispersion in Time domain

It was discussed that mitigation of chromatic dispersion was carried out using raised cosine filter and Kaiser window. The GUI has been created for generating the response of raised cosine filter as shown in Fig. 11.

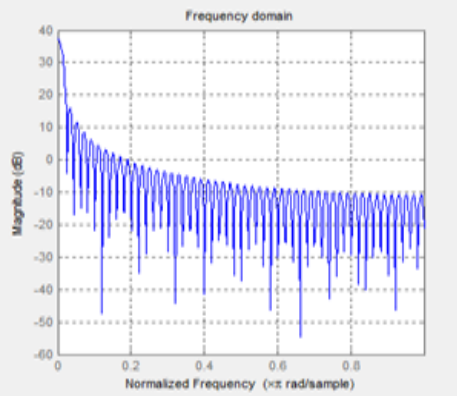

Fig. 11. Response of GUI for Raised Cosine Filter Output

After improving the shape of the pulse the phase is improved through the Kaiser window as shown in GUI in Fig.12 at frequency of 1G Hz:

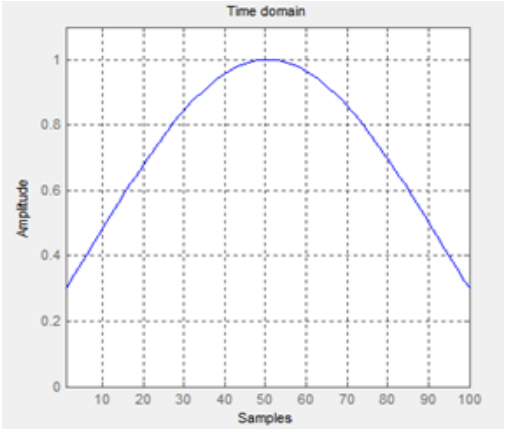

Fig. 12. Fig. 12. Response of GUI for Time domain Window filtration

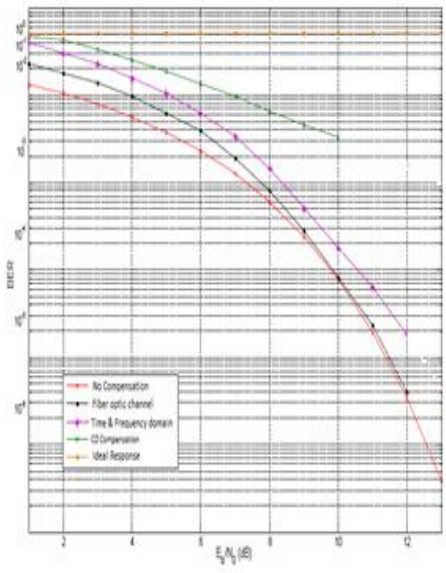

Fig. 13. The response of GUI for generating the BER for mitigation of chromatic dispersion

After applying the chromatic dispersion mitigation. It is important to show the performance of the system. It was discussed that chromatic dispersion mitigation is carried out using Bit Error Rate and Eye Diagram. The BER diagram is developed using GUI as shown in Fig. 13

Bit error rate is calculated by the SP tool of MATLAB. The semianalytic type model is selected in which Eb/No range is 0:19 dB, channel is optical fiber, Modulation is 16-QAM and samples per symbols are 256. After that response of chromatic dispersion mitigation is generated via Eye-diagram that is generated via GUI as shown in Fig. 14.

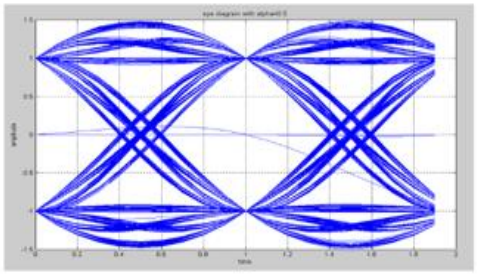

The response of GUI for Eye diagram before CD reduction

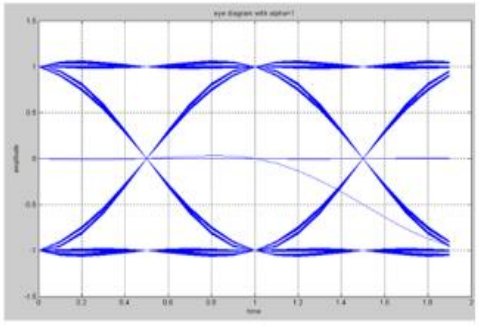

The response to GUI for Eye diagram after CD reduction

Fig. 14. The response of GUI for generating the Eye diagram for performing mitigation of chromatic dispersion

It is really important to shows the original signal which is transmitted at optical fiber channel. If the designed system was not developed. Every time have to execute simulation and programming need to be dine for that. The response of signal transmitted can be easily developed and displayed via GUI as shown in Fig. 15.

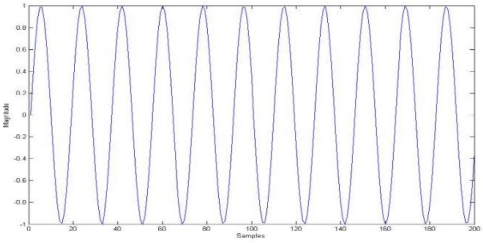

Fig. 15. Response of GUI for Input Signal to be transmitted

Similarly, the GUI has the capability to generate the response and difference between the signals transmitted and signal that is corrupted via chromatic dispersion. The response of noisy signal due to chromatic dispersion is shown in Fig. 16. This shows that after propagation at fiber optic at receiver we get this noisy signal due to chromatic dispersion.

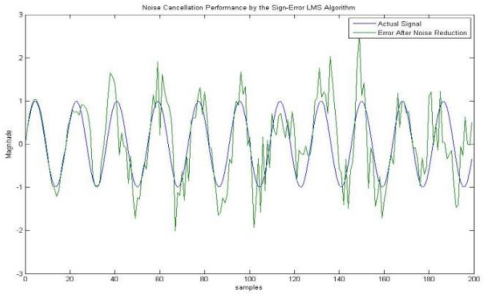

Fig. 16. Response of GUI for Noisy signal received at end of Fiber channel

Finally, after applying the proposed technique that mitigates the chromatic dispersion via our method. The final output of the signal in which chromatic dispersion is removed can be depicted as well. This is only possible due to the development of GUI. The response of the output signal that is generated form which chromatic dispersion is mitigated is shown in Fig. 17.

In this work, the development of chromatic dispersion is carried out via digital signal processing technique i.e. raised cosine filter, window and filtration method. The GUI is designed in order to ease the system designer, in terms eliminate the need of re-

programming for each change in parameters and running whole simulation again and again.

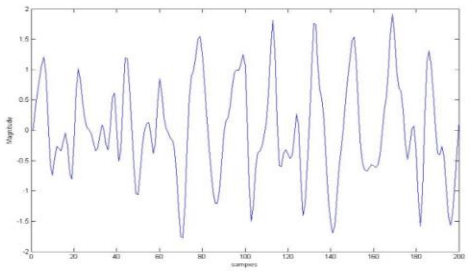

Fig. 17. The response of GUI for output Signal after mitigation of Chromatic Dispersion.

In the past, the work also carried out related to reducing the chromatic dispersion. Alfiad M.S et al, (2009) [21], worked on digital modulation scheme in an electrical and optical chromatic dispersion compensation for low frequency. Every time when changing the permanents, the re-programming of algorithm was required. Cherbi L et al, (2006) [22], worked on measures CD in optical networks in which compensators is designed for certain wavelength. Phase-shift modulation scheme is adopted for the measurement of CD SMF for 10 km distance only. Li, Xu et al, (2020) [23] worked transmission systems artificial CD and DGD is compensated can be compensated but without simplifying system. Goldfarb Gilad and Li Guifang, (2007) [24] worked on Digital IIR filtering to control CD in system with DSP. There are less number of taps are used in IIR filtering as compared in FIR filtering, complex programming and no re-programming feature was there. Borjesson (2016) [25] worked on design of compensator for CD. Compensator works on lookup table function along with usage of BPSK with low BER. Xu Tianhua, (2012) [26] worked on digital filters for compensation of CD and n improved feature recorded.

From above it was concluded that in the past lack of programming, re-programming, visualization, execution of models, complex modeling, low data rate, lack of data analysis and several issues left unaddressed. Taking the benefits of all that our work proposed the chromatic dispersion is carried out via digital signal processing technique for better BER performance. One of the main novelty of the work is design and development of GUI that is not descripted yet in the literature. The designed provided various feature to communication system designer that reduces the efforts of programming, not only this the system characterization can be changed easily. The designed system will be helpful for many researcher those who are working on optical system as it is giving the fast and accurate way of analyzing the results.

In this work, the mitigation of chromatic dispersion is carried out along with design of Graphical User Interface (GUI). The designed offers great feature of mitigating chromatic dispersion using the less complex algorithms, better BER and Eye diagram and one of the main novelty and contribution of the work is system changes in parameters and characterization is developed and designed are made ease. The existing system offering the output execution separately and changing of parameters is also challenging.

In developing the GUI there are many features are added such as overserving results in faster development of optical fiber channel in a GUI is not done before. The designed system can be beneficial for the student's ad researcher that are working of optical system design via this system they can design, analysis, and output can be observe. The designer can work other aspects such as developing advanced algorithm in the system.

It is concluded that the designed work offer the GUI in order to mitigate the chromatic dispersion from the optical systems. The system has been developed for the 10 Gb/s data rate and the compensation of more than 40 % has been attained during the proposed system and the BER of 10-3 is achieved. The system is considered to be the good step as in the past discussed in literature review that no such type of GUI was report. The designed system will be helpful for the optical designer and researchers as it will be great platform to demonstrate the chromatic

dispersion compensation by configuring their system requirements and they can see the output at the same time.

The authors would like thanks Department of Electronic Engineering, Quaid-e-Awam University of Engineering, Science and Technology, Nawabshah, Sindh, Pakistan for the technical support in carrying this research work.

REFERENCES

[1] M. F. L. Abdullah, B. Das, and M. S. N. Shahida, "Frequency domain technique for reducing chromatic dispersion," In 2014 Electrical Power, Electronics, Communicatons, Control and Informatics Seminar (EECCIS), 2014, pp. 56-61.

[2] M. F. L. Abdullah, B. Das, and N. S. M. Shah, "DSP techniques for reducing chromatic dispersion in optical communication systems," In 2014 International Conference on Computer, Communications, and Control Technology (I4CT), 2014, pp. 305-309.

[3] Ahmed, R. K., & Mahmood, H. A. (2018, January). Performance analysis of PAM intensity modulation based on dispersion compensation fiber technique for optical transmission system. In Engineering Sciences-3rd Scientific Conference of Engineering Science (ISCES), 2018 1st International Scientific Conference of (pp. 126-130). IEEE.

[4] Yang, A., Guo, P., Wang, W., Lu, Y., & Qiao, Y. (2019). Joint monitoring of chromatic dispersion, OSNR and inter-channel nonlinearity by LFM pilot. Optics & Laser Technology, 111, 447-451.

[5] Amiri, I. S., Rashed, A. N. Z., Kader, H. M. A., Al-Awamry, A. A., Abd El-Aziz, I. A., Yupapin, P., & Palai, G. (2020). Optical communication transmission systems improvement based on chromatic and polarization mode dispersion compensation simulation management. Optik, 207, 163853.

[6] Neumann, S. P., Ribezzo, D., Bohmann, M., & Ursin, R. (2021). Experimentally optimizing QKD rates via nonlocal dispersion compensation. Quantum Science and Technology, 6(2), 025017.

[7] Wu, Z., Li, S., Huang, Z., Shen, F., & Zhao, Y. (2021, November). Chromatic Dispersion Equalization FIR Digital Filter for Coherent Receiver. In Photonics (Vol. 8, No. 11, p. 478). Multidisciplinary Digital Publishing Institute.

[8] Udayakumar, R., Khanaa, V., & Saravanan, T. (2013). Chromatic dispersion compensation in optical fiber communication system and its simulation. Indian Journal of Science and Technology, 6(6), 4762-4766.

[9] Mustafa, F. M., Zaky, S. A., Khalaf, A. A., & Aly, M. H. (2021). Dispersion compensation in silica doped fiber using soliton transmission technique over cascaded FBG. Optical and Quantum Electronics, 53(5), 1-17.

[10] Galvis-Velandia, J. E., Puerto-López, K., & Ramírez-Mateus, J. (2021, November). Analysis of linear and non-linear effects in the frequency domain for a three-channel optical transmission system. In Journal of Physics: Conference Series (Vol. 2102, No. 1, p. 012017). IOP Publishing.

[11] Novick, A., Castro, J. M., Pimpinella, R., Kose, B., Huang, P., & Lane, B. (2018, March). Study of Dispersion Compensating Multimode Fiber for Future VCSEL PAM-4 Channels at Data Rates over 100 Gb/s. In 2018 Optical Fiber Communications Conference and Exposition (OFC) (pp. 1-3). IEEE.

[12] Zeng, Z., Yang, A., Guo, P., & Feng, L. (2018, January). Weighted finite impulse response filter for chromatic dispersion equalization in coherent optical fiber communication systems. In 2017 International Conference on Optical Instruments and Technology: Optoelectronic Devices and Optical Signal Processing (Vol. 10617, p. 106170U). International Society for Optics and Photonics.

[13] Konishi, T., Murakawa, T., Nagashima, T., Hasegawa, M., Shimizu, S., Hattori, K., ... & Wada, N. (2015). Flexible OFDM-based access systems with intrinsic function of chromatic dispersion compensation. Optical Fiber Technology, 26, 94-99.

[14] Ranzini, S. M., Parahyba, V. E., Júnior, J. H. D. C., Guiomar, F., & Carena, A. (2019). Impact of Nonlinear Effects and Mitigation on Coherent Optical Systems. In Optical Communications (pp. 93-120). Springer, Cham.

[15] Ji, J., Zheng, S., & Zhang, X. (2019). Pre-distortion compensation for optical-based broadband LFM signal generation system. Optics Communications, 435, 277-282.

[16] Fu, S., Chen, C., Gao, F., Li, X., Deng, L., Tang, M., & Liu, D. (2018). Digital chromatic dispersion pre-management enabled single-lane 112 Gb/s PAM-4 signal transmission over 80 km SSMF. Optics letters, 43(7), 1495-1498.

[17] Kumar, P., Kumar, V., & Roy, J. S. (2019). Design of quad core photonic crystal fibers with flattened zero dispersion. AEU-International Journal of Electronics and Communications, 98, 265-272.

[18] Hu, Y., Wang, Y., & Chee, K. W. (2019). Optical Communications and Modulation Techniques in 5G. In Smart Grids and Their Communication Systems (pp. 401-464). Springer, Singapore.

[19] Nain, H., Jadon, U., & Mishra, V. (2018). Performance Exploration of Different Dispersion Compensation Schemes with Binary and Duo Binary Modulation Formats Over Fiber-Optic Communication. In Information and Communication Technology for Sustainable Development (pp. 281-290). Springer, Singapore.

[20] Sharma, D., & Prajapati, Y. K. (2018). Analytical Study of DWDM Optical Long Haul Network with Symmetrical Dispersion Compensation. Indian Journal of Science and Technology, 8(1).

[21] Alfiad, M. S., van den Borne, D., Jansen, S. L., Wuth, T., Kuschnerov, M., Grosso, G., ... & De Waardt, H. (2009). A comparison of electrical and optical dispersion compensation for 111-Gb/s POLMUX–RZ–DQPSK. Journal of Lightwave Technology, 27(16), 3590-3598.

[22] Cherbi, L., Azrar, A., Mehenni, M., & Aksas, R. (2009). Characterization of the polarization in the spun fibers. Microwave and Optical Technology Letters, 51(3), 725-731.

[23] Liu, X., Lun, H., Fu, M., Fan, Y., Yi, L., Hu, W., & Zhuge, Q. (2020). AI-Based Modeling and Monitoring Techniques for Future Intelligent Elastic Optical Networks. Applied Sciences, 10(1), 363.

[24] Goldfarb, G., & Li, G. (2007). Chromatic dispersion compensation using digital IIR filtering with coherent detection. IEEE Photonics Technology Letters, 19(13), 969-971.

[25] Börjesson, E. (2018). Implementation of Blind Carrier Phase Recovery for Coherent Fiber-Optical Receivers (Master's thesis).

[26] Xu, T., Karanov, B., Shevchenko, N. A., Lavery, D., Liga, G., Killey, R. I., & Bayvel, P. (2017). Digital nonlinearity compensation in high-capacity optical communication systems considering signal spectral broadening effect. Scientific reports, 7(1), 1-10

[27] Kaim Khani, T., Mushtaq, Z., Waqas, A., Chowdhry, B. S., & Uqaili, M. A. (2021). Improving VLC Data Rate and Link Range Using Commercial Electronic Components. Wireless Personal Communications, 1-13.

[28] Shaikh, M. N., Waqas, A., Chowdhry, B. S., & Umrani, F. A. (2012). Performance and Analysis of FSO link availability under different weather conditions in Pakistan. Journal of The Institution of Electrical & Electronics, 76, 1-5.

[29] Arain, S., Shaikh, M. N., Waqas, A., Chowdhry, B. S., & Themistos, C. (2016, July). Performance analysis of advance modulation schemes for free space optical networks. In 2016 18th International Conference on Transparent Optical Networks (ICTON) (pp. 1-4). IEEE.

[30] Mushtaq, Z., Uqaili, M. A., Waqas, A., & Chowdhry, B. S. (2021). Multi-Stage Mach–Zehnder Based Continuously Tunable Photonic Delay Line. Wireless Personal Communications, 1-11.

Vol. 5, No. 1 | January – June 2022

MnO2@Co3O4 nanocomposite based electrocatalyst for effective oxygen evolution reaction

Muhammad Yameen Solangi[1], Abdul Hanan Samo[2], Abdul Jaleel Laghari[1], Umair Aftab[1], Rehan Ali Qureshi[1], Muhammad Ishaque Abro[1] Muhammad Imran Irfan[3]

Abstract:

For large-scale energy applications, conceiving low-cost and simple earth-abundant electrocatalysts are more difficult to develop. By using an aqueous chemical technique, MnO2 was added into Co3O4 with varying concentrations to prepare MnO2@Co3O4 nanocomposite (CM). In an aqueous solution of 1 M KOH, the electrocatalyst with a greater concentration of MnO2 outperforms in terms of OER. To confirm the composition, crystalline structure, and morphology of the electrocatalyst, analytical methods such as X-ray diffraction (XRD) techniques, Fourier transformed infrared spectroscopy (FTIR) and scanning electron microscopy (SEM) were used. At 20 mA/cm2 current density, the electrocatalyst had a lowest overpotential of 310 mV verses Reversible hydrogen electrode (RHE). The CM-0.4 electrocatalyst has a small Tafel slope value and charge transfer resistance of approximately 72 mV/dec and 74 Ω which confirm its high catalytic activity. The electrocatalyst reveals a double layer capacitance (Rct) of 18 µF/cm2 and an electrochemical active surface area (ECSA) of 450 cm2, demonstrating that addition of MnO2 impurities into Co3O4 enhances the active catalyst sites. These findings contribute to the knowledge of these kind of catalysts, that will assist in the development of novel electrocatalysts which are feasible for prospective energy generation technologies.

Keywords: *Electrocatalyst; oxygen evolution reaction; cobalt oxide; manganese oxide; alkaline media.*

1. Introduction

Growing energy consumption and the depletion of fossil fuels are two major challenges which have led to the discovery of earth abundant alternative sources and the development of effective energy storage systems [1-3]. For this fact, electrochemical water electrolysis is one of the most efficient methods to obtain hydrogen [4,5].

Herein, hydrogen evolution reaction (HER) takes place at the cathode while oxygen evolution reaction (OER) happens at the anode in an electrochemical water splitting mechanism. Nevertheless, the efficient electrocatalysts were utilized for effective water splitting [6-8]. Currently, the RuO2/IrO2 based noble electrocatalysts have superiority for OER with lower low overpotential value for higher electro-catalytical activity [9,10].

However, they are rare in nature and massive cost electrocatalyst that restrict the usage in industrial applications. To achieve cost-effective hydrogen generation, creating an electro-catalyst for water splitting that are

[1]Dept. of Metallurgy & Materials Engineering, MUET, Jamshoro, Pakistan.
[2]College of Materials & Chemical Engineering, Harbin Engineering University, Harbin, China.
[3]Institute of Chemistry, University of Sargodha, Sargodha- 40100 Pakistan
Corresponding Author: yameen.engineer14@gmail.com

efficient, inexpensive, earth-abundant, stable, and operate at low overpotential is critical [11-13].

The OER mechanism contains 4 electron charge transfer kinetics [14]. Therefore, OER mechanism is slow process as compared to HER and responsible for overall performance of water splitting. In this regard, OER requires more overpotential for water oxidation which provide the major hindrance in water splitting technology [15-17]. So that, researchers are developing electrocatalysts for OER with low overpotential, ease of synthesis and low-cost. In this fact, various transition metal oxides, sulfides, selenides, and phosphide based electrocatalysts were developed to overcome such problems [18-20].

In this work, the impurity addition strategy was applied to create nanocomposite for essential OER performance. Wherein, MnO2 as an impurity was added in Co3O4 to create oxygen vacancies in the Co3O4 nanostructures which may be responsible for increase in active sites and decrease the overpotential of catalyst that leads to superior OER performance. The synthesized nanocomposite was characterized by XRD, FTIR, SEM and Electrochemical Analysis for the determination of crystallinity, phase purity, morphology, and electrochemical investigation respectively.

2. Experimental Work

2.1 Materials and Methods

Cobalt chloride hexahydrate (CoCl2.6.H2O), urea (CH_4N_2O) and potassium permanganate (KMnO4) were brought from Sigma Aldrich, Karachi, Pakistan. The synthesis of MnO2@Co3O4 nanocomposite was developed by aqueous chemical method [21]. Herein, 0.1M solution of CoCl2.6.H2O and CH_4N_2O was added into 100 ml deionized water. After that, KMnO4 with two different concentrations i.e., 0.2 g and 0.4 g were added separately in different breakers containing cobalt oxide precursor. These samples were labeled as Co3O4 pristine, CM-0.2 and CM-0.4. The label CM denotes the composite of MnO2@Co3O4. These samples were mixed properly and placed into an electric oven at 95OC for 5 h. Once the reaction time was completed then samples were taken out from oven and washed multiple times with deionized (DI) water to remove the extra impurities. After that, nanocomposite material was collected through sedimentation method in china dish and dried in oven at 100OC for moisture content removal. The dried samples were placed into furnace for calcination to convert hydroxide phase into oxide phase at 500OC for 5 h. When the calcination time finished then sample were taken from furnace and nanocomposite was achieved for further characterization.

2.2 Physical Characterization

Powder X-ray diffraction (XRD) was performed on a Philips PAN analytical powder x-ray diffractometer at 45 kV and 45 mA using Cu Kα radiation (λ = 0.15406 nm). The lattice parameters were calculated by Bragg's law in cubic formula.

$$d_{(hkl)} = \frac{a}{\sqrt{h^2 + k^2 + l^2}}$$

Whereas, "d(hkl)" is the atomic planer spacing, "a" is lattice constant and "(h,k,l)" is the diffracted plane.

The Crystallite size of sample was computed by Debye's Scherrer equation at (311) plane.

$$D = \frac{k\lambda}{\beta Cos\theta}$$

where "D" is the crystallite size (Å), "k" is Scherrer constant that is equal to 0.9, "λ" is the wavelength of source CuKα, "β" is the full width at half maximum (Radians) and "θ" is the peak position (Radians).

Fourier transform infrared spectroscopy (FTIR) was obtained on a Perkin Elmer FTIR Spectrometer spectrum two. Scanning electron microscopy (SEM) images were achieved on JSM-6380L JEOL scanning electron microscope.

2.3 Electrochemical Analysis

Electrochemical measurements were carried out on a VERSASTAT 4-500 Potentiostat consisting of a three-electrode assembly i.e., working electrode, reference

electrode and counter electrode made up of glassy carbon electrode, silver-silver chloride electrode and Pt wire respectively. Glassy carbon electrodes were modified with the electrocatalyst, and various experiments were performed in 1M KOH solution. The linear sweep voltammetry (LSV) was done to determine the polarization curves at a scan rate of 5 mV/s and cyclic voltammetry (CV) was used to investigate the effective active surface area at 10, 20 and 30 mV/s scan rates. The chrono-potentiometric analysis was accomplished for durability as synthesized electrocatalyst at 20 mA/cm2 for 40 h.

3. Results and Discussion

3.1 Physical Characterization

The XRD spectrum of pristine Co3O4, CM-0.2 and CM-0.4 can be seen in Fig.1. The XRD spectra of pristine Co3O4 resembled with JCPDS card no. 01-080-1536. The diffraction pattern revealed at the planes of (111), (220), (311), (222), (400), (331), (422), (511), (440), (531), (442), (620), (533) and (622) at the 2 theta angles of 18.848o, 31.017o, 36.461o, 38.231o, 44.436o, 48.669o, 55.177o, 58.842o, 64.656o, 68.011o, 69.111o, 73.437o, 76.618o and 77.668o respectively. This JCPDS card validates that the Co3O4 has cubic crystalline structure [22,23]. Whereas XRD spectrum of MnO2 are matched with JCPDS card no. 00-044-0992 that diffracted at 2θ values of 19.112o, 37.121o, 38.958o, 45.068o, 49.498o, 59.599o, 65.703o and 69.583o corresponded at the planes (111), (311), (222), (400), (331), (511), (531) and (440). which revealed that MnO2 is also in cubic crystalline phase.

In addition, other structural features such atomic planer spacing, lattice constant and crystallite size of samples are given in the Table 1. The lattice constant of pristine Co3O4 is higher but the addition of MnO2 reduces its lattice constant that leads to reduction in crystallite size. Here, the substitution of large Co2+ atom (0.72 Å) with small Mn4+ atom (0.67 Å) carried out that may be responsible for shrinkage of unit cell and achieved reduction in the lattice constant. However, the major peak of Co3O4 at (311) diffracted plane shifted toward right side as the concentration of MnO2 increases as shown in Fig 1(b) which also suggested the substitution of Co atom by Mn atom. Therefore, crystallite size of composite decreases as the concentration of MnO2 increases [24,25].

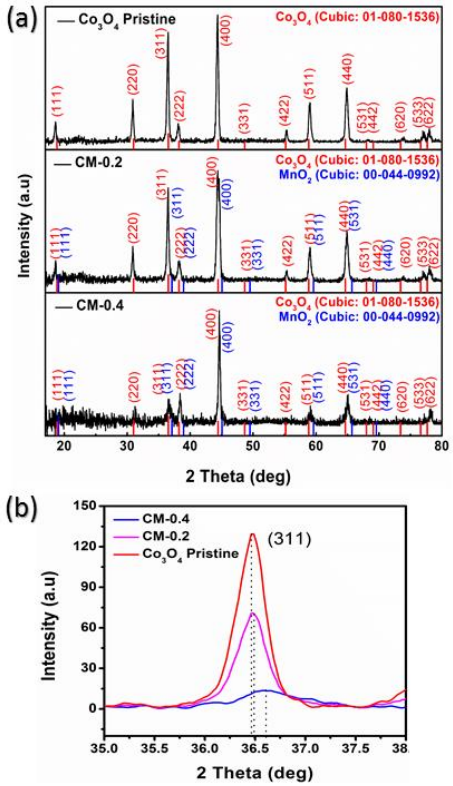

Fig. 1. (a) XRD pattern of various samples (b) Zoom in view of XRD peak shift

The FTIR spectra of various samples are shown in Fig. 2. It represented that pristine Co3O4, CM-0.2 and CM-0.4 involved same peak of O-H, C-H, C=O, O-H, C-O and C=C corresponding to 3438 cm-1, 2927cm-1, 1797cm-1, 1035 cm-1 and 878 cm-1. These organic bonds achieved from the Potassium bromide (KBr) that were used for the making the pallet of KBr and sample for FTIR measurement. Despite this, the main difference was observed in pristine Co3O4 and nanocomposite (CM-0.4) of metal oxide M-O peaks which represent O-Co-O at 570 cm-1 and Co-O at 663 cm-1. However, the presence

of MnO2 in Co3O4 nanostructures sharpen the metal oxide peaks due to the addition of MnO2 impurities [22,26,27].

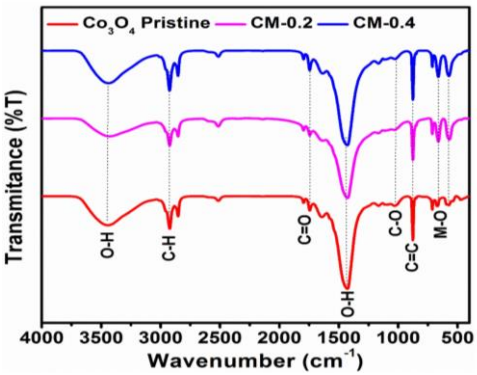

Fig. 2. FTIR spectra of different samples

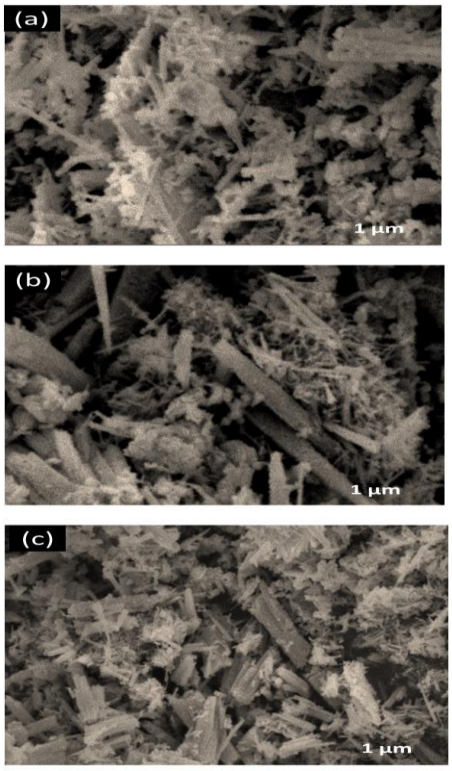

Fig. 3. SEM images of (a) Pristine Co_3O_4 (b) CM-0.2 (c) CM-0.4

The morphology of prepared Co3O4 pristine and nanocomposites was examined by scanning electron microscopy (SEM). The SEM images of samples are shown in Fig. 3. The morphology of pristine Co3O4 showed nano needles like structure as shown in Fig. 3(a) while the morphology of CM-0.2 and CM-0.4 contained nano flakes in the matrix of nano needles like structure as shown in Fig. 3(b, c). It can be seen that CM-0.2 nanocomposite contained fewer nano flakes than CM-0.4. which stated that as the amount of MnO2 increase then nano flakes concentration increases in nano needle matrix.

3.2 Electrochemical Analysis

The electrochemical analysis of various samples was investigated in 1M KOH environment. The LSV polarization curves can be seen in Fig. 4(a) that shows CM-0.4 has lowest overpotential of 310 mV as compare to the overpotential of pristine Co3O4 and CM-0.2 as 430 mV and 350 mV vs RHE at the current density of 20 mA/cm2. The CM-0.4 electrocatalyst exhibits high OER performance due to lowest overpotential as compare to updated electrocatalyst that can be seen in Table 3. The Tafel values were obtained by linear fit region of polarization curves as shown in Fig. 4(b). The Tafel values of pristine Co3O4, CM-0.2 and CM-0.4 are calculated as 102 mV/dec, 86 mV/dec and 72 mV/dec respectively.

The oxygen evolution reaction (OER) takes place through four electron transfer mechanism which is given as under.

1. $M + OH^- \rightarrow MOH + e^-$
2. $MOH + OH^- \rightarrow MO^- + H_2O$
3. $MO^- \rightarrow MO + e^-$
4. $2MO \rightarrow 2M + O_2 + 2e -$

The OER kinetic and theoretical Tafel values in alkaline media of 1, 2, 3 and 4 sub reactions are 120 mV/dec, 60 mV/dec, 40 mV/dec and 15 mV/dec respectively [28, 29]. Therefore, the current study contains 72 mV/dec Tafel value of best composite which suggest that step-1 is rate determining step for effective OER performance.

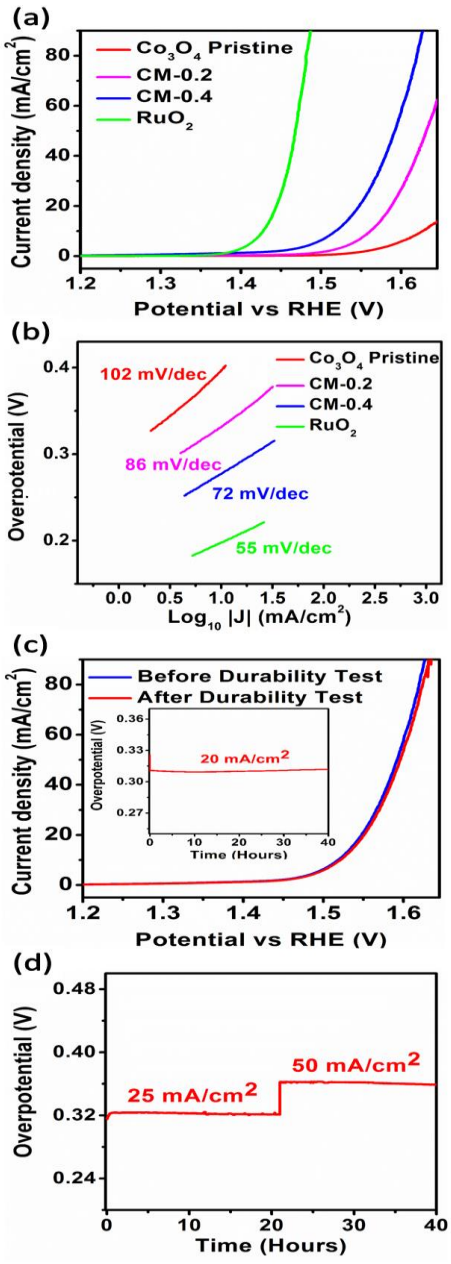

Fig. 4. Electrochemical Analysis of various electrocatalysts (a) Polarization curve (b) Tafel plot (c) Stability & Durability of best sample (d) Durability of best electrocatalyst at different current densities.

The stability test was performed by measuring LSV before and after chronopotentiometry at 20 mA/cm2. The stability of CM-0.4 illustrated in Fig. 4(c) which represented its overpotential did not drop after long operation. Furthermore, the durability of CM-0.4 can be seen inside Fig. 4(c) which showed that CM-0.4 electrocatalyst is long term durable for 40 h. In addition, durability test was also performed at different current densities i.e., 25 mA/cm2 and 50 mA/cm2 as shown in Fig. 4(d). It revealed that the potential does not drop at various current densities which give significant proof of electrocatalyst's stability.

The cyclic voltammetric (CV) experiment was performed at different scan rates on various electrocatalysts as shown in Fig. 5. The cyclic voltammetry of CM-0.4 has highest current density that represent its highest catalytical active sites as seen in Fig. 5(c). In addition, the double layer capacitance Cdl value plots were extracted from CV curves as illustrated in Fig. 5(d). The Cdl values of pristine Co3O4, CM-0.2 and CM-0.2 have been calculated as 3.6 µF/cm2, 7.8 µF/cm2 and 18 µF/cm2. The CM-0.4 electrocatalyst has high double layer capacitance than other as prepared electrocatalysts.

The electrochemical active surface area ESCA was calculated by Cdl/Cs expression, whereas specific capacitance of the electrolyte (Cs) in 1M KOH is about 0.04 [30]. The electrochemical active surface area (ECSA) was calculated as 450 cm2, 195 cm2, and 90 cm2 for CM-0.4, CM-0.2 and Pristine Co3O4 respectively which are mentioned in Table 2. This data also authenticates the catalytical performance of CM-0.4.

The electrochemical impedance spectroscopy data represented by Nyquist plot and Bode (1, 2) of various samples are shown in Fig. 6. The EIS data was fitted via Z view software and fitted equivalent circuit is enclosed in Fig. 6(a). The solution resistance Rs is almost similar to all samples due to similar electrolyte conditions. The charge transfer resistance Rct was obtained as 74 **Ω**, 240 **Ω** and 460 **Ω** of CM-0.4, CM-0.2 and pristine Co3O4 respectively. The results also

validate that the Rct of nanocomposite based electrocatalyst is lower than pristine electrocatalyst which facilitates the movement of charge in between anode and cathode via electrolyte.

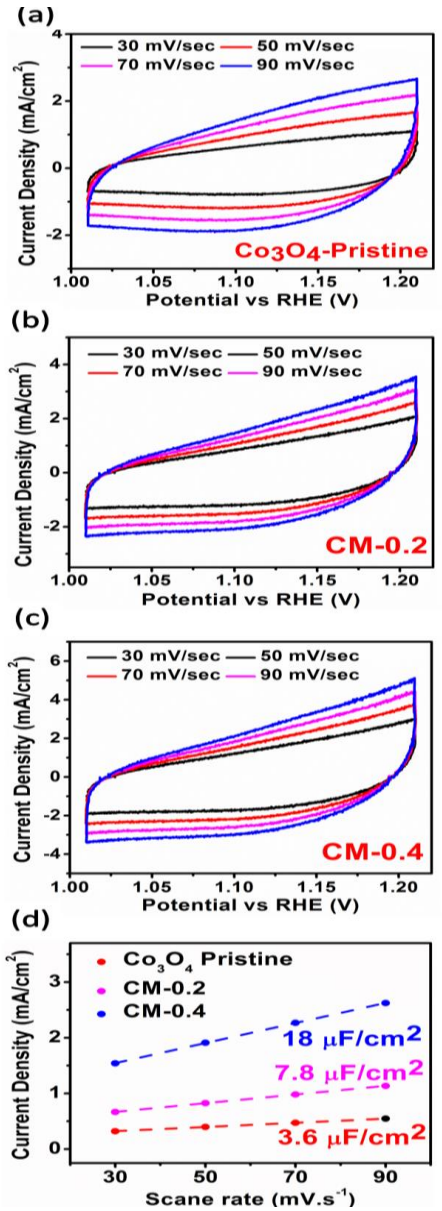

Fig. 5. Cyclic voltammetry of various electrocatalysts (a) Pristine Co_3O_4 (b) CM-0.2 (c) CM-0.4 (d) Double layer capacitance (C_{dl}) plot.

The bode-1 plot gives the information about gain parameter and phase angle in the range of 0.1Hz to 100kHz frequency at 1.45V applied potential. The phase angles obtained as pristine Co3O4 (50.123o), CM-0.2 (45.537o) and CM-0.4 (31.289o) that confirm the superior activity of CM-0.4 electrocatalyst. Furthermore, the bode-2 plot provides the knowledge about maximum oscillation frequency of catalyst. It was noticed that CM-0.4 contained least oscillation frequency as compared to other two catalyst. Therefore, better adsorption of reactive species on the surface of electrocatalysts is attributed due to greater electron recombination lifetime. From these outcomes, it is suggested that CM-0.4 electrocatalyst can be potential candidate for superior water oxidation reaction.

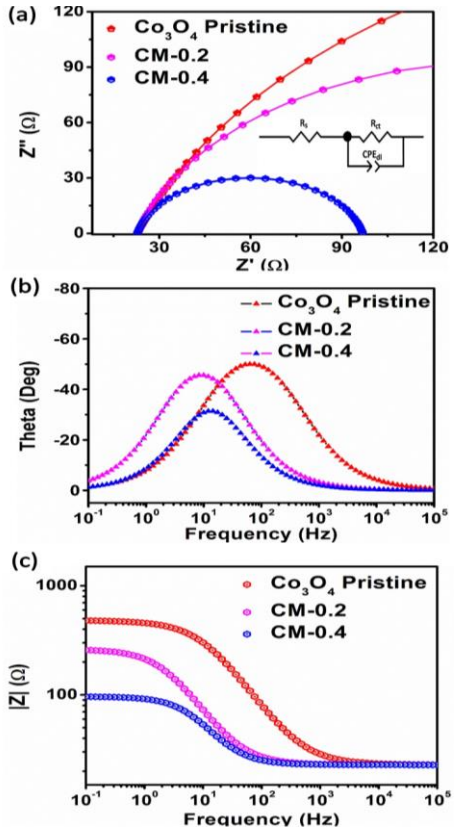

Fig. 6. Electrochemical impedance spectroscopy data of pristine Co_3O_4, CM-0.2 and CM-0.4 (a) Nyquist plot (b) Bode plot-1 and (c) Bode plot-2

TABLE I. XRD STRUCTURAL FEATURES OF PRISTINE AND COMPOSITE SAMPLES.

Sample IDs	**(hkl)**	**2 Theta**	**d spacing**	**Lattice Constant**	**FWHM**	**Crystallite Size (D)**
		Degree	**Å**	**Å**	**Degree**	**Å**
Co_3O_4 Pristine	(311)	36.4617	2.4622	8.4118	0.28356	294.96
CM-0.2	(311)	36.470	2.4617	8.4051	0.30115	277.74
CM-0.4	(311)	36.658	2.4495	8.3821	0.60382	138.59

TABLE II. SUMMARY OF UNIQUE FEATURES OF PRESENTED OER CATALYSTS

Catalyst	**Calculated from LSV**	**Calculated from EIS**		**Calculated from CV**	
	Tafel Slope	**Charge Transfer Resistance**	**Double Layer Capacitance**	**Double Layer Capacitance**	**Electrochemically active surface area**
	B	***R_{ct}***	***CPE_{dl}***	***C_{dl}***	***ECSA***
	mV/dec	**Ω**	***Mf***	***(μF/cm²)***	***cm²***
Co_3O_4 Pristine	102	460	0.04	3.6	90
CM-0.2	86	240	0.31	7.8	195
CM-0.4	72	74	0.37	18	450

TABLE III. COMPARISON OF CM-0.4 COMPOSITE AS OER CATALYST WITH RECENTLY REPORTED ELECTROCATALYSTS.

Electrocatalyst	**Electrolyte**	**Current Density**	**Overpotential**	**References**
MnO_2@Co_3O_4 (CM-0.4)	1 M KOH	20 mA/cm^2	310 mV	This work
Mg/Co_3O_4	1 M KOH	20 mA/cm^2	320 mV	[31]
Fe_3O_4/Co_3O_4	1 M KOH	10 mA/cm^2	370 mV	[13]
$CoSe_4$	1 M KOH	10 mA/cm^2	320 mV	[32]
Mn-Co Phosphide	1 M KOH	10 mA/cm^2	330 mV	[33]
$NiCo_2S_4$/RGO	1 M KOH	10 mA/cm^2	366 mV	[34]
CoOx-N-C/TiO_2C	1 M KOH	10 mA/cm^2	350 mV	[35]

4. Conclusion

The summery of present work involves the MnO2@Co3O4 nanocomposite based electrocatalysts which have been synthesized by aqueous chemical method. The XRD pattern and FTIR spectrum validate the synthesis of pristine Co3O4 and CM-nanocomposite. The CM-0.4 catalyst having morphology of nano flakes in the matrix of nano needles exhibits lowest overpotential of 310 mV at current density of 20 mA/cm2. It also contains low Tafel slope value and Rct value as 72 mv/dec and 74 Ω respectively. This electrocatalyst has expressed higher ECSA of 450 cm2. In addition, it is stable and long-term durable for 40 h that makes it superior for OER activity.

DATA AVAILABILITY STATEMENT

It is stated that this data is soul property of authors and not taken from any data base. The authors also declare that this data is not published in any other journal.

AUTHOR CONTRIBUTION

All authors equally contribute for this work

CONFLICT OF INTEREST

The authors declare no conflict of interest.

ACKNOWLEDGMENT

This research work was accomplished in Department of Metallurgy and Materials Engineering and Advanced Research Laboratory, MUET, Jamshoro, Sindh, Pakistan.

REFERENCES

[1] U. Aftab, A. Tahira, R. Mazzaro, M. I. Abro, M. M. Baloch, M. Willander, et al., "The chemically reduced CuO–Co3O4 composite as a highly efficient electrocatalyst for oxygen evolution reaction in alkaline media," Catalysis Science & Technology, vol. 9, pp. 6274-6284, 2019.

[2] A. Mehboob, S. R. Gilani, A. Anwar, A. Sadiqa, S. Akbar, and J. Patujo, "Nanoscale cobalt-oxide electrocatalyst for efficient oxygen evolution reactions in alkaline electrolyte," Journal of Applied Electrochemistry, vol. 51, pp. 691-702, 2021.

[3] P. F. Liu, H. Yin, H. Q. Fu, M. Y. Zu, H. G. Yang, and H. Zhao, "Activation strategies of water-splitting electrocatalysts," Journal of Materials Chemistry A, vol. 8, pp. 10096-10129, 2020.

[4] A. Tahira, U. Aftab, M. Y. Solangi, A. Gradone, V. Morandi, S. S. Medany, et al., "Facile deposition of palladium oxide (PdO) nanoparticles on CoNi2S4 microstructures towards enhanced oxygen evolution reaction," Nanotechnology, 2022.

[5] Z. H. Ibupoto, A. Tahira, A. A. Shah, U. Aftab, M. Y. Solangi, J. A. Leghari, et al., "NiCo2O4 nanostructures loaded onto pencil graphite rod: An advanced composite material for oxygen evolution reaction," International Journal of Hydrogen Energy, vol. 47, pp. 6650-6665, 2022.

[6] A. Q. Mugheri, A. Tahira, U. Aftab, A. L. Bhatti, R. Lal, M. A. Bhatti, et al., "Chemically Coupled Cobalt Oxide Nanosheets Decorated onto the Surface of Multiwall Carbon Nanotubes for Favorable Oxygen Evolution Reaction," Journal of Nanoscience and Nanotechnology, vol. 21, pp. 2660-2667, 2021.

[7] B. Paul, P. Bhanja, S. Sharma, Y. Yamauchi, Z. A. Alothman, Z.-L. Wang, et al., "Morphologically controlled cobalt oxide nanoparticles for efficient oxygen evolution reaction," Journal of Colloid and Interface Science, vol. 582, pp. 322-332, 2021.

[8] C. L. I. Flores and M. D. L. Balela, "Electrocatalytic oxygen evolution reaction of hierarchical micro/nanostructured mixed transition cobalt oxide in alkaline medium," Journal of Solid State Electrochemistry, vol. 24, pp. 891-904, 2020.

[9] W. H. L. P. D. Jaekyung Yia, Chang Hyuck Choi (Ph.D.), Yuri Lee (Ph.D.), Kyung Su Park (Ph.D.), Byoung Koun Min (Ph.D.), Yun Jeong Hwang (Ph.D.), Hyung-Suk Oh (Ph.D., "Effect of Pt introduced on Ru-based electrocatalyst for oxygen evolution activity and stability," Electrochemistry Communications, vol. 104, p. 106469, 2019.

[10] Q. Shi, C. Zhu, D. Du, and Y. Lin, "Robust noble metal-based electrocatalysts for oxygen evolution reaction," Chem Soc Rev, vol. 48, pp. 3181-3192, 2019.

[11] D. Zhao, Z. Zhuang, X. Cao, C. Zhang, Q. Peng, C. Chen, et al., "Atomic site electrocatalysts for water splitting, oxygen reduction and selective oxidation," Chemical Society Reviews, vol. 49, pp. 2215-2264, 2020.

[12] A. Tahira, Electrochemical water splitting based on metal oxide composite nanostructures vol. 2066. Linköping: Linköping University Electronic Press, 2020.

[13] A. L. Bhatti, U. Aftab, A. Tahira, M. I. Abro, R. H. Mari, M. K. Samoon, et al., "An Efficient and Functional Fe3O4/Co3O4 Composite for Oxygen Evolution Reaction," Journal of Nanoscience and Nanotechnology, vol. 21, pp. 2675-2680, 2021.

[14] A. Hanan, A. J. Laghari, M. Y. Solangi, U. Aftab, M. I. Abro, D. Cao, et al., "CdO/Co3O4

Nanocomposite as an Efficient Electrocatalyst for Oxygen Evolution Reaction in Alkaline Media," International Journal of Engineering Science Technologies, vol. 6, pp. 1-10, 2022.

[15] Y. V. Kaneti, Y. Guo, N. L. W. Septiani, M. Iqbal, X. Jiang, T. Takei, et al., "Self-templated fabrication of hierarchical hollow manganese-cobalt phosphide yolk-shell spheres for enhanced oxygen evolution reaction," Chemical Engineering Journal, vol. 405, p. 126580, 2021.

[16] I. M. Abdullahi, J. Masud, P.-C. Ioannou, E. Ferentinos, P. Kyritsis, and M. Nath, "A Molecular Tetrahedral Cobalt–Seleno-Based Complex as an Efficient Electrocatalyst for Water Splitting," Molecules, vol. 26, p. 945, 2021.

[17] A. L. Bhatti, U. Aftab, A. Tahira, M. I. Abro, M. Kashif samoon, M. H. Aghem, et al., "Facile doping of nickel into Co3O4 nanostructures to make them efficient for catalyzing the oxygen evolution reaction," RSC Advances, vol. 10, pp. 12962-12969, 2020.

[18] C. Linder, S. G. Rao, A. le Febvrier, G. Greczynski, R. Sjövall, S. Munktell, et al., "Cobalt thin films as water-recombination electrocatalysts," Surface and Coatings Technology, vol. 404, p. 126643, 2020.

[19] A. Badreldin, A. E. Abusrafa, Abdel, and A. Wahab, "Oxygen-Deficient Cobalt-Based Oxides for Electrocatalytic Water Splitting," ChemSusChem, vol. 14, pp. 10-32, 2021.

[20] A. Badruzzaman, A. Yuda, A. Ashok, and A. Kumar, "Recent advances in cobalt based heterogeneous catalysts for oxygen evolution reaction," Inorganica Chimica Acta, vol. 511, p. 119854, 2020.

[21] M. R. S. A. Janjua, "Synthesis of Co3O4 Nano Aggregates by Co-precipitation Method and its Catalytic and Fuel Additive Applications," Open Chemistry, vol. 17, pp. 865-873, 2019.

[22] D. D. M. Prabaharan, K. Sadaiyandi, M. Mahendran, and S. Sagadevan, "Precipitation method and characterization of cobalt oxide nanoparticles," Applied Physics A, vol. 123, 2017.

[23] M. Y. Solangi, U. Aftab, A. Tahira, M. I. Abro, R. Mazarro, V. Morandi, et al., "An efficient palladium oxide nanoparticles@Co3O4 nanocomposite with low chemisorbed species for enhanced oxygen evolution reaction," International Journal of Hydrogen Energy, vol. 47, pp. 3834-3845, 2022.

[24] L. Abdelhak, B. Amar, B. Bedhiaf, D. Cherifa, and B. Hadj, "Characterization of Mn-Doped Co3O4 Thin Films Prepared by Sol Gel-Based Dip-Coating Process," High Temperature Materials and Processes, vol. 38, pp. 237-247, 2019.

[25] N. Manjula, M. Pugalenthi, V. S. Nagarethinam, K. Usharani, and A. R. Balu, "Effect of doping concentration on the structural, morphological, optical and electrical properties of Mn-doped CdO thin films," Materials Science-Poland, vol. 33, pp. 774-781, 2015.

[26] T. Athar, A. Hakeem, N. Topnani, and A. Hashmi, "Wet Synthesis of Monodisperse Cobalt Oxide Nanoparticles," ISRN Materials Science, vol. 2012, pp. 1-5, 2012.

[27] A. N. Naveen and S. Selladurai, "Investigation on physiochemical properties of Mn substituted spinel cobalt oxide for supercapacitor applications," Electrochimica Acta, vol. 125, pp. 404-414, 2014.

[28] U. Aftab, A. Tahira, R. Mazzaro, V. Morandi, M. I. Abro, M. M. Baloch, et al., "Facile NiCo2S4/C nanocomposite: an efficient material for water oxidation," Tungsten, vol. 2, pp. 403-410, 2020.

[29] A. Q. Mugheri, A. Tahira, U. Aftab, M. I. Abro, A. B. Mallah, G. Z. Memon, et al., "An advanced and efficient Co3O4/C nanocomposite for the oxygen evolution reaction in alkaline media," RSC Advances, vol. 9, pp. 34136-34143, 2019.

[30] A. Tahira, Z. H. Ibupoto, M. Vagin, U. Aftab, M. I. Abro, M. Willander, et al., "An efficient bifunctional electrocatalyst based on a nickel iron layered double hydroxide functionalized Co3O4 core shell structure in alkaline media," Catalysis Science & Technology, vol. 9, pp. 2879-2887, 2019.

[31] A. H. Samo, U. Aftab, M. Yameen, A. J. Laghari, M. Ahmed, M. N. Lakhan, et al., "MAGNESIUM DOPED COBALT-OXIDE COMPOSITE FOR ACTIVE OXYGEN EVOLUTION REACTION," Journal of Applied and Emerging Sciences, vol. 02, pp. 210-216, 2021

[32] I. M. Abdullahi, J. Masud, P.-C. Ioannou, E. Ferentinos, P. Kyritsis, and M. Nath, "A Molecular Tetrahedral Cobalt–Seleno-Based Complex as an Efficient Electrocatalyst for Water Splitting," Molecules, vol. 26, p. 945, 2021.

[33] Y. V. Kaneti, Y. Guo, N. L. W. Septiani, M. Iqbal, X. Jiang, T. Takei, et al., "Self-templated fabrication of hierarchical hollow manganese-cobalt phosphide yolk-shell spheres for enhanced oxygen evolution reaction," Chemical Engineering Journal, vol. 405, p. 126580, 2021.

[34] C. Shuai, Z. Mo, X. Niu, X. Yang, G. Liu, J. Wang, et al., "Hierarchical NiCo2S4 nanosheets grown on graphene to catalyze the oxygen evolution reaction," Journal of Materials Science, vol. 55, pp. 1627-1636, 2020.

[35] L. He, J. Liu, B. Hu, Y. Liu, B. Cui, D. Peng, et al., "Cobalt oxide doped with titanium dioxide and embedded with carbon nanotubes and graphene-like nanosheets for efficient trifunctional electrocatalyst of hydrogen evolution, oxygen reduction, and oxygen evolution reaction," Journal of Power Sources, vol. 414, pp. 333-344, 2019.

Vol. 5, No. 1 | January – June 2022

Assessment of Rice Residues as Potential Energy Source in Pakistan

Tarique Ahmed Memon[1,2], Mujeeb I. Soomro[3], Khanji Harijan[4], Sajjad Bhangwar[5] Sabab Ali Shah[6]

Abstract:

Pakistan produces a huge amount of biomass wastes such as rice straw (RS) and rice husk (RH), wheat straw (WS), and other biomass wastes that are being burned in the field after crop harvest to prepare the land for the next crop. Biomass is known as a potential energy source that can be effectively utilized as an alternative to fossil fuels. This study aims to assess the energy potential and gaseous pollutant emissions from rice residues such as RS and RH. The Energy potential of crop residues in Pakistan was estimated by considering the residual characteristics such as residue to crop product ratio, moisture level and lower heating value of dry biomass obtained from the South Asian countries. The mathematical models were defined for the assessment of amount of residues, available energy potential, and emissions of gaseous pollutants. The estimated amount of rice residues found to be 10147.65 thousand tons of dry biomass. The theoretical and available energy potential of the rice residues were estimated as 159219 TJ, and 100,431 TJ, respectively. Based on dry matter fraction and proportion of crop residue burnt, the total amount of crop residue burnt for RS and RH were 1356.38 thousand tons and 307.7 thousand tons respectively. Total emissions from burning of rice residues were estimated as 1749.59, 27.639, 2.432, 1.265, 4.997, and 0.549 Gg for CO_2, CO, NO, NO_2, NOx, and SO_2, respectively. It was concluded that the crop residues generated in Pakistan can be effectively utilized as an alternative energy source, to reduce electricity demand supply gap, reliance on fossils fuels, and lower contribution to global warming.

Keywords: *Rice Husk; Rice Straw; Energy Potential; Pollutant emissions; Crop residues*.

1 Introduction

Pakistan is currently facing confronting industrial and economic challenges since couple of decades due to various factors such as energy crisis, rapid rising population, changing lifestyle of people [1][2]. Among them, the energy crisis are caused by poor planning and mismanagement of energy sector in terms of poor market instruments, inefficient energy mix and higher transmission and distribution losses which has ultimately caused reduced employment and production of industries, and increased electricity prices [3].

[1]Department of Mechanical Engineering, Quaid-e-Awam University of Engineering, Science, and Technology (QUEST) Campus Larkana, Sindh, Pakistan.

[2]Department of Engineering Mechanics, Zhejiang University, China 310058

[3]Department of Mechanical Engineering, Mehran University of Engineering and Technology (MUET) SZAB Campus Khairpur Mirs, Sindh, Pakistan.

[4]Department of Mechanical Engineering, Mehran University of Engineering and Technology Sindh Pakistan

[5]Department of Mechanical Engineering, Quaid-e-Awam University of Engineering, Science & Technology Pakistan.

[6]Department of Department of Civil and Environmental Engineering, Hanyang University, Seoul 04763, S. Korea.

Corresponding Author: tariquememon@quest.edu.pk

The electricity is mainly produced from conventional thermal resources sharing 58.4% followed by hydro 31%, nuclear 2.8 %, and other renewable sources 2.4% [4].

The thermal energy sources for electricity generation cannot be relied as primary energy sources due to their high prices and adverse environmental impacts [5].

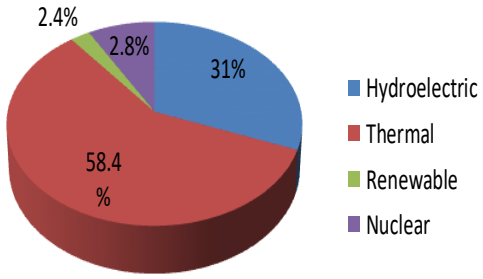

Fig. 1. Sources contribution in Electricity Generation [4]

Utilization of fossil fuels for electricity generation has resulted greenhouse gases (GHGs) emissions into the environment [6]. The major emissions are sulphur oxides (SOx), sulphur dioxide (SO_2), and nitrogen oxides (NOx), carbon dioxide (CO_2), carbon mono oxide (CO) and particulate matters (PM) [7][8]. The overall emissions in Pakistan are estimated to increase in future from 557 Million tons CO_2 equivalent (Mt CO_2-eq) in 2020 to 4621 Mt CO_2-eq in 2050 as shown in Fig. 2 [9]. The trend of utilizing biomass as a potential source has been increasing throughout the world because of certain advantages such as abundant availability, lower environmental impacts through modern biomass conversion technologies, increased energy security and supply, development of rural areas and job opportunities. Biomass is more economical in comparison with other renewable energy sources because of less capital and investment cost per unit of production [10]. Pakistan is still inefficient to implement advanced technologies for efficient utilization of alternative renewable energy resources. However, some of the renewable energy projects are installed such as biomass [11], Solar [12], Wind [13]. The different energy sources and their conversion routes are presented in the Fig. 2 [14].

Pakistan is an agrarian country in which the contribution of agriculture sector in country's Gross Domestic Product (GDP) is 21%. The major crops are rice, sugarcane, wheat, cotton, and maize producing waste in the form of straw and husk, bagasse, wheat straw (WS), cotton straw and corn stover respectively [4].

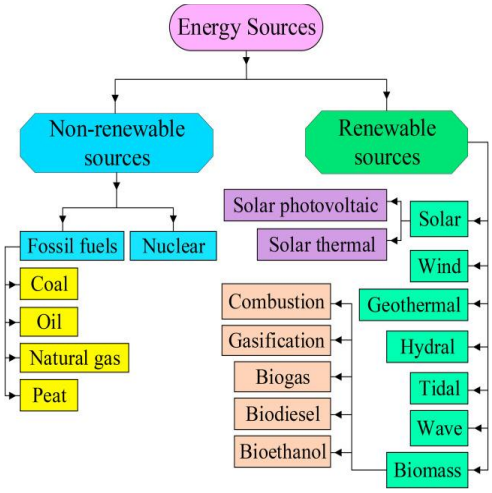

Fig. 2. Classification of energy resources [14]

Pakistan is an agrarian country in which the contribution of agriculture sector in country's Gross Domestic Product (GDP) is 21%. The major crops are rice, sugarcane, wheat, cotton and maize producing waste in the form of straw and husk, bagasse, wheat straw (WS), cotton straw and corn stover respectively [4]. Rice is considered as one of the most commonly produced and consumed grains in the world population. It is known as prominent staple food in many countries as it is rich in proteins, lipids, carbohydrates, phytic and phenolic acids, minerals, vitamins B and E [16].

Agricultural residues are produced from harvesting and processing of crops and are categorized as primary and secondary residues. Primary residues such as RS, WS, and sugar cane tops are those residues which

are produced in the field when harvesting the crop, while secondary residues such as rice husk (RH), wheat husk (WH) and bagasse are produced at processing mills. Primary residues have lower availability because of difficulty in the collection, and farmers utilize as fertilizer, animal feed. Availability of secondary residues is comparatively high at the processing mills with little handling and transportation cost [18]. Being an agrarian country, Pakistan produces massive quantity of crop residues like stems, leaves, and seed pots that can be efficiently utilized as energy source. Huge amount of crop residues such as RS, RH, WS, sunflower stems, garden biomass wastes, dates, mangoes, and orange tree biomass are burned in the field after crop harvest every year to prepare the land for next crop [19]. The amount of crop residue directly depends upon the crop production. The amount of crop residue generated directly depends upon the yield of crop. Rice crop has two main types of residues, the field residues such as RS and the process residues such as RH and bran. RS is dry stalks of cereal plants collected at the time of harvest in the field. RH is outer most layer of rice grain and is known as process residue. Rice bran is used as cattle, poultry and fish food [20][21]. RS is used as feedstock and bedding material for livestock, domestic fuel as well as building material in rural areas [22]. The burning of crop residues is a common activity in developing countries because of unawareness of benefits related to its alternative uses as an energy source [23][24]. Crop and agricultural residues are being used as domestic fuels for heating and cooking purpose since ancient times. Almost half of the people in the world especially in developing countries are utilizing the agricultural and crop residues as a primary energy source and are known as fourth major energy source after coal, gas and oil [25]. After harvesting rice crop, the farmers usually burn residues because they believe that it has advantageous effects on crop yields [26][27]. Many studies proposed that burning rice residues have positive as well as negative effects on the soil quality. Burning increases the availability of phosphorous and potassium nutrients for short time [28]. According to [29] burning rice residues in the field enhance the crop productivity for the next crop season. Some researchers have found negative effects of residues burning such as [30] and [31], according to them burning causes loss of plant nutrients such as nitrogen, potash and sulphur and microbial population and organic carbon is reduced. On the other hand, some practices alternative to burning of crop residues such as (1) recycling of residue in the soil through incorporation, surface retention to improve soil's physio-chemical and biological properties [32]. (2) Animal feed [36], (3) mushroom cultivation or bioenergy production [34]. (4) For cooking and lighting purpose [35]. Burning RS has many negative impacts, producing smoke, gaseous and particulate emissions (PM 10, PM 2.5, NOx, SO_2) in the atmosphere which ultimately affects health of population and climate [36][37].

Fig. 3. Open field burning of rice straw [38]

Fig. 4. Rice husk used in brick manufacturing industries [40]

RH is supplied to brick manufacturing industries where it is being burned, which causes release of CO_2 and methane into

atmosphere which takes part in greenhouse effect and poor air quality. The amount of CO_2 released from burning depends upon the amount of RH burned and its carbon fraction [39].

The burning of rice residues has also adverse environmental impacts in terms of air pollution and climate change. Incomplete combustion of agricultural residues produces emissions of toxic air pollutants and greenhouse gases, black carbon which is a second largest source of global warming contribution after carbon dioxide. It captures radiations and warms the atmosphere and ultimately enhances glacier melting [26][41][24].

RH generated in the mill is partly used for heating purposes. Surplus amount of RH is supplied to brick manufacturing industries. RH is also agricultural waste generated after paddy rice milling. It is often used as fuel for green technology. RH is used in boilers to produce steams, in brick kilns to fire clay bricks, in boilers for rice processing industry, where RH have gone through self-burning process [42].

Limited studies have been conducted in Pakistan for the estimation of rice residues without taken into account the variation of residual characteristics such as residue to crop product ratio, lower heating values, availability factor and relative moisture content.

There have been many studies related to the utilization of rice residues as energy source. [1] Estimated that 17.86 million tons of RS from the rice crop are produced. [43] concluded that RH based electricity generation is more economically and environmentally viable compared to coal-based electricity generation. [44] estimated that RS and husk generated in the Punjab province of India contributed 33.43% of total residue potential. [45] have estimated that Bangladesh produces enormous amount of rice residues such as RS and husk. The available energy potential from rice residues was estimated to be 425.324 PJ during the year 2015-16. [39] estimated that annually 1328 GWh electricity can be generated from the available quantity of RH in Pakistan and 36,042 tons of CO_2 equivalent (tCO_2-eq) per year of methane can be avoided by utilizing RH instead of conventional fossil fuels. [46] have studied biomass residues as potential energy source of electricity generation in Punjab province of Pakistan. It is concluded that lot of potential is available to generate electricity of 1700 MW. [47] studied that the open field burning of RS release CO_2 and methane which contributes global warming. They have concluded that RS can be utilized for electricity generation through efficient conversion technologies. [48] have estimated that total residue potential from arable field crops and horticulture crops were 59.432 million tons, and 15.652 million tons, respectively. The available energy potential from arable field crops was 298,955 TJ and from horticultural crops was 65,491 TJ. [49] studied the resource potential of agricultural and animals waste for the generation of electricity and greenhouse gases mitigation potential. It was estimated that annual potential of 62,808 GWh from the total waste can be generated which accounts 27% of the total electricity consumption in the country. Moreover, the mitigation of greenhouse gases emissions from the biomass wasted based electricity generation were about 4,096 thousand t CO_2 per year. [50] studied agricultural crop residues as renewable energy source in Pakistan. A model based on MATLAB was developed to estimate the existing and future accessibility of the selected biomass residues as an energy source. They have estimated that 11000 MW electricity can be produced from the selected crop residues. Forecast shows that the plant capacity can be increased up to 16,000 MW by the year 2035. [51] studied the availability of RH for the generation of electricity in Bangladesh. They have proposed that RH is a viable option for the electricity generation in the country. [52] conducted experimental work on the open field burning of RS. They have found that the percentage of CO_2, CO, and NOx to the total emissions were 15.3%, 13.9%, and 31.4% respectively.

The purpose of this study was to assess the potential of rice residues as an energy source

and to estimate the gaseous pollutant emissions like CO, CO_2, NO, NO_2, NOx, and SO_2 caused by open field burning of rice residues. In this study we have estimated the potential of rice residues as dry mass, theoretical and available energy potential by taking into account the residual characteristics from the previous studies conducted in South Asian countries such as Pakistan, India, Bangladesh, Sri Lanka, and Afghanistan and limit values have been estimated.

2 Methodology

In order to estimate the residue potential, the first stage is to get primary input data relevant to rice crop production for the estimation of amount of available residue and energy potential from the crop residues. In the next step, biomass crop residues such as RS and RH is estimated from the annual crop production by considering residue to crop product ratio (RPR) and moisture level (M).

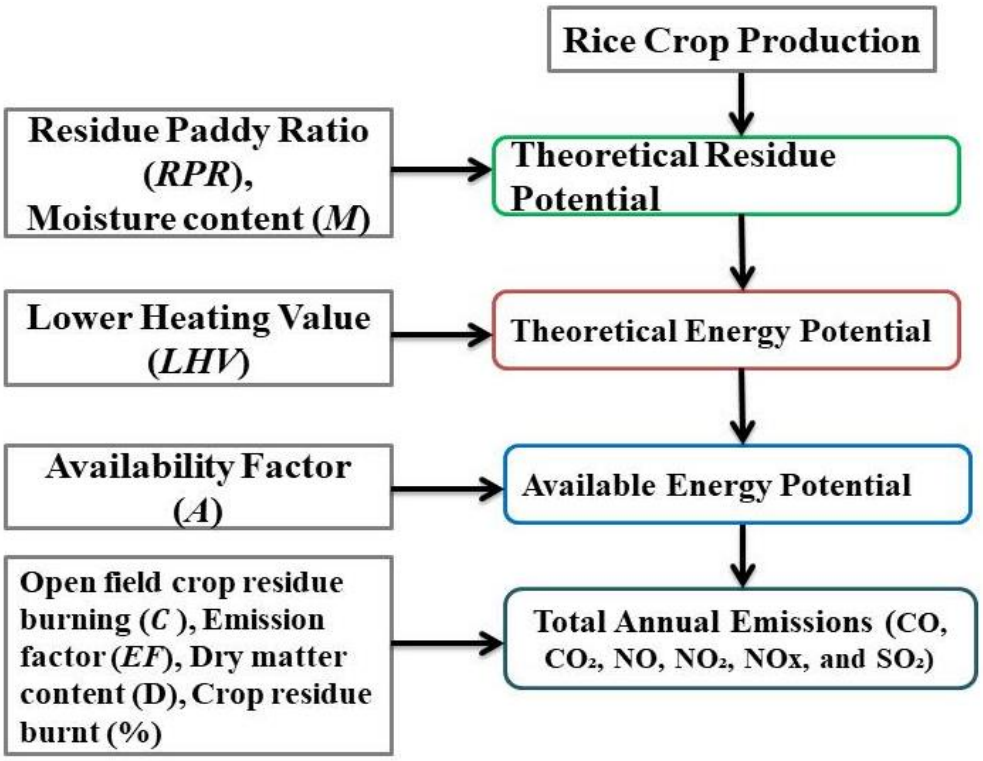

Fig. 5. Flow diagram for assessing the energy and emissions reduction potential from rice residues

The energy potential from the crop residue can be estimated by considering energy content value and availability factor of the particular residue. The amount of emissions from open field burning of residues is estimated by considering open field burning of the particular residue, emissions factors of particular gaseous pollutants and dry matter content. The methodology flow diagram is presented in the Fig. 5.

2.1 Rice Crop Production

According to Pakistan Economic Survey Report 2020, rice crop area was increased by 8% to 3.034 million hectares during 2019-20, therefore, the production increased by 2.9% to

7.410 million tons compared to previous year 2018-19. Paddy rice production data in Pakistan from 2012-13 to 2019-20 is taken from Pakistan Economic survey reports [4][54] and is presented in Table 1.

TABLE I. PADDY RICE PRODUCTION IN PAKISTAN [4]

Year	Potential of Paddy (Thousand Tons)
2012-13	5536
2013-14	6798
2014-15	7003
2015-16	6801
2016-17	6849
2017-18	7450
2018-19	7202
2019-20	7410
Average	**6881**

For the estimation of energy potential and gaseous pollutant emissions, the average value of the crop production was 6881 thousand tons which is considered as input data in order to reduce the yearly crop yield fluctuations.

2.2 Characterization of Rice Crop Residues

The evaluation of biomass characteristics is an important step for the assessment of energy potential through the conversion process prior to it utilization. The properties of biomass change rapidly with certain factors such as climatic conditions and seasonal variations which affect the thermal decomposition behavior, the product yield and quality [55]. Literature shows that there is considerable difference in characteristics and quantity of the crop residues depends upon many factors such as local climate conditions, difference in agricultural practices, crop production, crop type and varies from region to region [46][48][50][56]. Hence, the residual characteristics of biomass vary region to region. In this study, residual characteristics like residue crop production ratio (RPR), moisture level (M) and lower heating value (LHV) of dry biomass residues were taken into account from different studies in South Asian countries such as Pakistan, India, Bangladesh, Sri Lanka, and Afghanistan. The average values of residual properties were considered in order to reduce fluctuations in the data and results. The energy potential of rice residues was estimated by considering RPR, M, and LHV of dry matter of residues.

Moisture level plays a pivotal role in selection of biomass to energy conversion process [57]. M content indicates the presence of water in biomass and is an important factor for conversion of biomass feedstock to energy. High M decreases the heating value of the feedstock due to mass of water [19]. Therefore, the energy intensive drying process is required to reduce the M according to the conversion technology [58]. Residual characteristics values of rice straw and husk are presented in Table 3 and 4 respectively. It can be observed in the Table 3 and 4 that amount of residues generated from the crop production varies from region to region. For example, from Table 3, residue to crop ratio of RS ranges from 1 to 1.76 in different countries. The RPR of rice straw in Pakistan was given as 1. 1.5, 1.54, and 1.757. but these values were different for Bangladesh as 1.695 and 1.76. for India and Afghansitan it was close to Pakistan that is 1.5, for Sri Lanka it was 1.76. moisture content values of rice straw in these countries were near to each other and varies from 7.43 to 12.7%. however lower heating values of moisture varied from 12.81 to 18.74 MJ/kg. there were, 13.8, 17, and 18.74 MJ/kg for Pakistan. For India it was 15.03 and 15.54 MJ/kg, for Afghanistan it was 12.81 MJ/kg, for Sri Lanka, it was 16 MJ/kg, and for Bangladesh it was 16.3 MJ/kg.

TABLE II. ELEMENTAL ANALYSIS OF RICE RESIDUES [39][56]

Composition (%)	Rice straw (RS)	Rice husk (RH)
Carbon	28.55	44.13
Hydrogen	3.98	5.01
Nitrogen	1.15	0.39
Sulphur	0.61	0.07
Oxygen	65.71	50.40

TABLE III. CHARACTERISTICS OF RICE STRAW

Characteristics	Rice Straw	Country Reference
Residue Crop Ratio, (*RPR*)	(1-1.76)	Pakistan-[18][50] [46][59][60][61] India-[62][44][22] Afghanistan- [20] [63]. Sri Lanka-[64] Bangladesh-[21] [45][65].
Lower Heating Value, (*LHV*) (MJ/kg)	(12.81-18.74)	Pakistan-[50] [46] [60] [56]. India- [66] [62][44]. Afghanistan-[20]. Sri Lanka-[64]. Bangladesh- [21] [45].
Moisture content, (*M*) (%)	(7.43-12.7)	Pakistan-[59] [56]. Afghanistan-[20]. Sri Lanka-[64]. Bangladesh-[21]. India-[66].

2.3 Theoretical Residues Potential

Theoretical rice residues (RH and RS) potential indicates the amount of residue j generated per year from the rice crop production. The amount of residues generated depends upon annual crop production, ratio of residue to crop product (RPR), and moisture level (M). Theoretical amount of residue j is estimated from the equation (1) by taking relevant data from Table 3, and 4.

$$TRP_j = Cp \times RPR_j \times [\frac{100-Mj}{100}] \qquad (1)$$

Where, Cp is the annual amount of the crop production in thousand tons, RPR is the residue j to crop production ratio. Thus, RPR=1 indicates that, 1 ton of the crop residue is produced from the 1 tons of crop production. M indicates the relative moisture content (%) of residue j.

Amount of residue generated depends upon the crop varieties, environmental factors region and agricultural practices of the concerned region. For example, RPR becomes 1.75 when the rice crop is harvested at 5cm above the ground level. RPR could decrease to 0.45, if the crop is cut by more than 5 cm above the ground [28][44]. The eight years average data related to the rice crop production from 2012-13 to 2019-20 is taken from Pakistan Economic Survey reports in 2018-19 and 2019-20 in order to reduce crop yield fluctuations per year.

TABLE IV. CHARACTERISTICS OF RICE HUSK

Characteristics	Rice Husk	Country Reference
Residue Crop Ratio, (*RPR*)	(0.20-0.321)	Pakistan- [18][50] [46][59][60][61][39] India-[62][44][22] Afghanistan-[20][63]. Sri Lanka-[64] Bangladesh-[21][45] [65].
Lower Heating Value, (*LHV*) (MJ/kg)	(13.48-17)	Pakistan-[50] [46] [60] [56]. India-[66] [62] [44]. Afghanistan-[20]. Sri Lanka-[64]. Bangladesh- [45].
Moisture content, (*M*) (%)	(7.88-12.4)	Pakistan-[59] [56] [39]. Afghanistan-[20]. Sri Lanka-[64]. Bangladesh-[21]. India-[66].

2.4 Theoretical Energy Potential

The theoretical or ideal energy potential represents the total amount of energy potential from the generated dry biomass residues and can be estimated by the following equation (2).

$$TEP_j = TRP_j \times LHV_j \qquad (2)$$

Where, LHV indicates lower heating value (MJ/kg) of particular residue j

2.5 Available Energy Potential

The available energy potential indicates the amount of energy that can be technically and economically generated from the crop

residues. Its value depends upon certain factors such as collection mechanism, characteristics of biomass and the conversion technology [44]. The theoretical energy potential is constraints by alternative uses of crop residues and agricultural practices of particular region [44]. Therefore, availability factor is incorporated in the following equation to estimate the available energy potential from the crop residues.

$$AEP_j = TEP_j \times A_j \quad (3)$$

Where A is the availability of the residue j, which is 0.6 for RS and 0.8 for RH [45].

TABLE V. RESIDUE PRODUCT RATIO, LHV, AND MOISTURE, OF RICE CROP RESIDUES.

	Rice Straw		Rice Husk	
	Range	Mean	Range	Mean
RPR	1-1.76	1.38	0.20-0.321	0.26
M (%)	7.43-12.7	10.065	7.88-12.4	10.14
LHV) (MJ/kg)	12.81-18.74	15.775	13.48-17	15.24

2.6 Estimation of total annual gases Emissions

In order investigate/estimate the amount of gaseous emissions such as (CO, CO_2, NO, NO_2, NOx, and SO_2) caused by open field burning of rice RS and RH. The total amount of gaseous pollutant emissions can be estimated by the following Eq. (4).

$$E_{i,j} = C_j \times EF_{i,j} \quad (4)$$

Where, E is total annual emissions (Gg) from the pollutant i emitted from the crop residue j. EF is the specific emission factor (g/kg) of pollutant i from burning of the residue j, and C is the total amount (kg) of burnt crop residue j.

2.6.1 Estimation of crop residues burnt

The crop residues burned in the field depends upon the amount of crop production, dry matter content, portion of the residue burned. The total amount of the crop residue burnt can be estimated by the following Eq. (5).

$$C_j = Cp \times RPR_j \times D_j \times \emptyset_j \quad (5)$$

Where, TRP is theoretical biomass potential (Thousand tons) of the residue j, $\emptyset$ is Crop residue j burnt (%) and D is dry matter content of residue j. Dry matter content for RH and straw is taken from [67] and proportion of burnt residue (%) is taken as 25% as estimated by [68].

2.6.2 Emission Factors

Emission factors are used to estimate and quantify the pollutant emissions from burning of biomass residues vary with time, space and largely depend upon type, quality and biomass fuel composition and climate and burning condition and onsite experiments such as indoor and in-field [69][24]. The mean values of emission factors of different gaseous pollutants from the open field burning of rice residues as estimated by [24] have presented in the Table 6.

TABLE VI. EMISSIONS FACTORS (EF) (G/KG) FOR GASEOUS POLLUTANTS [24].

Rice Residues	Rice Straw	Rice Husk
CO_2	1090.1	880.48
CO	17.19	14.05
NO	1.48	1.38
NO_2	0.89	0.19
NOx	3.16	2.31
SO_2	0.38	0.11

3 Results and Discussion

The theoretical crop residues potential from RS and RH, the theoretical and available energy potential and total emissions of gaseous pollutants is estimated from RS and RH.

3.1 Total Amount of Residues and Energy Potential

The mean value eight years from 2012 to 2020 of rice crop production is taken as 6881 thousand tons in order to reduce yearly crop yield fluctuations. The total amount of rice residues obtained as dry substance and is estimated as 10,147.65 thousand tons. The amount of RS produced is 8,540 thousand tons

while the amount of RH generated is 1607.65 thousand tons of dry mass. Theoretical energy potential was estimated as 159,219 TJ out of which 134,718.5 TJ was estimated from RS and 24,500.586 TJ from RH.

The limit values of rice crop residues characteristics were considered, and maximum, minimum and average potential values were estimated as presented in Table 5. The residual properties of rice residues (residue crop ratio, lower heating value, and relative moisture content) values vary among the countries as shown in Table 3 and 4. Therefore, the estimated potential values from crop residues change within the limits. The location of the crop and its characteristics such as crop production and agricultural practices also affect the quantity of residues generated. As shown in Fig. 6, when estimating the energy potential of RS, the energy potential of 81,600 TJ was obtained when the minimum values of properties such as ratio of residue to product, moisture level, and lower heating values were taken. Similarly, energy values of 134,718.5 TJ and 198,129 TJ from RS were obtained when average and maximum limit values were considered respectively.

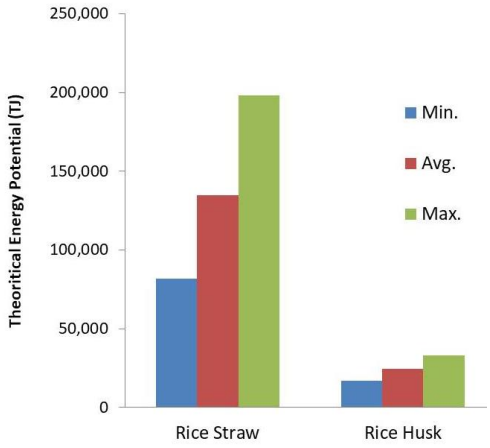

Fig. 6. Comparison of TEP of rice residues

Fig. 7 shows total theoretical and available estimated potential from the crop residues in Pakistan. Potential values were estimated as minimum, maximum and average of residual characteristics. The total theoretical energy potential of the rice residues obtained from the rice crop production has minimum 98,692.64 TJ, an average 159,219 TJ, and maximum of 231,024 TJ. While the total available energy potential obtained from the rice residues were estimated as minimum 62,634 TJ, an average 100,431 TJ, and maximum value of 145,193 TJ.

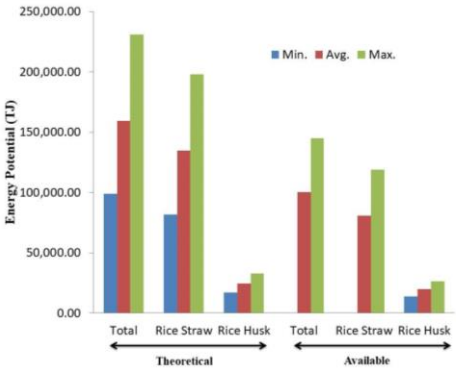

Fig. 7. Total Theoretical and Available Energy Potential of Rice residues

3.2 Estimation of gaseous Emissions

The amount of gaseous pollutants such as CO, CO_2, NO, NO_2, NOx, and SO_2 emissions (Gg) from the rice residues open field burning are estimated by considering the proportion of residue burn, dry matter content, and specific emission factors of gaseous pollutants. Based on dry matter fraction and proportion of burnt crop residue, the total amount of burnt crop residue for RS and RH was 2017.85 thousand tons and 380 thousand tons respectively as presented in the Table 7. The amount of crop residue such as RS burnt is more than the RH. Because the yield value of RS is more.

TABLE VII. AMOUNT OF BURNT RESIDUES IN PAKISTAN

Rice Residues	Rice Straw	Rice Husk
RPR	1.38	0.26
Amount of Crop residue (Th. Tons)	9495.78	1789
Dry matter content [70]	0.85	0.85

Crop residue/dry matter burnt (%) [68]	25	25
Amount of Burnt Residue, C_j (Th. Tons)	2017.85	380

Total amount of pollutant emissions (Gg) from rice residues for CO_2, CO, NO_2, NO, NOx, and SO_2 are presented in Fig. 10. Total pollutant emissions from rice residues were 2534.58, 40.025, 3.51, 1.868, 7.254, and 0.808 Gg for CO_2, CO, NO, NO_2, NOx, and SO_2 respectively. Total pollutant emissions from burning of RS were 2200 Gg for CO_2, 34.686 Gg for CO, 2.986 Gg for NO, 1.796 Gg for NO_2, 6.376 Gg for NOx, and 0.766 Gg for SO_2. It can be observed from the Fig. 8 that the gaseous pollutants emissions from the burning of RS is more than the RH because of emissions factors of RS is higher than rice husk.

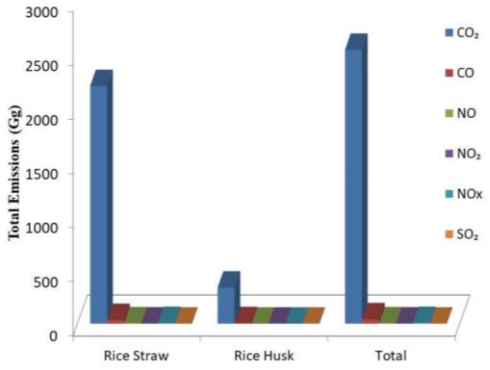

Fig. 8. Emissions from Rice straw and Rice husk

4 Conclusion

This study focuses on the exploitation of rice crop residues as an energy source and assessment of gaseous pollutants emissions caused by open field burning. The average amount of rice residues is estimated to be 10147.65 thousand tons that can be efficiently utilized to produce 159219 TJ of energy which is approximately 3803 kilo tons of oil equivalent (ktoe). If this amount of residues is properly utilized for electricity generation, 44,229 GWh can be produced annually. The available energy potential is estimated as 100,431TJ. This available energy potential is 2398.75 ktoe. If the available amount of residues is efficiently utilized for electricity generation, an annual amount of 27,897GWh electricity could be produced. Total emissions from burning of rice residues were 1749.59, 27.639, 2.432, 1.265, 4.997, and 0.549 Gg for CO_2, CO, NO, NO_2, NOx, and SO_2 respectively. Hence it is concluded that the crop residues generated in Pakistan can be effectively utilized as an alternative energy source, to reduce the demand supply gap, reduce reliance on fossil fuels and prevent environmental degradation.

5 Recommendations

There are certain issues related to utilization of crop residues as an energy source such as residues availability, agricultural practices, and unawareness about the efficient utilization of residues as alternative source of energy. Therefore, the Government of Pakistan should institute and implement proper policies and regulations among the public and private sectors to encourage renewable energy technologies by providing subsidies, incentives and reducing taxes, and creating awareness among the farmers about the utilization of crop residues as an alternative energy source.

REFERENCES

[1] M. Irfan et al., "Assessing the energy dynamics of Pakistan: Prospects of biomass energy," Energy Reports, vol. 6, pp. 80–93, 2020, doi: 10.1016/j.egyr.2019.11.161.

[2] K. R. Abbasi, M. Shahbaz, Z. Jiao, and M. Tufail, "How energy consumption, industrial growth, urbanization, and CO2 emissions affect economic growth in Pakistan? A novel dynamic ARDL simulations approach," Energy, vol. 221, p. 119793, 2021, doi: 10.1016/j.energy.2021.119793.

[3] M. O. Chaudhry, M. Z. Faridi, and S. Riaz, "Energy Crisis and Macroeconomic Stability in Pakistan.," Pakistan J. Soc. Sci., vol. 35, no. 1, pp. 425–436, 2015.

[4] G. of P. Finance Division, Pakistan Economic Survey Report 2019-20. .

[5] T. Iqbal et al., "Sketching Pakistan's energy dynamics: Prospects of biomass energy," J. Renew. Sustain. Energy, vol. 10, no. 2, 2018, doi: 10.1063/1.5010393.

[6] N. Hossain, M. A. Bhuiyan, B. K. Pramanik, S. Nizamuddin, and G. Griffin, "Waste materials for wastewater treatment and waste adsorbents for biofuel and cement supplement applications: A critical review," J. Clean. Prod., vol. 255, 2020, doi: 10.1016/j.jclepro.2020.120261.

[7] K. Harijan, M. A. Uqaili, M. Memon, and U. K. Mirza, "Forecasting the diffusion of wind power in Pakistan," Energy, vol. 36, no. 10, pp. 6068–6073, 2011, doi: 10.1016/j.energy.2011.08.009.

[8] H. Zhang et al., "A laboratory study of agricultural crop residue combustion in China: Emission factors and emission inventory," Atmos. Environ., vol. 42, no. 36, pp. 8432–8441, 2008, doi: 10.1016/j.atmosenv.2008.08.015.

[9] N. Abas, A. Kalair, N. Khan, and A. R. Kalair, "Review of GHG emissions in Pakistan compared to SAARC countries," Renew. Sustain. Energy Rev., vol. 80, no. January 2016, pp. 990–1016, 2017, doi: 10.1016/j.rser.2017.04.022.

[10] M. M. Rahman and J. V. Paatero, "A methodological approach for assessing potential of sustainable agricultural residues for electricity generation: South Asian perspective," Biomass and Bioenergy, vol. 47, no. 0, pp. 153–163, 2012, doi: 10.1016/j.biombioe.2012.09.046.

[11] N. A. Khan and H. el Dessouky, "Prospect of biodiesel in Pakistan," Renew. Sustain. Energy Rev., vol. 13, no. 6–7, pp. 1576–1583, 2009, doi: 10.1016/j.rser.2008.09.016.

[12] M. M. Rafique and H. M. S. Bahaidarah, "Thermo-economic and environmental feasibility of a solar power plant as a renewable and green source of electrification," Int. J. Green Energy, vol. 16, no. 15, pp. 1577–1590, 2019, doi: 10.1080/15435075.2019.1677237.

[13] H. Yaqoob et al., "Feasibility Study of a 50 MW wind farm project in Pakistan," J. Adv. Res. Fluid Mech. Therm. Sci., vol. 74, no. 2, pp. 27–42, 2020, doi: 10.37934/ARFMTS.74.2.2742.

[14] H. Yaqoob et al., "Case Studies in Chemical and Environmental Engineering Energy evaluation and environmental impact assessment of transportation fuels in Pakistan," Case Stud. Chem. Environ. Eng., vol. 3, no. December 2020, p. 100081, 2021, doi: 10.1016/j.cscee.2021.100081.

[15] G. of P. Finance Division, Pakistan Economic Survey 2017-18. 2019.

[16] L. A. Silva, I. F. S. dos Santos, G. de O. Machado, G. L. Tiago Filho, and R. M. Barros, "Rice husk energy production in Brazil: An economic and energy extensive analysis," J. Clean. Prod., vol. 290, p. 125188, 2020, doi: 10.1016/j.jclepro.2020.125188.

[17] K. Ahmed, S. Shahid, and N. Nawaz, "Impacts of climate variability and change on seasonal drought characteristics of Pakistan," Atmos. Res., vol. 214, no. August, pp. 364–374, 2018, doi: 10.1016/j.atmosres.2018.08.020.

[18] A. W. Bhutto, A. A. Bazmi, and G. Zahedi, "Greener energy: Issues and challenges for Pakistan - Biomass energy prospective," Renew. Sustain. Energy Rev., vol. 15, no. 6, pp. 3207–3219, 2011, doi: 10.1016/j.rser.2011.04.015.

[19] A. Abdullah et al., "Bioenergy potential and thermochemical characterization of lignocellulosic biomass residues available in Pakistan," vol. 37, no. 2, pp. 1–8, 2020, doi: 10.1007/s11814-020-0624-0.

[20] A. G. Noori, P. A. Salam, and A. M. Fazli, "Assessment of Selected Biomass Energy Potential in Afghanistan," vol. 4, no. 6, pp. 6–14, 2019.

[21] A. S. N. Huda, S. Mekhilef, and A. Ahsan, "Biomass energy in Bangladesh : Current status and prospects," Renew. Sustain. Energy Rev., vol. 30, pp. 504–517, 2014, doi: 10.1016/j.rser.2013.10.028.

[22] M. Hiloidhari and D. C. Baruah, "Rice straw residue biomass potential for decentralized electricity generation: A GIS based study in Lakhimpur district of Assam, India," Energy Sustain. Dev., vol. 15, no. 3, pp. 214–222, 2011, doi: 10.1016/j.esd.2011.05.004.

[23] R. Azhar, M. Zeeshan, and K. Fatima, "Crop residue open fi eld burning in Pakistan ; multi-year high spatial resolution emission inventory for 2000 – 2014," Atmos. Environ., vol. 208, no. September 2018, pp. 20–33, 2019, doi: 10.1016/j.atmosenv.2019.03.031.

[24] M. Irfan et al., "Estimation and characterization of gaseous pollutant emissions from agricultural crop residue combustion in industrial and household sectors of Pakistan," Atmos. Environ., vol. 84, pp. 189–197, 2014, doi: 10.1016/j.atmosenv.2013.11.046.

[25] G. CAO, X. ZHANG, S. GONG, and F. ZHENG, "Investigation on emission factors of particulate matter and gaseous pollutants from crop residue burning," J. Environ. Sci., vol. 20, no. 1, pp. 50–55, 2008, doi: 10.1016/S1001-0742(08)60007-8.

[26] T. Ahmed, B. Ahmad, and W. Ahmad, "Why do farmers burn rice residue? Examining farmers' choices in Punjab, Pakistan," Land use policy, vol. 47, pp. 448–458, 2015, doi: 10.1016/j.landusepol.2015.05.004.

[27] A. Junpen, J. Pansuk, O. Kamnoet, and P. Cheewaphongphan, "Emission of Air Pollutants from Rice Residue Open," 2018, doi: 10.3390/atmos9110449.

[28] O. Erenstein, "Crop residue mulching in tropical and semi-tropical countries: An evaluation of residue availability and other technological

implications," Soil Tillage Res., vol. 67, no. 2, pp. 115–133, 2002, doi: 10.1016/S0167-1987(02)00062-4.

[29] M. Haider, Published by the South Asian Network for Development and Environmental Economics (SANDEE) PO Box 8975, EPC 1056, Kathmandu, Nepal. Tel: 977-1-, no. 71. 2012.

[30] P. K. Gupta et al., "Residue burning in rice-wheat cropping system: Causes and implications," Curr. Sci., vol. 87, no. 12, pp. 1713–1717, 2004.

[31] B. J. Heard, C. Cavers, and G. Adrian, "Up in Smoke—- Nutrient Loss with Straw Burning," Better Crop., vol. 90, no. 3, pp. 10–11, 2006.

[32] K. G. Mandal, A. K. Misra, K. M. Hati, K. K. Bandyopadhyay, and P. K. Ghosh, "Rice residue-management options and effects on soil properties and crop productivity," vol. 2, no. January, pp. 224–231, 2004.

[33] R. Article, S. Devi, C. Gupta, S. L. Jat, and M. S. Parmar, "Crop residue recycling for economic and environmental sustainability : The case of India," pp. 486–494, 2017.

[34] C. Román-Figueroa, N. Montenegro, and M. Paneque, "Bioenergy potential from crop residue biomass in Araucania Region of Chile," Renew. Energy, vol. 102, pp. 170–177, 2017, doi: 10.1016/j.renene.2016.10.013.

[35] A. Vatsanidou, C. Kavalaris, S. Fountas, N. Katsoulas, and T. Gemtos, "A life cycle assessment of biomass production from energy crops in crop rotation using different tillage system," Sustain., vol. 12, no. 17, 2020, doi: 10.3390/SU12176978.

[36] I. Kumar, V. Bandaru, S. Yampracha, L. Sun, and B. Fungtammasan, "Limiting rice and sugarcane residue burning in Thailand: Current status, challenges and strategies," J. Environ. Manage., vol. 276, no. January, p. 111228, 2020, doi: 10.1016/j.jenvman.2020.111228.

[37] M. Z. Haider, "Determinants of rice residue burning in the field," J. Environ. Manage., vol. 128, pp. 15–21, 2013, doi: 10.1016/j.jenvman.2013.04.046.

[38] C. Menke, S. Garivait, and B. Gadde, "Air pollutant emissions from rice straw open field burning in India , Thailand and the Philippines," Environ. Pollut., vol. 157, no. 5, pp. 1554–1558, 2009, doi: 10.1016/j.envpol.2009.01.004.

[39] O. Mohiuddin, A. Mohiuddin, M. Obaidullah, H. Ahmed, and S. Asumadu-Sarkodie, "Electricity production potential and social benefits from rice husk, a case study in Pakistan," Cogent Eng., vol. 3, no. 1, 2016, doi: 10.1080/23311916.2016.1177156.

[40] P. Ahmed Ali SOhu (Quaid-e-Awam University of Engineering, Science and Technology Nawabshah, Sindh, "Study and Analysis of the potential of Rice Husk (biomass) as a viable source of Energy in Larkano and Kamber Shahdadkot districts of Sindh."

[41] P. Forster et al., "Bounding the role of black carbon in the climate system : A Scientific assessment Bounding the role of black carbon in the climate system : A scienti fi c assessment," no. November 2017, 2013, doi: 10.1002/jgrd.50171.

[42] G. H. M. J. S. De Silva, S. Vishvalingam, and T. Etampawala, "Effect of waste rice husk ash from rice husk fuelled brick kilns on strength , durability and thermal performances of mortar," Constr. Build. Mater., vol. 268, p. 121794, 2021, doi: 10.1016/j.conbuildmat.2020.121794.

[43] L. Q. Luu and A. Halog, "Rice Husk Based Bioelectricity vs. Coal-fired Electricity: Life Cycle Sustainability Assessment Case Study in Vietnam," Procedia CIRP, vol. 40, pp. 73–78, 2016, doi: 10.1016/j.procir.2016.01.058.

[44] J. Singh, "Overview of electric power potential of surplus agricultural biomass from economic, social, environmental and technical perspective - A case study of Punjab," Renew. Sustain. Energy Rev., vol. 42, pp. 286–297, 2015, doi: 10.1016/j.rser.2014.10.015.

[45] M. A. Salam, K. Ahmed, N. Akter, and T. Hossain, "ScienceDirect A review of hydrogen production via biomass gasification and its prospect in Bangladesh," Int. J. Hydrogen Energy, vol. 43, no. 32, pp. 14944–14973, 2018, doi: 10.1016/j.ijhydene.2018.06.043.

[46] M. Uzair, S. S. Sohail, N. U. Shaikh, and A. Shan, "Agricultural residue as an alternate energy source: A case study of Punjab province, Pakistan," Renew. Energy, vol. 162, pp. 2066–2074, 2020, doi: 10.1016/j.renene.2020.10.041.

[47] J. Logeswaran, A. H. Shamsuddin, A. S. Silitonga, and T. M. I. Mahlia, "Prospect of using rice straw for power generation: a review," Environ. Sci. Pollut. Res., vol. 27, no. 21, pp. 25956–25969, 2020, doi: 10.1007/s11356-020-09102-7.

[48] A. O. Avcıoğlu, M. A. Dayıoğlu, and U. Türker, "Assessment of the energy potential of agricultural biomass residues in Turkey," Renew. Energy, vol. 138, pp. 610–619, 2019, doi: 10.1016/j.renene.2019.01.053.

[49] S. M. Safieddin Ardebili, "Green electricity generation potential from biogas produced by anaerobic digestion of farm animal waste and agriculture residues in Iran," Renew. Energy, vol. 154, pp. 29–37, Jul. 2020, doi: 10.1016/j.renene.2020.02.102.

[50] M. Kashif et al., "Untapped renewable energy potential of crop residues in Pakistan: Challenges and future directions," J. Environ. Manage., vol. 256, no. September 2019, p. 109924, 2020, doi: 10.1016/j.jenvman.2019.109924.

[51] M. R. Abedin and H. S. Das, "Electricity from rice husk: A potential way to electrify rural Bangladesh," Int. J. Renew. Energy Res., vol. 4, no. 3, pp. 604–609, 2014, doi: 10.20508/ijrer.15831.

[52] H. Zhang et al., "A laboratory study of agricultural crop residue combustion in China: Emission factors and emission inventory," Atmos. Environ., vol. 42,

no. 36, pp. 8432–8441, Nov. 2008, doi: 10.1016/j.atmosenv.2008.08.015.

[53] M. Adnan, J. Ahmad, S. Farooq, and M. Imran, "A techno-economic analysis for power generation through wind energy : A case study of Pakistan," Energy Reports, vol. 7, pp. 1424–1443, 2021, doi: 10.1016/j.egyr.2021.02.068.

[54] G. of P. Finance Division, Pakistan Economic Survey Report 2018-19. 2020.

[55] A. Ahmed, S. Hidayat, M. S. Abu Bakar, A. K. Azad, R. S. Sukri, and N. Phusunti, "Thermochemical characterisation of Acacia auriculiformis tree parts via proximate, ultimate, TGA, DTG, calorific value and FTIR spectroscopy analyses to evaluate their potential as a biofuel resource," Biofuels, vol. 12, no. 1, pp. 9–20, 2021, doi: 10.1080/17597269.2018.1442663.

[56] A. Abdullah et al., "Potential for sustainable utilisation of agricultural residues for bioenergy production in Pakistan: An overview," J. Clean. Prod., vol. 287, p. 125047, 2021, doi: 10.1016/j.jclepro.2020.125047.

[57] S. Reza, A. Ahmed, W. Caesarendra, and M. S. A. Bakar, "Acacia Holosericea : An Invasive Species for Bio-char , Bio-oil , and Biogas Acacia Holosericea : An Invasive Species for Bio-char , Bio-oil , and Biogas Production," no. April, 2019, doi: 10.3390/bioengineering6020033.

[58] M. Danish, M. Naqvi, U. Farooq, and S. Naqvi, "Characterization of South Asian agricultural residues for potential utilization in future ' energy mix ,'" Energy Procedia, vol. 75, pp. 2974–2980, 2015, doi: 10.1016/j.egypro.2015.07.604.

[59] U. U. Rehman Zia, T. ur Rashid, W. N. Awan, A. Hussain, and M. Ali, "Quantification and technological assessment of bioenergy generation through agricultural residues in Punjab (Pakistan)," Biomass and Bioenergy, vol. 139, no. July, p. 105612, 2020, doi: 10.1016/j.biombioe.2020.105612.

[60] S. Butt, I. Hartmann, and V. Lenz, "Bioenergy potential and consumption in Pakistan," Biomass and Bioenergy, vol. 58, pp. 379–389, 2013, doi: 10.1016/j.biombioe.2013.08.009.

[61] Eaz. husnain, "02-Agriculture finl," pp. 19–40, 2016, [Online]. Available: http://www.finance.gov.pk/survey/chapters_17/02-Agriculture.pdf.

[62] M. Hiloidhari, D. Das, and D. C. Baruah, "Bioenergy potential from crop residue biomass in India," Renew. Sustain. Energy Rev., vol. 32, pp. 504–512, 2014, doi: 10.1016/j.rser.2014.01.025.

[63] A. Milbrandt, R. Overend, A. Milbrandt, and R. Overend, "Assessment of Biomass Resources in Afghanistan Assessment of Biomass Resources in Afghanistan," no. January, 2011.

[64] K. K. C. K. Perera, P. G. Rathnasiri, S. A. S. Senarath, and A. G. T. Sugathapala, "Assessment of sustainable energy potential of non-plantation biomass resources in Sri Lanka," vol. 29, pp. 199–213, 2005, doi: 10.1016/j.biombioe.2005.03.008.

[65] A. K Hossain and O. Badr, "Prospects of renewable energy utilisation for electricity generation in Bangladesh," Renew. Sustain. Energy Rev., vol. 11, no. 8, pp. 1617–1649, 2007, doi: 10.1016/j.rser.2005.12.010.

[66] J. Singh, B. S. Panesar, and S. K. Sharma, "Energy potential through agricultural biomass using geographical information system-A case study of Punjab," Biomass and Bioenergy, vol. 32, no. 4, pp. 301–307, 2008, doi: 10.1016/j.biombioe.2007.10.003.

[67] D. G. Streets, K. F. Yarber, J. H. Woo, and G. R. Carmichael, "Biomass burning in Asia: Annual and seasonal estimates and atmospheric emissions," Global Biogeochem. Cycles, vol. 17, no. 4, 2003, doi: 10.1029/2003gb002040.

[68] M. M. Iqbal and A. M. Goheer, "Greenhouse gas emissions from agro-ecosystems and their contribution to environmental change in the Indus Basin of Pakistan," Adv. Atmos. Sci., vol. 25, no. 6, pp. 1043–1052, 2008, doi: 10.1007/s00376-008-1043-z.

[69] X. Zhang, Y. Lu, and X. Qian, "A high-resolution inventory of air pollutant emissions from crop residue burning in China," Atmos. Environ., vol. 213, no. September 2018, pp. 207–214, 2019, doi: 10.1016/j.atmosenv.2019.06.009.

[70] G. R. Carmichael, Biomass burning in Asia : Annual and seasonal estimates and atmospheric emissions Biomass burning in Asia : annual and seasonal estimates and atmospheric emissions, no. June. 2014.

Abbreviations

IEA, International Energy Agency; FY, Fiscal Year; RH, Rice Husk; RS, Rice Straw; M, Moisture Level; TEP, Theoretical Energy Potential; AEP, Available Energy Potential; LHV, Lower Heating Value; CO, Carbon mono oxide; CO_2, Carbon dioxide; NO, Nitrogen mono oxide; NO_2, Nitrogen di oxide; NOx, Nitrogen oxides; SOx, Sulphur oxides; GHG, Green House Gases; PM, Particulate matter; Mt CO_2-eq, Million tons CO_2 equivalent; EF, Emission Factor; toe, tons of oil equivalent; GWh, Gega Watt Hour; RPR, Residue to Crop Production Ratio; MJ, Mega Joule; TJ, Tera Joule; kg, kilo gram; Gg, Gega grams; USD, United States Dollar; GDP, Gross Domestic Product.

Vol. 5, No. 1 | January – June 2022

Multi-Scale Pooling In Deep Neural Networks For Dense Crowd Estimation

Ali Raza Radhan[1], Fareed Ahmed Jokhio[2], Ghulam Hussain[1,3], Kamran Javed[4], Arsalan Ahmed[1]

Abstract:

State-of-the-art-methods for counting persons in dense crowded places lack in estimating accurate crowd density due to following reasons. They typically apply the same filters over a complete image or over big image patches. Only then the perspective distortion can be compensated by estimating local scale. It is achieved by training an additional classifier with the optimal kernel size chosen from limited choices. These methods are restricted to the context they are applied on because they are not end-to-end trainable; cannot justify quick scale changes because they allocate a single scale to big image patches; and can only utilize a narrow range of receptive fields for the networks to be of a feasible size. In this study, we bring in an end-to-end trainable deep architecture that merges features achieved from multiple kernels of different sizes and learns various essential features such as quick scale changes and to utilize the right context at each image location. This technique flexibly encodes scale of related information to precisely predict crowd density. The training and validation loss of the proposed approach is 5% and 4% lower than the state-of-the-art context aware method, respectively.

Keywords: *Perspective Distortion, local scale, image patches, crowd counting, deep learning*.

1 Introduction

Crowd counting has become an interesting topic in the recent years for researchers due to its broad applications, including crowd monitoring, traffic control, public safety, and event planning, video surveillance and city management. Over the last few years, the density map generation methods have been developed to count people in a scene by training regressors to estimate people density per unit area and get total number of counts by integration without detecting people individually. Currently deep learning methods [28-33] have become prevailing tool for crowd counting, due to powerful learning ability of convolutional neural networks (CNNs). Although crowd counting algorithms have been broadly examined by previous methods [20-22, 28- 33], but handling large density variance in crowd images which causes occlusion and perspective distortion that still remained a challenging problem. As illustrated in fig.1, the densities of a crowd vary significantly from low crowd (e.g. Venice dataset) to extremely dense crowd (Shanghai Part A dataset). Such large variation in density of people is a great challenge for CNN models and creates problems for predicting accurate density map. Most deep learning-based approaches [30-36] use same filters and

[1]Dept. Electronic Engineering, Quaid-e-Awam University, Larkana, Pakistan.
[2]Dept. Computer System Engineering, Quaid-e-Awam University, Nawabshah, Pakistan
[3]Dept. Electronic Engineering, Sungkyunkwan University, Suwon, South Korea
[4]National Centre of Artificial Intelligence (NCAI), Saudi Data and Artificial Intelligence
Corresponding Author: fajokhio@quest.edu.pk

pooling operations on a complete image. These depend upon fix sizes of receptive fields. However, one ought to alter receptive field size over an image to get better results. Stunning advancement has been attained by learning a density map by designing multi-scale structures [39] or accumulating multi-scale features [40,41], which shows capacity to manage with density variation is tuff for crowd counting approaches and remains a huge challenge. Figure 2 compares the Mean Absolute Error of several techniques on three standard benchmark crowd counting datasets having different crowd densities. Result indicates the strength of proposed method to high scale variance.

Low Medium High

Fig. 1. Crowd Types

Such large variation in density of people is a great challenge for CNN models and creates problems for predicting accurate density map. Most deep learning-based approaches [30-36] use same filters and pooling operations on a complete image. These depend upon fix sizes of receptive fields. However, one ought to alter receptive field size over an image to get better results. Stunning advancement has been attained by learning a density map by designing multi- scale structures [39] or accumulating multi- scale features [40,41], which shows capacity to manage with density variation is tuff for crowd counting approaches and remains a huge challenge. Figure 2 compares the Mean Absolute Error of several techniques on three standard benchmark crowd counting datasets having different crowd densities. Result indicates the strength of proposed method to high scale variance.

In this paper, we introduce a deep learning method that gets features from different receptive field sizes and learn the importance of each feature at different image locations and accounts for rapid scale changes. Our method can alleviate the problem of density variation, occlusion, and perspective distortion by using multi-scale pooling operation and give better results than other state-of-art methods. This is contrast to crowd counting methods that work on the density variation as in [19, 42], but different only in the loss function as we get the accurate multi-scale features with minimum error. Experiments are done on several standard crowds counting benchmark datasets such as ShanghaiTech Part A, Part B and Venice which show large density variation as shown in figure 1.

2 Letrature Review

Most of the initial research was centered on detection-based crowd counting, where rectangular bounding boxes were used to detect persons in the scene [1] and this information was used to count the number of persons [2]. People are counted either by whole body detection or by different body parts-based detection. Same class detection techniques [3,4] generally are conventional pedestrian detection ways which train a

classifier using attributes (such as Haar wavelets [5], histogram-oriented gradients [4], edgelet [6] and shapelet [7]) taken out from a full body. Several learning methods such as Support Vector Machines, boosting [8] and random forest [9] have been used with different level of success. Though fruitful in small scale crowd scenes, these methods are badly affected in dense crowd places. Analysts have endeavored to address this issue by embracing part-based detection methods [10, 11], where one applies boosted classifiers for particular body parts such as the head and shoulder to approximate the people counts in that specific area [2].

Though part-based detectors were used to reduce the problems of overlapping, these mechanisms had not fruitful results in the presence of highly congested crowds and high background litter.

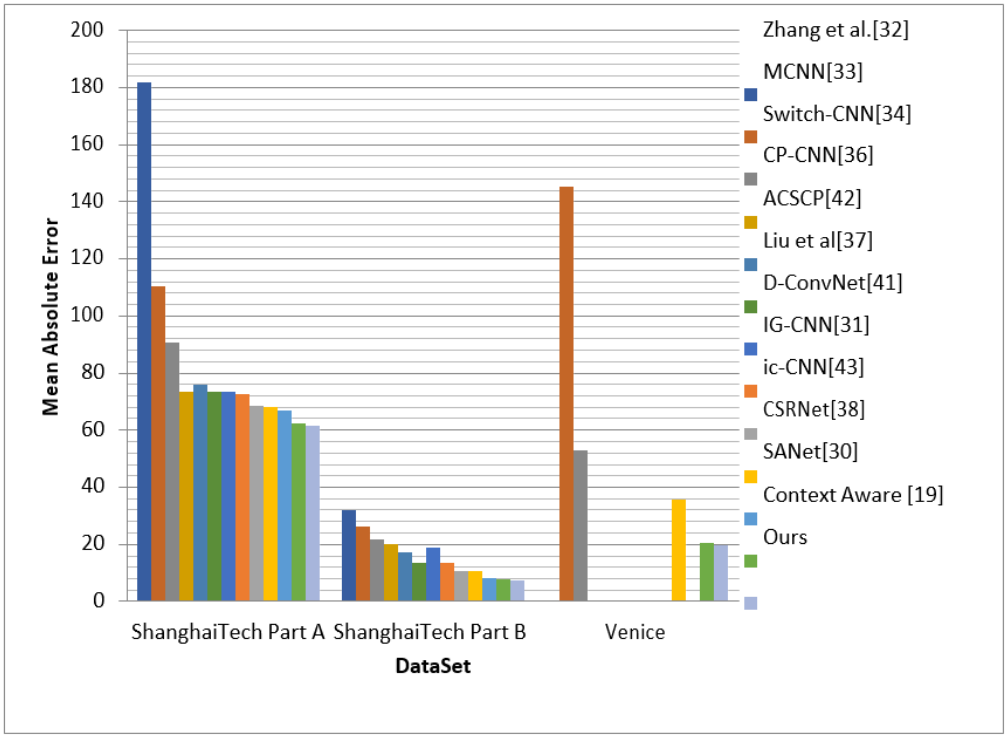

Fig. 2. The performance comparison of the state-of-the-art methods

To solve these problems researchers tried to count by regression where they apply a mapping between features brought out from local image patches to their researcher's counts [12, 13]. By counting using regression, these strategies dodge reliance on teaching detectors which could be a generally complex task. In recent research, Idrees et al. [23] recognized that in congested crowds, no any detection method is effective enough to give precise data for counting people due to problems of overlapping, low quality images and perspective distortion. Furthermore, they noticed that there exists a spatial relationship that can be utilized to oblige the count approximation in adjacent local regions. With these ideas in mind, they suggest finding features using various methods that gather different information. By treating thickly populated crowds of people as irregular and non-homogeneous surface, they applied

Fourier analysis along with head detections and Scale-Invariant Feature Transform (SIFT) interest point based counting in local adjacent regions. The three sources, i.e., Fourier, interest points and head detection are then merged with their respective confidences and counts at localized patches are determined independently.

As the previous methods were successful in addressing the problems of occlusion and clutter, they mostly neglected important spatial information as they were regressing on the global count. In variance, Lempitsky et al. [24] proposed a method to learn a linear mapping between local patch features and object density maps, thereby absorbing spatial information in the learning procedure. Perceiving that it is hard to learn a linear mapping, Pham et al. [25] proposed a method to learn a non-linear mapping between local patch features and density maps. They take multiple image patches using random forest regression to vote for densities of various target objects to learn a non-linear mapping.

Similar to the above technique, Wang and Zou [26] proposed a fast method for density estimation based on subspace learning viewing the computational complication point of view of the existing methods. In a recent approach, Xu and Qiu [27] perceiving that the existing crowd density estimation strategies utilized a smaller set of features results in limiting their capability to perform better. They put forward a method to increase the accuracy of crowd density estimation by utilizing a large set of features. As the regression methods used by previous methods (based on Gaussian process regression or Ridge regression) are computationally complex and are not able to operate very high-dimensional features, they utilized random forest as the regression model whose tree structure is speedy and flexible. Unlike conventional methods to random forest construction, they inserted random projection in the tree nodes to tackle the problem of dimensionality and to introduce randomness in the tree structure.

Now density-based counting methods are mostly superseded by convolutional neural networks-based methods where instead of looking at the patches of an image, researchers form an end-to-end regression method using CNNs. Wang et al. [28] applied CNNs firstly for the task of crowd density estimation. Wang et al. gave an end-to-end deep CNN regression model for counting persons from images in highly dense crowds. In addition, to minimize false responses background like trees and buildings in the images, training data is increased with extra negative samples having ground truth count is fixed as zero. In another approach, Fu et al. introduced to divide the image into one of the five categories: very high density, high density, medium density, low density and very low density rather than estimating density maps, they utilized a combination of two classifiers to acquire boosting in which the first classifier samples misclassified images and the other one reclassifies rejected samples.

The approach of [29, 30] utilizes image patches taken out at multiple scales as source to a multi stream network. They then either combine the features for final density prediction [29] without continuous scale changes or introduce an adhoc term in the training loss function [30] predict consistency across scales forcibly. This, however, does not take contextual information into the features achieved by the algorithm, so has limited effect. Whereas approach [31] learns multi-scale features, by utilizing various receptive fields, they merge all of these features to estimate the density.

While the earlier approaches account for scale, they neglect the reality that the suitable scale changes smoothly over the image should be controlled dynamically. This was proposed in [32] by weighting various density maps generated from input images at different scales. As the density map at each scale just relies upon features extracted from a specific scale, and consequently be ruined by the absence of versatile-scale reasoning. Here, we content that one should rather extract features at various scales and figure out how to adaptively merge them. While this, basically was also the inspiration of [33] , which train an additional classifier to dole out the best receptive field for each image patch, these

techniques stay restricted in many significant manners. Firstly, they depend on classifiers, which need pre-training the network before training the classifier, and in this way it is not end-to-end trainable. Secondly, they commonly assign a single scale to a whole image patch that can still be large and in this manner don't represent quick scale changes. Lastly, the range of receptive field sizes they reliance remain limited in part because using much bigger ones would need using more complex architectures, which may be difficult to train given sort of networks being used.

In this study, we bring in an end-to-end trainable deep architecture that merges features achieved from multiple kernels of different sizes and learns various essential features such as quick scale changes and to utilize the right context at each image location. This technique flexibly encodes scale of related information to precisely predict crowd density. The training and validation loss is relatively low than above methods.

3 Method

3.1 Overview

As discussed above, we target the perspective distortion problem in crowd counting methods where density of people varies from low to extreme level. For decreasing the training and validation loss and to improve the generalization of the model with density variation, we trained it on optimal number of epoch and batch size to get the final density map.

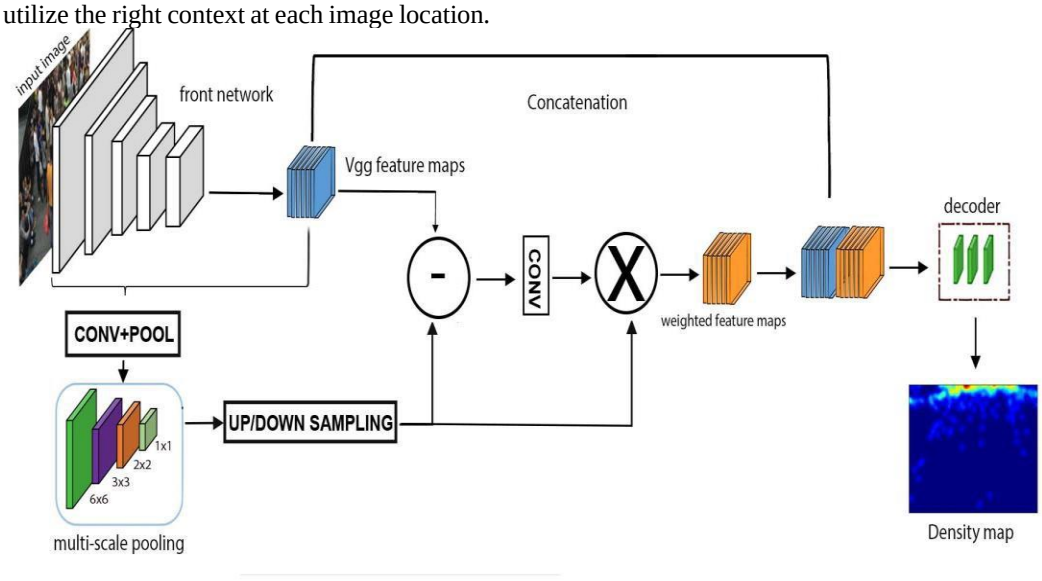

Fig. 3. The proposed methodology

3.2 Scale Learning Module

We aim to generate an estimated density map that is very similar to ground-truth density map of the given set of M training images with corresponding ground-truth density maps. Images are given to initial point of our network having first ten layers of pre- trained *VGG-16* network to get *Vgg* feature maps as shown in fig.2. These *Vgg* features are the base to our learning-scale model. As discussed earlier in section 2, *Vgg-16* network use same filters and pooling operations on a complete image and depends upon fix sizes of receptive fields. So, it is less efficient in rapid scale change scenarios. To solve this, we alter receptive field size over an image to get learning-scale features by applying multi- scale pooling 1X1, 2X2, 3X3 and 6X6 on Vgg features. This forms a pyramid structure. Each pooling

feature shows a density map, hence four different densities extract information from the given image.

These multi-scale densities are then up sampled to the size of convolution layers by linear interpolation and finally combined to give the weighted features. In the end weighted features are concatenated with *Vgg* features to predict the final density map of underlying image as shown in Figure 3.

Scale Learning Network is illustrated in figure 3. RGB images are at input to a front network that contains the first 10 layers of the *VGG-16* network. The resulting *Vgg* features are organized in blocks of various sizes by average pooling succeeded by a 1×1 convolutional layer. They are then up-sampled back to the original feature size to form the weighted features. Contrast or weighted features are further utilized to memorize the weights for the learning-scale features that are then fed to a back-end network to deliver the ultimate density map.

3.3 Training Details and Loss Function

Our network is end-to-end trainable which involves L2 loss defined as

$$L(\sigma) = \frac{1}{2B} \sum_{i=1}^{B} \{ D_i^{gt} - D_i^{pre} \}_2^2 \qquad (1)$$

Where B is the batch size, $\boldsymbol{\sigma}$ is the non-linear mapping parameter that maps an input image $\boldsymbol{I}$i to a predicted density map $\boldsymbol{D_i^{pre}}$. $\boldsymbol{D_i^{gt}}$ is the ground-truth density map that we get as in [19] by convolving an image having ones at people head's locations and zeros elsewhere with a Gaussian kernel $\boldsymbol{N^{gt}}$ $(\boldsymbol{p \backslash \mu, \delta^2})$ we have

$$\forall p \in I_i, D_i^{gt} (\mathrm{p} \backslash I_i) = \sum_{j=1}^{ci} N^{gt} \left(p \backslash \mu = P_i^j, \delta^2\right) \qquad (2)$$

Where $\boldsymbol{\mu}$ and $\boldsymbol{\delta}$ are the mean and standard deviation of the normal distribution. To reduce the loss, we apply stochastic Gradient Descent with batch size 1 for ShanghaiTech Part_A dataset because it has various size images and got impressive results after training the model for 150 epochs. For other two Venice and ShanghaiTech_Part_B fixed image size datasets, we use Adam with batch size 16 and trained the model for 100 epochs

4 Experiments

4.1 Evaluation Matrices

We apply two standard error terms, i.e. Mean Absolute Error (MAE) and Mean Squared Error (MSE) for evaluation purpose and compare our results with other methods. These are defined as

$$MAE = \frac{1}{K} \sum_{i=1}^{K} |x_i - \hat{x}_i| \ , MSE = \sqrt{\frac{1}{K} \sum_{i=1}^{K} (x_i - \hat{x}_i)^2}, \qquad (3)$$

Where K is the total number of images of test images, $\boldsymbol{x_i}$ represents the ground-truth and $\boldsymbol{\hat{x}_i}$ is the predicted number of people in the $\boldsymbol{i^{th}}$ image.

4.2 Benchmark Datasets and Ground-Truth Data

We took three standard benchmark datasets including ShanghaiTech Part_A, ShanghaiTech Part_B and Venice to compare our method with other approaches. ShanghaiTech [27]. The shanghaiTech crowd counting dataset comprises of 1198 images with approximately 330,165 people in them. It is divided in two parts ShanghaiTech Part_A with 482 images which are randomly taken from internet and ShanghaiTech Part_B having 716 images taken from busy streets of metropolitan area in Shanghai city. In part_A 300 images and in Part_B 400 images are reserved for training set. The remaining images of both parts are used for testing purposes. The ground-truth density maps for part_A were generated by adaptive Gaussian kernels and for part_B by fixed kernels. Venice [19]. Venice dataset contains 167 fixed size 1280X720 resolution images from Piazza San Marco in Venice. In this dataset 80 images forms a training data set, and 87 images are used for testing purpose. The images of Venice dataset are more calibrated than

ShanghaiTech. The ground-truth density maps are generated by fixed Gaussian kernels as in ShanghaiTech part_B data set.

4.3 Ablation Study

Ablation study is mainly performed on ShanghaiTech and Venice datasets, as there could be the more problem of rapid scale change due to density variation. Here we confirm the benefits of specific features.

Table 1 shows comparison of Mean Absolute Error and Root Mean Square Error of different approaches on three standard benchmark crowd counting datasets having people density variation. Results in Figure 4 indicate the strength of proposed method on low, medium, and high types of crowds.

TABLE I. COMPARATIVE RESULTS ON THE VENICE DATASET & SHANGHAITECH DATASET VARIATION IN CROWD COUNTING. WE SUMMED UP

	Venice		**Shanghai Part-A**		**Shanghai Part-B**	
Method	MAE	RMSE	MAE	RMSE	MAE	RMSE
Zhang et al.[32]	-	-	181.8	277.7	32.0	49.8
MCNN [33]	145.4	147.3	110.2	173.2	26.4	41.3
Switch-CNN[34]	52.8	59.5	90.4	135.0	21.6	33.4
CP-CNN[36]	-	-	73.6	106.4	20.1	30.1
ACSCP[42]	-	-	75.7	102.7	17.2	27.4
Liu et al.[37]	-	-	73.6	112.0	13.7	21.4
D-ConvNet[41]	-	-	73.5	112.3	18.7	26.0
IG-CNN[31]	-	-	72.5	118.2	13.6	21.1
Ic-CNN[43]	-	-	68.5	116.2	10.7	16.0
CSRNet[38]	35.8	50.0	68.2	115.0	10.6	16.0

SANet[30]	-	-	67.0	104.5	8.4	13.6
Context aware[19]	20.5	29.9	62.3	100.0	7.8	12.2
Ours approach	**19.8**	**29.3**	**61.5**	**100.0**	**7.2**	**12.0**

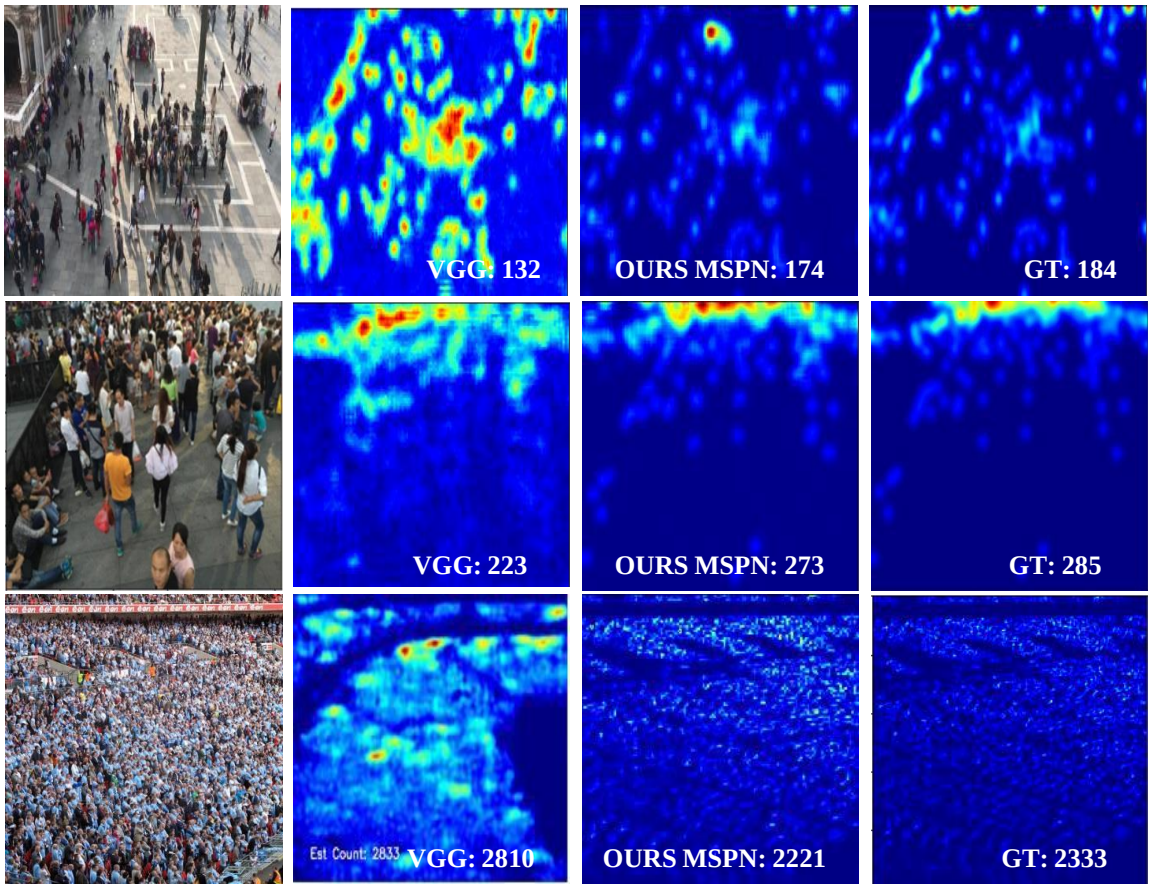

Fig. 4. The performance of the proposed approach on three different density level scenes for crowd density estimation

5 Conclusion and Future perspectives

In this paper, we propose a learning scale model by applying multi-scale pooling network to solve the problem of density four different scale density maps of an image to generate the final one. Experiments were performed on three different standard benchmark datasets having density variations and the generalization ability of the model was quite

impressive than other state-of-art methods. These datasets were formed by fixed cameras, so in future we will work on the images taken from moving cameras e.g. drones. We will enhance our model to process consecutive images and their ground- truth data simultaneously

Funding:
This research received no external funding.

Conflicts of Interest:
The authors declare no conflict of interest.

REFERENCES

[1] Dollar, P., Wojek, C., Schiele, B., Perona, P., 2012. Pedestrian detection: An evaluation of the state of the art. IEEE transactions on pattern analysis and machine intelligence 34, 743–761.

[2] Li, M., Zhang, Z., Huang, K., Tan, T., 2008. Estimating the number of people in crowded scenes by mid based foreground segmentation and head-shoulder detection, in: Pattern Recognition, 2008. ICPR 2008.19th International Conference on, IEEE. pp. 1–4.

[3] Leibe, B., Seemann, E., Schiele, B., 2005. Pedestrian detection in crowded scenes, in: Computer Vision and Pattern Recognition, 2005. CVPR 2005. IEEE Computer Society Conference on, IEEE. pp. 878–885.

[4] Tuzel, O., Porikli, F., Meer, P., 2008. Pedestrian detection via classification on riemannian manifolds. IEEE transactions on pattern analysis and machine intelligence 30, 1713–1727.

[5] Viola, P., Jones, M.J., 2004. Robust real-time face detection. International journal of computer vision 57, 137–154.

[6] Wu, B., Nevatia, R., 2005. Detection of multiple, partially occluded humans in a single image by bayesian combination of edgelet part detectors, in: Computer Vision, 2005. ICCV 2005. Tenth IEEE International Conference on, IEEE. pp. 90–97.

[7] Sabzmeydani, P., Mori, G., 2007. Detecting pedestrians by learning shapelet features, in: Computer Vision and Pattern Recognition, 2007. CVPR'07. IEEE Conference on, IEEE. pp. 1–8.

[8] Viola, P., Jones, M.J., Snow, D., 2005. Detecting pedestrians using patterns of motion and appearance. International Journal of Computer Vision 63, 153–161.

[9] Gall, J., Yao, A., Razavi, N., Van Gool, L., Lempitsky, V., 2011. Hough forests for object detection, tracking, and action recognition. IEEE transactions on pattern analysis and machine intelligence 33, 2188–2202.

[10] Felzenszwalb, P.F., Girshick, R.B., McAllester, D., Ramanan, D., 2010. Object detection with discriminatively trained part- based models. IEEE transactions on pattern analysis and machine intelligence 32, 1627–1645.

[11] Wu, B., Nevatia, R., 2007. Detection and tracking of multiple, partially occluded humans by bayesian combination of edgelet based part detectors. International Journal of Computer Vision 75, 247–266.

[12] Chan, A.B., Vasconcelos, N., 2009. Bayesian poisson regression for crowd counting, in: 2009 IEEE 12th International Conference on Computer Vision, IEEE. pp. 545–551.

[13] Ryan, D., Denman, S., Fookes, C., Sridharan, S., 2009. Crowd counting using multiple local features, in: Digital Image Computing: Techniques and Applications, 2009. DICTA'09., IEEE. pp. 81–88.

[14] Babu Sam, D., Surya, S. and Venkatesh Babu, R., 2017. Switching convolutional neural network for crowd counting. In Proceedings of the IEEE conference on computer vision and pattern recognition (pp. 5744-5752).

[15] Zhang, L., Shi, M. and Chen, Q., 2018, March. Crowd counting via scale-adaptive convolutional neural network. In 2018 IEEE Winter Conference on Applications of Computer Vision (WACV) (pp. 1113-1121). IEEE.

[16] Chen, J., Su, W. and Wang, Z., 2020. Crowd counting with crowd attention convolutional neural network. Neurocomputing, 382, pp.210-220.

[17] Zhang, Y., Zhou, D., Chen, S., Gao, S. and Ma, Y., 2016. Single-image crowd counting via multi-column convolutional neural network. In Proceedings of the IEEE conference on computer vision and pattern recognition (pp. 589-597).

[18] Sam, D.B. and Babu, R.V., 2018, April. Top- down feedback for crowd counting convolutional neural network. In Thirty- second AAAI conference on artificial intelligence.

[19] Liu, W., Salzmann, M. and Fua, P., 2019. Context-aware crowd counting. In Proceedings of the IEEE/CVF Conference on Computer Vision and Pattern Recognition (pp. 5099-5108).

[20] Zhang, C., Li, H., Wang, X. and Yang, X., 2015. Cross-scene crowd counting via deep convolutional neural networks. In Proceedings of the IEEE conference on computer vision and pattern recognition (pp. 833-841).

[21] Hu, Y., Chang, H., Nian, F., Wang, Y. and Li, T., 2016. Dense crowd counting from still images with convolutional neural networks. Journal of Visual Communication and Image Representation, 38, pp.530-539.

[22] Boominathan, L., Kruthiventi, S.S. and Babu, R.V., 2016, October. Crowdnet: A deep convolutional network for dense crowd counting. In Proceedings of the 24th ACM international conference on Multimedia (pp. 640-644).

[23] Idrees, H., Saleemi, I., Seibert, C., Shah, M., 2013. Multi-source multiscale counting in extremely dense crowd images, in: Proceedings of the IEEE Conference on Computer Vision and Pattern Recognition, pp. 2547–2554.

[24] Lempitsky, V., Zisserman, A., 2010. Learning to count objects in images, in: Advances in Neural Information Processing Systems, pp. 1324–1332.

[25] Pham, V.Q., Kozakaya, T., Yamaguchi, O., Okada, R., 2015. Count forest: Co-voting uncertain number of targets using random forest for crowd density estimation, in: Proceedings of the IEEE International Conference on Computer Vision, pp. 3253– 3261.

[26] Wang, Y., Zou, Y., 2016. Fast visual object counting via example-based density estimation, in: Image Processing (ICIP), 2016 IEEE International Conference on, IEEE. pp. 3653–3657.

[27] Xu, B., Qiu, G., 2016. Crowd density estimation based on rich features and random projection forest, in: 2016 IEEE Winter Conference on Applications of Computer Vision (WACV), IEEE. pp. 1–8.

[28] Wang, C., Zhang, H., Yang, L., Liu, S., Cao, X., 2015. Deep people counting in extremely dense crowds, in: Proceedings of the 23rd ACM international conference on Multimedia, ACM. pp. 1299–1302.

[29] Daniel Onoro-Rubio and Roberto J. L´opez- Sastre. Towards Perspective-Free Object Counting with Deep Learning. In European Conference on Computer Vision, pages 615– 629, 2016.

[30] Xinkun Cao, ZhipengWang, Yanyun Zhao, and Fei Su. Scale Aggregation Network for Accurate and Efficient Crowd Counting. In European Conference on Computer Vision, 2018.

[31] Deepak Babu Sam, Neeraj N. Sajjan, R. Venkatesh Babu, and Mukundhan Srinivasan. Divide and Grow: Capturing Huge Diversity in Crowd Images with Incrementally Growing CNN. In Conference on Computer Vision and Pattern Recognition, 2018.

[32] Cong Zhang, Hongsheng Li, Xiaogang Wang, and Xiaokang Yang. Cross-Scene Crowd Counting via Deep Convolutional Neural Networks. In Conference on Computer Vision and Pattern Recognition, pages 833–841, 2015.

[33] Yingying Zhang, Desen Zhou, Siqin Chen, Shenghua Gao, and Yi Ma. Single-Image Crowd Counting via Multi-Column Convolutional Neural Network. In Conference on Computer Vision and Pattern Recognition, pages 589–597,2016.

[34] Deepak Babu Sam, Shiv Surya, and R. Venkatesh Babu. Switching Convolutional Neural Network for Crowd Counting.In Conference on Computer Vision and Pattern Recognition, page 6, 2017.

[35] Feng Xiong, Xinjian Shi, and Dit-Yan Yeung. Spatiotemporal Modeling for Crowd Counting in Videos. In International Conference on Computer Vision, pages 5161–5169, 2017.

[36] Vishwanath A. Sindagi and Vishal M. Patel. Generating High-Quality Crowd Density Maps Using Contextual Pyramid CNNs. In International Conference on Computer Vision,pages 1879–1888, 2017.

[37] Xialei Liu, Joost van de Weijer, and Andrew D. Bagdanov. Leveraging Unlabeled Data for Crowd Counting by Learning to Rank. In Conference on Computer Vision and Pattern Recognition, 2018.

[38] Yuhong Li, Xiaofan Zhang, and Deming Chen. CSRNet: Dilated Convolutional Neural Networks for Understanding the Highly Congested Scenes. In Conference on Computer Vision and Pattern Recognition, 2018.

[39] Wei Liu, Dragomir Anguelov, Dumitru Erhan, ChristianSzegedy, Scott E. Reed, Cheng-Yang Fu, and Alexander C.Berg. SSD: Single Shot Multibox Detector. In European Conference on Computer Vision, 2016.

[40] Vijay Badrinarayanan, Alex Kendall, and Roberto Cipolla. Segnet: A Deep Convolutional Encoder-Decoder Architecture for Image Segmentation. arXiv Preprint, 2015.

[41] Zenglin Shi, Le Zhang, Yun Liu, and Xiaofeng Cao. Crowd Counting with Deep Negative Correlation Learning. In Conference on Computer Vision and Pattern Recognition, 2018.

[42] Zan Shen, Yi Xu, Bingbing Ni, Minsi Wang, Jianguo Hu, and Xiaokang Yang. Crowd Counting via Adversarial Cross-Scale Consistency Pursuit. In Conference on Computer Vision and Pattern Recognition, 2018.

[43] Viresh Ranjan, Hieu Le, and Minh Hoai. Iterative Crowd Counting. In European Conference on Computer Vision,2018

Vol. 5, No. 1 | January – June 2022

Contrast Normalization Filtering Modules for Segmentations of Retinal Blood Vessels from Color Retinal Fundus Images

Qamar un nisa[1], Toufique Ahmed Soomro[2], Mehboob khuwaja[1], Ahmed J. Afif[3], BS Chowdhry[1]

Abstract:

Vision loss is one of the main complications of eye disease, especially diabetic retinopathy (DR), because DR is a silent disease affecting the retina of the eye and resulting in loss of vision. Manual observation of eye disease takes time and delays effective treatment, so computerized methods are used to diagnose eye disease by extracting their features such as blood vessels, optic disc, and other abnormalities. Many computerized methods are proposed but they are still lacking to obtain small vessels. To overcome this problem, we have proposed digital image enhancement methods based on image processing techniques for detection of retinal vessels. The proposed method is based on the elimination of uneven illumination using morphological tactics and Principal Component Analysis (PCA). The main propose to use the PCA to convert the Red-Green- Blue (RGB) channels into signal well contrast image. Since the PCA technique is used in the preprocessing module to get well contrast image. These initial steps are known as the preprocessing module, and our post-processing module contains the vessel coherence and the double threshold binarization method to obtain an image of the segmented vessels. Our proposed method obtained comparable results against existing methods with sensitivity: 0.78, specificity: 0.95 and precision: 0.951 on two databases namely Digital Retinal Images for Vessel Extraction (DRIVE) and Structured Analysis of The Retina (STARE). Such performance shows that our proposed method has capability to segment the retinal blood more accurately. As well as it can be tool for ophthalmologist to diagnosis the eye disease.

Keywords: *Diabetic retinopathy: retinal image: optic disc: morphological tactics: Principle component analysis: double thershold..*

1. Introduction

The retina is the essential part of the human eye, composed of the light-sensitive layer in the back of the eye. The purpose of the retina is to transmit light into neural signals and accommodate the brain to get explicit knowledge. However, every part of the eye is essential for clear vision. The retina is placed beside the optic nerve, and a small darker round part is placed at the retina's central region, known as the macula. A major part of

[1]Electronic Engineering Department, Mehran University of Engineering and Technology, Jamshoro, Pakistan
[2]Electronic Engineering Department, Quaid-e-Awam University of Engineering, Science and Technology, Larkana Campus.
[3]Department of Exploration Helmholtz Institute Freiberg for Resource Technology (HIF), Germany.
Corresponding Author: qamarel10@gmail.com

the macula is called the fovea that gives clear vision.[1]

Retinal eye disease is one primary disease in the list of world health organization. DR has been happened suddenly, and many abnormalities in the retina occurred due to hypertension, unhealthy diet. These factors cause many eye diseases such as Retinal detachment, Hypertensive retinopathy, Neovascular glaucoma, Retinitis pigments, and Diabetic retinopathy. These kinds of diseases may cause complications, even vision loss impairment if they remain untreated. People having diabetic between ages 20 to 74 years can get diabetic retinopathy (DR). It is estimated that people with diabetes have increased by 20 to 25 million worldwide [2].

Diabetic retinopathy is an eye-related disease that affects the geometry of eye blood vessels that may distort or blur vision and cause blindness [3]. The retinal tissue in the human eye is similar to all other parts of human body tissues. The blood received by retinal tissue via small (micro) blood vessels also depends on a continuous blood flow to maintain blood sugar levels. Microaneurysms (MAs) are caused by an abnormal sugar level in the retinal blood vessels. The DR contains various retinal abnormalities such as cotton wool spots, microaneurysms, exudates, and hemorrhages. These abnormalities cause irreversible blindness due to retinal blood vessel damage.

The fundus camera gives the color retinal images. Fundus photography captures the interior of eye images via pupil to the back of the eye is called the fundus. Fundus camera consists of low power of microscope with an onboard flash camera. Optometrists uses low power fundus photography to help get deeper knowledge of ocular health. The fundus is composed of blood vessels, optic disc, retina, macula, and fovea; these are the main retina features of the eye's interior that gives a visualization of the retinal image. An ophthalmologist analyses the obtained retinal image by manually separating the vessels from their backgrounds. A significant number of observer interventions are required in manual segmentation, and it is a time-consuming process [4].

In the last few years, many researchers have been developing advanced techniques for the early detection of disease that can decrease the vision loss risk based on image processing techniques, especially image enhancement and segmentation. Many researchers have studied on computerized techniques for analyzing retinal blood vessel segmentation are implemented, but these studies have different issues, especially enhancement of tiny retinal blood vessels [5]. Multi-scale line detectors and morphological filters are methods based on the blood vessels segmentation. These methods are failed to address critical challenges in the analysis of retinal imaging, such as the tiny vessels detection before designing the vessel pre- detections and the removal of a noisy area of the vessels network [2]. However, a computerized system is reliable and able to create a segmented image that is highly desired to replace the previous systems of manual segmentation of blood vessel.

The automatic vessel optimization techniques require accurate segmentation of retinal blood vessels. Different algorithms are proposed for precise retinal vessel segmentation based on image processing by using filtering method. Many filters are used to remove noise pixels, but still, vessels need proper enhancement. Due to the noise issue, tiny vessels are not detected, leading to the low sensitivity of methods. We proposed pre-processing module based on adaptive wiener filtering and other basic image processing techniques. We also implemented a post-processing model based on histogram thresholding to segmented retinal blood vessels.

The paper is organized into six sections where: Section 1 is based on introduction on DR. Section 2 contain the related work, In the Section 3 explain the research methodology and elaborated each step of purposed model in detail, Section 4 based on database and measures three parameters, Section 5 contain on the result analysis and in the last section 6 based on research conclusion and future work.

2. Related Work

Many researchers have been working on different blood vessel segmentation methods in the fundus of Retinal images [6]. The blood vessels in the retinal images are multi-directionally distribute and make it is difficult to isolate accurately. The vascular network of retinal image containing veins as well as arteries. Since the blood vessels have root and branches that mimic tree. The blood vessels have a tabular shape with gradually varying orientations and widths. The low and varied contrast in the vessels makes it difficult to see the vessels accurately. Accurate segmentation of retinal blood vessels obtained by using different methods such as vessel tracking, morphological processing, filtering, machine learning, image processing techniques, and deep learning. Recently, Toufique et al. [7] developed several filter-based methods to increase the visibility of retinal blood vessels to get accurate segmentation of retinal blood vessels. Lathen et al. [8] implemented an enhanced local phase-based filter for optimal vessel improvement, and it extracts retinal blood vessels in the same vein using an intensity-based filter.

There are two automated retinal vessel segmentation methods: supervised and unsupervised retinal vessel segmentation [9]. The supervised retinal vessel segmentation method requires both user interruption and labeled data to train the vessels and non-vessel pixel classifier [10]. The classifiers are widely used in supervised retinal vessel segmentation methods, and these classifiers are Artificial Neural Networks (ANN) [11] SVM (Support Vector Machine) [12,13], GMM (Gaussian Mixture Models) [14,15], and K-Nearest Neighbors [10]. The unsupervised retinal vessel segmentation methods do not require any user interruption. The unsupervised retinal vessel segmentation methods use mathematical modeling tactics or imaging techniques to classify vessels and non-vessel pixels in an image, and they don't require any training data [9,16, 17]. The performance of supervised methods is significantly giving better result than unsupervised retinal vessel segmentation method. However, the segmentation of supervised method initially obtaining the required data, such as expert training sampling datasets, and might be problematic with time. The most significant supervised technique disadvantage during vessel segmentation is the arduous vessels classification and the pixel value of the background. Yin et al. [18] developed a method based on the segmentation of retinal blood vessel patterns. The proposed designs define which pixels are vessels and which are non-vessels. However, this approach gives false detection on pathology images. Although a learning method has been introduced to improve their method [19,20] it has yet to be validated with retinal vessels mapping, and the tiny vessels have not been detected. Our proposed method is the un-supervised retinal segmentation method. The pre-processing steps of our methods use in the supervised segmentation methods to improve the segmentation of retinal vessels.

Among the unsupervised methods, Mendonca et al. [21] introduced a method for segmentation of retinal blood vessels, and their approach is based on morphological reconstruction tactics. An offset difference of Gaussian filter threshold (DoOG) and their methods did not pick the small vessel, although it gave several erroneous pixel detections. The techniques of the multiscale retinal vessel [22] improved in [23] by exploiting the study of the intensities of retinal images, which is related to the pixels of the vessels responding to specific pixels during the process of image acquisition. After that, multiscale data is combined using a diameter-dependent equalization factor. However, their method provided pixel detection of false vessels on some retinal images, particularly those with a center light reflex.

Toufique Ahmed et al [24 proposed an unsupervised image processing method for detecting the small vessel based on the LoG filter. This method performs better, but some tiny vessels do not detectable. Shankar, K., et al. [25] developed an automated Hyperparameter Tuning Inception-v4 (HPTI-v4) model to classify and detect DR from color retinal images.

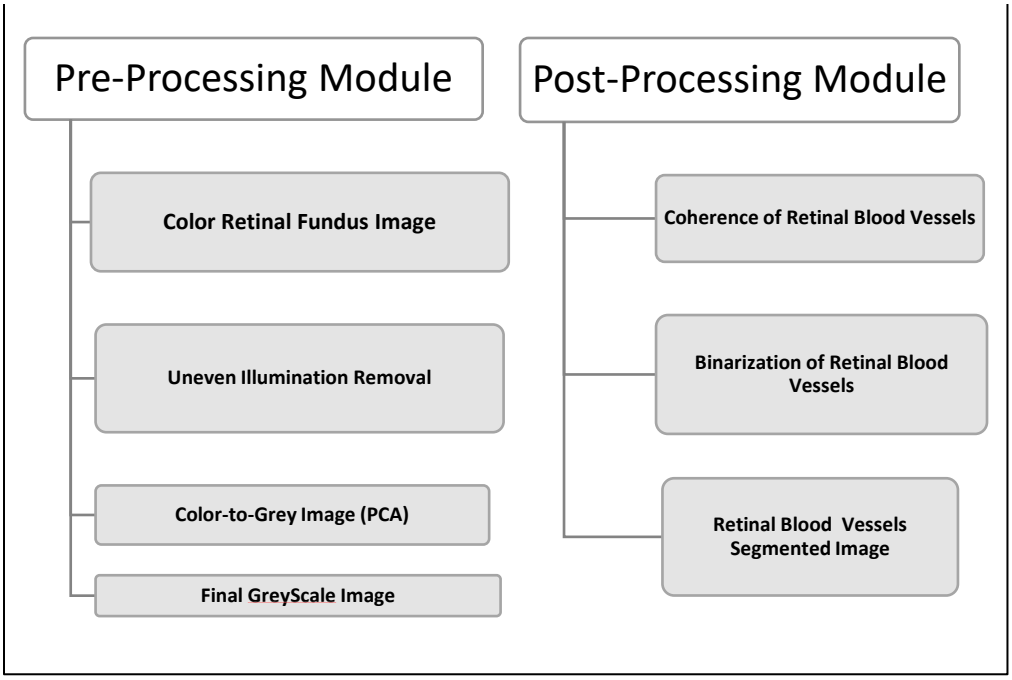

Fig. 1. Proposed Model

This model consists of various sub-processes such as initial step pre-processing, feature extraction, segmentation, and classification. Yin, Pengshuai et al. [26], implement a novel method, segment the biomedical images by deep guided network based on guided image filter for vessel segmentation, cup segmentation, and an optic disc of the retinal image. Toufique A., et al. [27] evaluated contrast normalization step for segmentation of retinal vessel.

3. Proposed Method

Segmentation of accurate blood vessels are a challenging task for the different applications of medical images specifically vessel image segmentation from color retinal fundus images. The segmented blood vessel retinal images contain several issues that make it difficult to diagnose the process of vessel segmentation due to uneven illumination, varying low contrast, and noise. Many researchers have been developing advanced techniques for the early detection of disease that can decrease vision loss and improve the detection of tiny vessels performance. Our proposed methodology is to improve the detection of tiny vessels and retaining an acceptable level of accuracy. This method is based on main two steps: pre-processing and post-processing to obtain an image of the well-segmented vessels. The proposed model is shown in the Figure.1 while all steps are elaborated as follows. Many systems for retinal image segmentation and analysis use preprocessing as the first step. The pre-processing step in our proposed model is based on two main steps to obtain the well-segmented image, while the process is shown in figure 1.

3.1 Processing of Color retinal fundus image

Our designed retinal segmentation algorithm used retinal color fundus images as input images to give an enhanced image in pre-

processing step. Our pre-processing module used monochrome-types input images while most of the retinal image databases are monochrome in nature and the publicly available databases contain color retinal images are captured by a camera known as fundus cameras. The color retinal images contain three types of channels: red, green, and blue channels (RGB channels). Each channel carries its own information and to get the appropriate input image for the further processing as shown in the Figure 2.

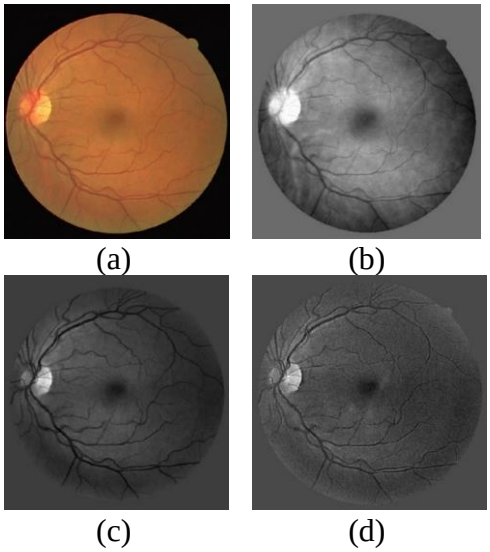

Fig. 2. Select the most suitable channel from retinal image. Where the original retinal color fundus image is shown in (a), and (b) retinal color image in RED channel, (c) retinal color image in GREEN channel, (d) retinal color image in BLUE channel.

The red channel contains both luminous information as well as noise [30] and the green channel contain least number of noisy pixel and give better vessels observation, and the blue channel contain shadow and more noise. However, green channel has a good contrast than the red and blue channels, and blood vessels are more visible in the green channel. A grayscale well-segmented output image will be obtained for further processing, and we select a grayscale image in our model for further processing because it requires less computing resources and takes less time of processing compared to a color (RGB) image. The color images have a minimal number of advantages in the application based on image processing. Color images do process additional information, which can increase the quantity of processing data required to obtain the intended result in any segmentation method. After the selection of the grayscale image, the removal of uneven illumination is analyzed in the next step to achieve a uniform level in the retinal blood vessel against their pixels in the background.

3.2 Removal of uneven illumination

Some basic image processing techniques are used to solve the issue of uneven illumination to obtain a well uniform contrast image. The main reason for eliminating the uneven illumination is each (RGB) channel appears large variation intensity background that effect on the observation of retinal blood vessel. However, we used morphological operations, Adaptive Wiener filtering, and Lee filtering.

We tested in three ways: one based on morphological operation, second based on adaptive wiener filtering, and last on Lee filtering.

Adaptive wiener filtering: Adaptive wiener filtering is based on the least mean square method, and it is applied to the noisy image according to statistical measurement. This filter can remove the noise from the image. Their main objective is to minimize the mean square error between the filtered image and tuoriginal images. This filter modifies each pixel's values properties, and it is required to remove the high-frequency region of image and achieve an edge-preserving of an image.

A local adaptive filter is dependent on in a defined window region of image M x N are the variance and mean. This filter work based on a computation of local image variance, however, when the local variance of the image is large the little smoothing is done in a lesser amount, and if the local variance of the image is smaller the filter performs more smoothing. An adaptive filter is more selective than a linear filter of comparable type because the adaptive

filter preserves the edges as well as other high-frequency regions of the image. The pixel-wise adaptive Wiener technique is used in the adaptive Wiener filter as shown in Figure 3.

The statistics variables are taken from a local neighborhood of each pixel are used in this method. The two statistical variables such as variance and means on which wiener filter in a window size of image is based. The adaptive Wiener filter has three steps with its operation. In the first step, the mask is created by calculating the mean of the noise-contained image. This calculation uses the M x N local neighborhood of each pixel in the image and the mathematical problem for this step is represented by

$$\mu = \frac{1}{NM}\sum_{n_1=1}^{N}\sum_{n_2=1}^{N} I(n_1, n_2) \qquad (1)$$

Next step, the mask is created by calculating the variance of the noise-contained image. This calculation uses the M x N local neighborhood of each pixel in the image and the mathematical problem for this step is represented by

$$\mu = \frac{1}{NM}\sum_{n_1=1}^{N}\sum_{n_2=1}^{N} I^2(n_1, n_2) - \mu^2 \quad (2)$$

In the last step, the adaptive Wiener creates a pixel-wise Wiener filter using these estimates. The mathematical problem at this step is expressed by the first step equation (1)

$$F(n_1 n_2) = \mu + \frac{\sigma^2 + v}{\sigma^2}\left(I(n_1, n_2)\right) - \mu) \quad (3)$$

Where, v is noise variance. If their noise variance is not specified, however, the adaptive Wiener filter will use the average of all calculated local variances. The adaptive wiener filter output of each channel of retinal color fundus image is shown in Figure 3.

Lee filtering: The Lee filter develops the output image via integrating the central pixel intensity in a neighborhood pixel with the mask's average intensity value. This filter is better in edge preservation. This approach uses local statistics to preserve details and is based on a multiplicative speckle model.

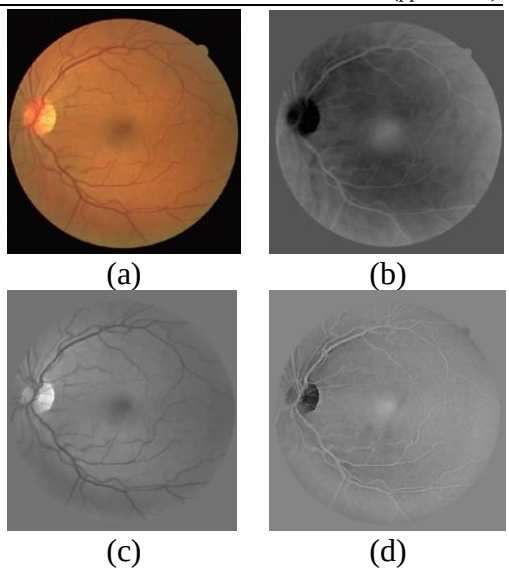

Fig. 3. Adaptive wiener filter output of each channel of retinal color fundus image. (a) input image (b) RED channel, (c) GREEN channel, (d) BLUE channel

This filter is better in edge preservation. This approach uses local statistics to preserve details and is based on a multiplicative speckle model. The lee filter works on mean and variance values [31]. If the variance area is small the smoothing operation is done but if an area of variance is high, then little smoothing is done. In contrast, this filter can preserve details in both low as well as in high contrast hence lee filter has adaptive in nature. The Lee filter mathematical method is expressed in equation (4).

$$img(m, n) = im + w \times (C_p - im) \quad .. (4)$$

Where, img represents the pixel value after filtering, and im means the filter window's mean intensity, C_p defines the center pixel, and w indicates the filter window's width. The filter window calculated by

$$w = \sigma^2(\sigma^2 + \rho^2) \qquad (5)$$

The ρ^2 represented as additive noise variance, and σ^2 is pixel variance calculated as

$$\sigma^2 = \frac{1}{N}\sum_{J=0}^{N-1} (X_j)^2 \qquad (6)$$

$$\rho^2 = \frac{1}{M}\sum_{J=0}^{M-1} (Y_j)^2 \qquad (7)$$

where M is the image size and N is the window size, X_j and Y_j are each pixel value in image at j. The Lee Filter has the drawback of being unable to efficiently eliminate speckle noise near edges. The output of lee filtering is shown in Figure 4.

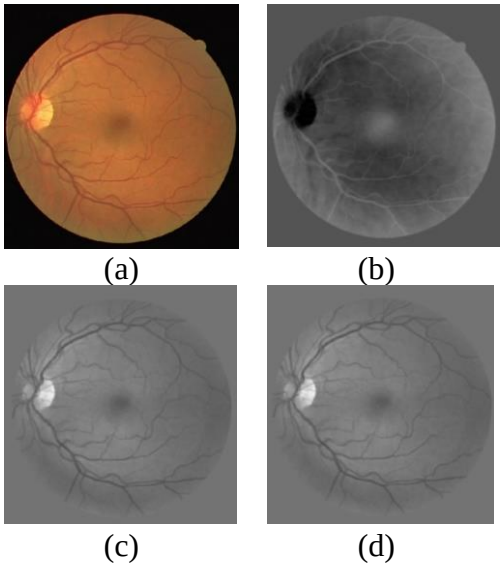

Fig. 4. Lee filter output of each channel of retinal color fundus image. (a) input image (b) RED channel, (c) GREEN channel, (d) BLUE channel.

We selected the best method by comparing the contrast level of the output image of each method and processed it for further processing. But these filtering techniques either adaptive wiener filtering and lee filtering do not give proper unform image as shown in Figure 3 and 4. We validated the morphological operation which works successfully and achieve well contrast image.

Morphological Image Processing Operations: Morphological image processing approaches are a set of digital image processing techniques which contains mathematical morphology tactics. The main functionality of Morphological operations is used for uniform contrast variation. Morphological operations are used to eliminate noisy pixels and uneven illumination of each grayscale retinal image. It is clearly observed that each channel has uneven illumination as well as noise as shown in the Figure 5. There are differences between background and intensities level of blood vessel, according to the analysis. The changes in these intensity levels produce an uneven illumination and noise problem since the blood vessel intensity levels are much lower than the background intensity level.

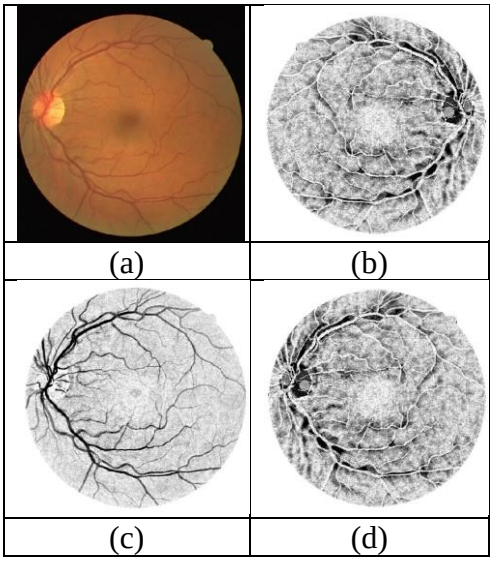

Fig. 5. Output of morphological Operation. (a) input image (b) RED channel, (c) GREEN channel, (d) BLUE channel.

There are many mathematical morphological approaches are used for image processing, the most used are closing and opening operations namely: top hat and bottom hat operation. Each RGB channel of retinal color fundus images are processed through both approaches to know how much noise affects the background of a retinal blood vessel. The top hat morphological operation is implemented as varying contrast of retinal blood vessels improved. The bottom hat morphological operation is implemented for improved the background of the image and give a sort of information to the retinal image, and it makes blood vessels more visible or enhanced while decreasing the level of noise effect on blood vessels. Finally, noise problem, as well as uneven illumination of background retinal image is eliminated

through subtracting top hat image from bottom hat image, with maintained these both issue: noise and uneven illumination, we obtained more enhanced final vessel image and observed that the vessels are more visible in Figure 5.

After comparing the output of all these filtering techniques, we can observe that more detailed of image is achieved from morphological operations as well as background contains uniformity also. As, we measured the contrasted of green channel of each vessel against their background of these techniques. The morphological techniques gave 60.12 contrast as compared to 37.28 of adaptive winner filter and 38.1 of lee filter.

3.3 Color conversion into grayscale image by PCA techniques

The grayscale images give more promising results because it used mainly for examining the details of an image. Grayscale image is crucial to maintain visual features in medical images to detect the most vital clues.

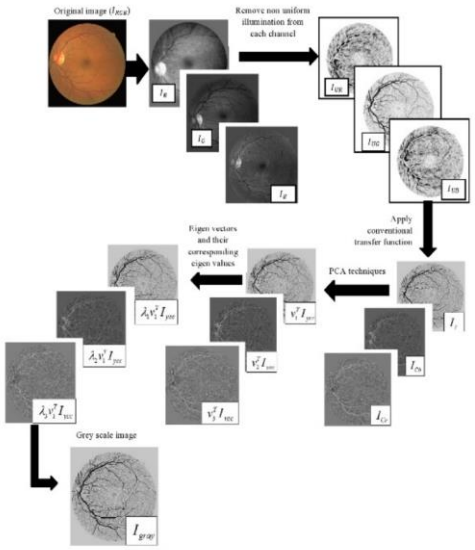

Fig. 6. PCA Based Conversion from RGB to Grayscale Image

The observation of retinal blood vessels plays a vital role in observing the progression of eye illnesses in the retinal image. In this stage, the main goal is to merge the three colors (RGB) channels into a single grayscale channel image while converting RGB to grayscale show more promising outcomes. Whereas RGB background equalization of the retinal channels provides adequate representation for subsequent processing. In order to create a single grayscale image, used all three channels: red, green, and blue channels instead of the single Green channel. The principal component analysis (PCA) is used to convert a color RGB image into a grayscale image. The process is shown in Figure 6.

Our method prefers to use all three RGB channels with the use of PCA to obtain a single grayscale image by including several processing steps:

1) the color to grayscale conversation method is concerned with the vector color RGB images formulation $(I_{rgb} \in R^3)$ through-loading three color channels: Red, Green, and Blue simultaneously. Further, a zero mean of YCbCr image $(I_{YCbCr} \in R^3)$is converted out by its RGB version to unlink such chrominance and luminance channels through transfer function *f (.)*.

2) The eigenvectors $(v_1 \geq v_2 \geq v_3 \in R^3)$ and their corresponding eigenvalues $(\lambda_1 \geq \lambda_2 \geq \lambda_3 \in R^1)$ are determined by the PCA method. The final $(I_{gray} \in R^3)$ grayscale image is determined via three projections of the weighted direct blend, where weights are determined by their eigenvalue's percentage. As seen in Figure , the final output is scaled to the [0, 1] range. Within three subframe projections, we achieved the final resulting grayscale image.

In the first subframe, projection leads the color-to-gray transfer results because of its

significantly larger eigenvalue while other two subframe projections assist in a limited way to filling a colored image detail in the final grayscale image as shown in figure 6. The principal component Analysis (PCA) conversion is utilized to the axes rotate from color space intensity values to orthogonal axes to get an effective color conversion.

In the first subframe, projection leads the color-to-gray transfer results because of its significantly larger eigenvalue while other two subframe projections assist in a limited way to filling a colored image detail in the final grayscale image as shown in figure 6. The principal component Analysis (PCA) conversion is utilized to the axes rotate from color space intensity values to orthogonal axes to get an effective color conversion.

4. Post Processing Module

The post-processing step is used to remove tiny objects from the binary image in order to binary image get well-connected vessels. This step contains the segmentation of the vessels in the retinal images. The main objective of post-processing is to analyze the effect of our pre-processing model and to assess its performance in the vessel segmentation. The post-processing step in our proposed model is based on two steps:

1. Coherence of Retinal Blood Vessels network using Contrast Normalization Filters.
2. Binarization method to achieve well segmented vessels image.

The homogenization of the background improves the overall contrast of the retinal image, it is observed that discontinuities in the vessels are present. To resolve this problem, we used a second order Gaussian derivative filter to normalize the pixels intensities between the connected vessels and give an initial coherent vessels image. But still, the small vessels do not maintain the same consistency with their background. It is therefore challenging to binarize the vessels, for getting well vessels image, we used Anisotropic diffusion filtering proposed by [32], anisotropic diffusion filtering is used to increase the coherence of tiny vessels. The output of both coherence filters is shown in Figure 7. It clearly observed that tiny vessels are more detected in final coherence image Fig 7(b), and it leads to give more accurate segmented image in binarization process.

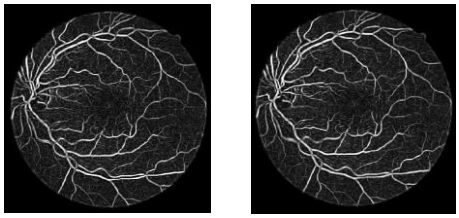

Fig(a) Fig(b)

Fig. 7. Coherence of vessels. Fig (a) represents the initial coherent image, and Fig (b) represents the final coherent image.

4.1 Binary Output: Final Segmented Image

The output images of final coherent vessels still having noisy pixels, as well as some intensity variations, remain and it makes it difficult to detect tiny vessels and connect them. A better vessel segmented output image is achieved here by using the double threshold method.

This method is based on morphological reconstruction images. This reconstruction morphological image is used for the final binary output image obtained and their structure is comprised of two binary images namely: 1. mask image 2. marker image.

We assume that A and B are two binary images: A is mask image and B is marker images of same type of domain D such as A ⊂ B i.e:$\forall p \in D, B(p) = 1 \Rightarrow A(p) = 1$ are used in reconstruction morphological image to provide binary image detail. Both marker and mask images are achieved by image histogram as shown in the Figure 8.

The Figure 8(a) shown the mask image, which is achieved by applying a mean image value based on the image histogram, and the marker image is achieved by multiplying with

standard derivation value 0.9 and subtract it by a mean image value image based on the histogram as shown in figure (b). The final binary output image as shown in Figure 8(c) and final binary image is achieved by applying morphological reconstruction operation. The mask image has more noise than the marker image and background noise is removed by multiply a standard derivation. The false pixels in the marker image background reduces, as a result, a small vessel is detected and get a better marker image by chosen 0.9 standard derivations.

We use image processing techniques to eliminate tiny objects against the binary image and obtain an accurate retinal vessel image. Because some isolated noise segments pixels are detected as false vessels because of the morphologically reconstructed process.

The small objects are removed from the reconstructed image so that the image only contains a well-connected vessel. Thus, small areas of fewer than 50 pixels are removed for this task to obtain the final binary image as shown in Figure 8(d).

4.2 Proposed algorithm

Our proposed method comprises of two main steps: 1. pre-processing 2. post processing.

The pre- processing step is based on following three stages.

1. Firstly, the retinal color fundus image proceeds as input and then convert the retinal image into RGB channels and subsequently each channel covert into greyscale images.

2. This stage is related to the removal of uneven illumination. To manage the uneven illumination from three channel by evaluated the morphological operation, lee filtering, and adaptive wiener filtering. When compared to the morphological operation, lee filter, and adaptive wiener filtering output result. The morphological operation produced well contrast image.

3. This stage is based on machine learning techniques for obtained the well contrasted grayscale image. We convert RGB image into grayscale image by using PCA techniques.

The post- processing steps are based on following stages.

4. The first stage of post processing related to examining the normalization of small vessel and it is crucial component in boosting the vessels sensitivity. Contrast coherent filters are used to obtain the coherent vessels image.

5. Stage 3. The third stage is based on double threshold binarization to get well segmented image.

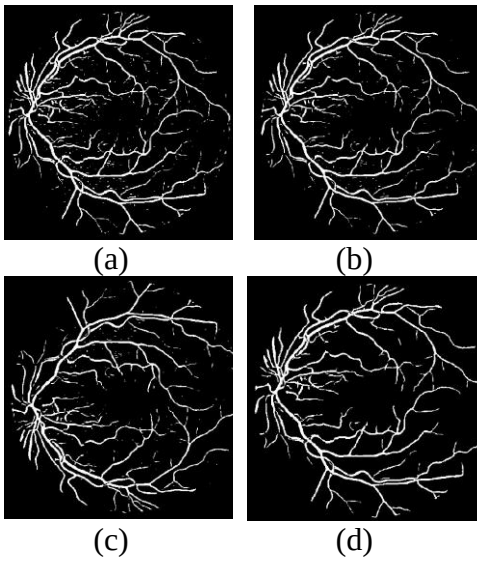

Fig. 8.

5. Database and Computing Parameters

We used two publicly available database for validating our proposed method. In this section, we introduce our database and measuring parameters also.

5.1 Database

We used the digital retinal images for vessel extraction (DRIVE) and structured analysis of the retina (STARE) database. These databases totally contained the 40 images, and each image have ground truth

image. Almost all researchers used these databases to validate their algorithm. It gives opportunity to compare the performance of our methods against existing methods.

5.2 Measuring Parameters

The most used parameters are computed, and these parameters are sensitivity, specificity, and accuracy. These three parameters are used to validate the retinal segmentation algorithm. The sensitivity and specificity is used to measure the ability of the vessels and non-vessels pixels classifications. Accuracy measured the overall performance of the algorithm. The mathematically representation of these parameters are shown below.

$$\text{Sensitivity (SE)} = \frac{\text{TP}}{\text{TP+FN}} \quad (8)$$

$$\text{Specificity (SP)} = \frac{\text{TN}}{\text{TN+FP}} \quad (9)$$

$$\text{Accuracy (AC)} = \frac{\text{TP+TN}}{\text{TP+FP+TN+FN}} \quad (10)$$

Where, TP, TN,FP and FN are true positive pixels intensity, true negative pixels intensity, false positive pixels intensity and false negative intensity.

6. Experimental Results Analysis

Our experimental result analysis section contains analysis of performance of our method on databases and comparison analysis with existing methods.

6.1 Performance on Database

The performance of our algorithm is shown in Table 1. It can be observed that our method gave accuracy of 0.948 on DRIVE and 0.941 on STARE with sensitivity of 0.80 on DRIVE and 0.79 on STARE. We analyzed the images also as shown in Figure 9. It is clearly analyzed that proposed method gives well segmented images and even tiny vessels are clearly observable and our method output is comparable with corresponding ground-truth.

TABLE I. PERFORMANCE OF OUR PROPOSED METHOD ON DATABASES

Database	SE	SP	AC
DRIVE	0.80	0.961	0.948
STARE	0.79	0.956	0.941

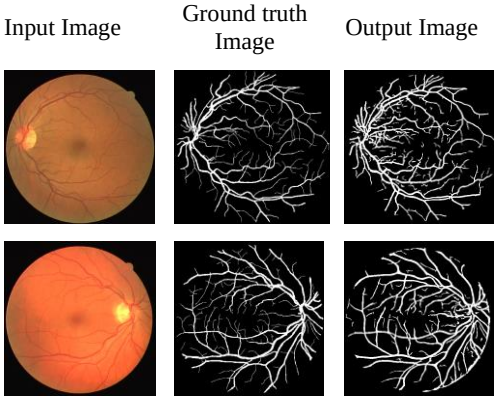

Fig. 9. Final output of proposed algorithm based on DRIVE and STARE database.

6.2 Comparison with Existing methods

The method's validation for accurate blood vessels segmentation is proven by comparing with performance of previous methods.

Many researchers use the two most extensively used publicly available databases, DRIVE and STARE, to evaluate their approaches. The Table 2 shows the comparison of performance of our proposed method with existing methods. our proposed method is based on tactics of image processing and has given higher sensitivity and accuracy (se=0.80, acc=0.948 and se=0.79, acc=0.941) on both DRIVE and STARE database than other pervious method except toufique et al [44] as well as toufique et al [45] method which have higher accuracy and sensitivity near to 96% and 81% respectively than our proposed method. It can be clearly observed that our method gave comparable performance as compared to existing methods, and it shows that our proposed method has capability to segment the retinal blood more accurately. This proposed method can be provided easy framework for ophthalmologist to more

accurately screen for retinal disorders and recommended for early treatment.

TABLE II. COMPARISON OF PROPOSED METHOD AGAINST EXISTING METHODS

Method	Year	DRIVE			STARE		
		SE	SP	AC	SE	SP	AC
Zhao et al [33]	2016	0.716	0.978	0.944	0.776	0.954	0.943
Melinscak et al [34]	2016	-	-	0.946	-	-	-
Toufique et al [35]	2016	0.714	0.968	0.946	0.709	0.965	0.942
Khan et al [36]	2016	0.737	0.967	0.951	0.736	0.971	0.951
Toufique et al [37]	2017	0.752	0.976	0.943	0.784	0.981	0.961
Toufique et al [38]	2017	0.746	0.966	0.952	0.755	0,959	0.951
Toufique et al [39]	2017	0.746	0.917	0.948	0.748	0,922	0.947
Toufique et al [40]	2018	0.752	0.976	0.953	0.786	0.982	0.967
Toufique et al [41]	2018	0.739	0.956	0.950	0.784	0.962	0.947
Khan et al [42]	2018	0.769	0.965	0.950	0.752	0.981	0.951
Toufique et al [43]	2019	0.745	0.962	0.948	0.784	0.976	0.951
Toufique et al [44]	2019	0.802	0.974	0.959	0.801	0.969	0,961
Toufique et al [45]	2021	0.812	0.971	0.963	0.809	0.969	0.958
Purposed method	2021	0.80	0.961	0.948	0.79	0.956	0.941

7. CONCLUSION

Changes in the structure of the retinal blood vessel in fundus image that can be used as a diagnostic parameter for eye diseases, especially DR. For the diagnosis of eye diseases, precise segmentation of the retinal vessels is required. Many methods have been proposed on the segmentation of retinal blood vessel but there is still need for improvement in the accurate detection of small vessels. In this research paper, we have implemented and validated the digital image contrast enhancement method based on image processing tactics and gives segmented vessels images accurately in which especially more tiny vessels are detected. The goal was to solve the issues of varying low contrast and other challenges in analysis of color fundus images, that make it challenging to accurate Segmentation of blood vessels. The segmentation is carried out in the post-processing, but the post-processing module depends on the pre-processing module. We proposed the well preprocessing module to get a well contrasted image, and it impacted the postprocessing modulus and gave a well segmented retinal vessel image. Our proposed method is validated on public databases, namely DRIVE and STARE. The method achieved performance comparable to existing methods and it achieved higher level of

sensitivity and segmentation accuracy. Our proposed method has capability to be used to a diagnostic tool for eye diseases in the future for timely recommended treatment.

REFERENCES

[1] Li, Xiaotao, and Xiang Li. "The antidepressant effect of light therapy from retinal projections." Neuroscience bulletin 34.2 (2018): 359-368.

[2] Soomro, Toufique A., et al. "Role of image contrast enhancement technique for ophthalmologist as diagnostic tool for diabetic retinopathy." 2016 International conference on digital image computing: techniques and applications (DICTA). IEEE, 2016

[3] S. Chaudhuri, S. Chatterjee, N. Katz, M. Nelson, and M. Goldbaum, ‘‘Detection of blood vessels in retinal images using two-dimensional matched filters,’’ IEEE Trans. Med. Imag., vol. 8, no. 3, pp. 263–269, Sep. 1989.

[4] Pakter, Helena M., et al. "Measuring arteriolar-to-venous ratio in retinal photography of patients with hypertension: development and application of a new semi automated method." American journal of hypertension 18.3 (2005): 417-421.

[5] Toufique Ahmed Soomro, Junbin Gao, Tariq M Khan, Ahmad Fadzil M Hani, Mohammad A. U. Khan, and Manoranjan Paul, “Computerised approaches for the detection of diabetic retinopathy using retinal fundus images: A survey,” Journal of Pattern Analysis and Application, pp. 1–35, 2017.

[6] Soomro, Toufique Ahmed, et al. "Deep learning models for retinal blood vessels segmentation: A review." IEEE Access 7 (2019): 71696-71717.

[7] Soomro, Toufique Ahmed, et al. "Impact of image enhancement technique on CNN model for retinal blood vessels segmentation." IEEE Access 7 (2019): 158183-158197

[8] Lathen, G.; Jonasson, J.; Borga, M. Blood vessel segmentation using multi-scale quadrature filtering. Pattern Recognit. Lett. 2010, 31, 762–67.

[9] Sun, K.; Chen, Z.; Jiang, S. Local Morphology Fitting Active Contour for Automatic Vascular Segmentation. IEEE Trans. -Bio-Med Eng. 2012, 59, 464–473

[10] Staal, J.; Abràmoff, M.D.; Niemeijer, M.; Viergever, M.A.; Van Ginneken, B. Ridge-based vessel segmentation in color images of the retina. IEEE Trans. Med. Imaging 2004, 23, 501–509.

[11] Sinthanayothin, C.; Boyce, J.F.; Cook, H.L.; Williamson, T.H. Automated localization of the optic disc, fovea, and retinal blood vessels from digital color fundus images. Br. J. Ophthalmol. 1999, 83, 890–902.

[12] Xing, Y.; Qinmu, P.; Yuan, Y.; Yiu-ming, C.; Jiajia, L. Segmentation of Retinal Blood Vessels Using the Radial Projection and Semi-supervised Approach. Pattern Recognit. 2011, 44, 10–11.

[13] Ricci, E.; Perfetti, R. Retinal Blood Vessel Segmentation Using Line Operators and Support Vector Classification. IEEE Trans. Med. Imaging 2007, 26, 1357–1365.

[14] Marin, D.; Aquino, A.; Gegundez-Arias, M.E.; Bravo, J.M. A New Supervised Method for Blood Vessel Segmentation in Retinal Images by Using Gray-Level and Moment Invariants-Based Features. IEEE Trans. Med. Imaging 2011, 30, 146–158.

[15] Soares, João VB, et al. "Retinal vessel segmentation using the 2-D Gabor wavelet and supervised classification." IEEE Transactions on medical Imaging 25.9 (2006): 1214-1222.

[16] Bankhead, Peter, et al. "Fast retinal vessel detection and measurement using wavelets and edge location refinement." PloS one 7.3 (2012): e32435.

[17] Al-Diri, Bashir, Andrew Hunter, and David Steel. "An active contour model for segmenting and measuring retinal vessels." IEEE Transactions on Medical imaging 28.9 (2009): 1488-1497

[18] Yin, Xiaoxia, et al. "Accurate image analysis of the retina using hessian matrix and binarisation of thresholded entropy with application of texture mapping." PloS one 9.4 (2014): e95943.

[19] Liskowski, Paweł, and Krzysztof Krawiec. "Segmenting retinal blood vessels with deep neural networks." IEEE transactions on medical imaging 35.11 (2016): 2369-2380.

[20] Li, Qiaoliang, et al. "A cross-modality learning approach for vessel segmentation in retinal images." IEEE transactions on medical imaging 35.1 (2015): 109-118.

[21] Mendonca, Ana Maria, and Aurelio Campilho. "Segmentation of retinal blood vessels by combining the detection of centerlines and morphological reconstruction." IEEE transactions on medical imaging 25.9 (2006): 1200-1213.

[22] Martínez-Pérez, M. Elena, et al. "Retinal blood vessel segmentation by means of scale-space analysis and region growing." International Conference on Medical Image Computing and Computer-Assisted Intervention. Springer, Berlin, Heidelberg, 1999.

[23] Martinez-Perez, M. Elena, et al. "Segmentation of blood vessels from red-free and fluorescein retinal images." Medical image analysis 11.1 (2007): 47-61.

[24] Shankar, K., et al. "Hyperparameter tuning deep learning for diabetic retinopathy fundus image classification." IEEE Access 8 (2020): 118164-118173.

[25] Yin, Pengshuai, et al. "Deep Guidance Network for Biomedical Image Segmentation." IEEE Access 8 (2020): 116106-116116.

[26] Soomro, Toufique Ahmed, et al. "Contrast normalization steps for increased sensitivity of a retinal image segmentation method." Signal, Image and Video Processing 11.8 (2017): 1509-1517.

[27] Azzopardi, George, et al. "Trainable COSFIRE filters for vessel delineation with application to retinal images." Medical image analysis 19.1 (2015): 46-57.

[28] Elseid, Arwa Ahmed Gasm, Mohamed Eltahir Elmanna, and Alnazier Osman Hamza. "Evaluation of spatial filtering techniques in retinal fundus images." American Journal of Artificial Intelligence 2.2 (2018): 16.

[29] Soomro, Toufique Ahmed, et al. "Retinal blood vessels extraction of challenging images." Australasian Conference on Data Mining. Springer, Singapore, 2018.

[30] J. Lee, "Digital image enhancement and noise filtering by use of local statistics," IEEE Trans. Pattern Anal. Mach. Intel., vol. Pami-2, no. 2, pp. 165–168, 1980 March.

[31] Gottschlich, Carsten, and C-B. Schönlieb. "Oriented diffusion filtering for enhancing low-quality fingerprint images." IET biometrics 1.2 (2012): 105-113.

[32] Y. Zhao, L. Rada, K. Chen, S. P. Harding, and Y. Zheng, ''Automated vessel segmentation using infinite perimeter active contour model with hybrid region information with application to retinal images,'' IEEE Trans. Med. Imag., vol. 34, no. 9, pp. 1797–1807, Sep. 2015.

[33] M. Melinščak, P. Prentašić, and S. Lončarić, ''Retinal vessel segmentation using deep neural networks,'' in Proc. Int. Conf. Comput. Vis. Theory Appl., 2015, pp. 1–6

[34] T. A. Soomro, M. A. U. Khan, J. Gao, T. M. Khan, M. Paul, and N. Mir, ''Automatic retinal vessel extraction algorithm,'' in Proc. Int. Conf. Digit. Image Comput., Techn. Appl. (DICTA), Nov. 2016, pp. 1–8

[35] M. A. U. Khan, T. A. Soomro, T. M. Khan, D. G. Bailey, J. Gao, and N. Mir, ''Automatic retinal vessel extraction algorithm based on contrast-sensitive schemes,'' in Proc. Int. Conf. Image Vis. Comput. New Zealand (IVCNZ), Nov. 2016, pp. 1–5

[36] T. A. Soomro, T. M. Khan, M. A. U. Khan, J. Gao, M. Paul, and L. Zheng, ''Impact of ICA-based image enhancement technique on retinal blood vessels segmentation,'' IEEE Access, vol. 6, pp. 3524–3538, 2018.

[37] T. A. Soomro, J. Gao, Z. Lihong, A. J. Afifi, S. Soomro, and M. Paul, ''Retinal blood vessels extraction of challenging images,'' in Data Mining (Communications in Computer and Information Science), vol. 996. Singapore: Springer, 2019, pp. 347–359.

[38] T. A. Soomro, A. J. Afifi, J. Gao, O. Hellwich, M. A. U. Khan, M. Paul, and L. Zheng, ''Boosting sensitivity of a retinal vessel segmentation algorithm with convolutional neural network,'' in Proc. Int. Conf. Digit. Image Comput., Techn. Appl. (DICTA), Nov. 2017.

[39] T. A. Soomro, T. M. Khan, M. A. U. Khan, J. Gao, M. Paul, and L. Zheng, ''Impact of ICA-based image enhancement technique on retinal blood vessels segmentation,'' IEEE Access, vol. 6, pp. 3524–3538, 2018.

[40] T. A. Soomro, A. J. Afifi, J. Gao, O. Hellwich, M. Paul, and L. Zheng, ''Strided U-net model: Retinal vessels segmentation using dice loss,'' in Proc. Digit. Image Comput., Techn. Appl. (DICTA), Dec. 2018, pp. 1–8.

[41] M. K. T. M. Khan and D. T. A. Bailey Soomro, ''A generalized multi-scale line-detection method to boost retinal vessel segmentation sensitivity,'' Pattern Anal. Appl., vol. 22, no. 3, pp. 1177–1196, 2018.

[42] T. A. Soomro, J. Gao, Z. Lihong, A. J. Afifi, S. Soomro, and M. Paul, ''Retinal blood vessels extraction of challenging images,'' in Data Mining (Communications in Computer and Information Science), vol. 996, nos. 1–12. Singapore: Springer, 2019.

[43] T. A. Soomro, A. J. Afifi, A. Ali Shah, S. Soomro, G. A. Baloch, L. Zheng, M. Yin, and J. Gao, ''Impact of image enhancement technique on CNN model for retinal blood vessels segmentation,'' IEEE Access, vol. 7, pp. 158183–158197, 2019.

[44] Soomro, T.A.; Ali, A.; Jandan, N.A.; Afifi, A.J.; Irfan, M.; Alqhtani, S.; Glowacz, A.; Alqahtani, A.; Tadeusiewicz, R.; Kantoch, E.; Zheng, L. Impact of Novel Image Preprocessing Techniques on Retinal Vessel Segmentation. Electronics 2021, 10, 2297. https://doi.org/10.3390/electronics10182297

Vol. 5, No. 1 | January – June 2022

Internet of Things Based Transducer Application to Harness Tidal Energy from coastal and offshore Pakistan

Suresh Kumar[1], Dr. Irfanullah Khan[2], Danish[1], Alveena Aslam[1], Dr. Muhammad Imran Majid[3,4]

Abstract:

This paper aims to transform tidal energy into rotation energy for electricity generation and in the course evaluating sea parameters. This is accomplished by integrating the Internet of Things with tidal energy off the coast (and in a home environment), which further enhances the capabilities of this prototype project to remotely monitor sea-like parameters to enable energy production using tidal energy. As South Korea is transducing tidal energy with a total installed tidal power capacity of above 500MW, Pakistan and Middle Eastern countries can benefit from its vast coastal line. This paper proposes a sustainable design that makes the turbine rotate at high speed. A vertical design is chosen, which is bi-directional. The design of the turbine consists of 3 blades, each occupying a 2 square feet area supported by an iron-rod frame. During the experimentation, an average voltage of 5V was generated, whereas the speed of the turbine generated was 75 RPM. It is the first known attempt of its kind supported by indigenous resources. It is proposed that this type of prototype can be scaled, to the coast to produce electrical energy to meet the energy production needs of the region.

Keywords: *Arduino; dc motors; internet of things; sensors; tidal energy; transducers; tidal turbines; underwater technology; wi-fi module.*

1 Introduction

Sourcing energy from renewable sources is presently a key subject in modern society [1]. It is known that more than 70% of the earth is covered with water [2]. We can use water as a renewable source for energy extraction. The electricity demand is growing, and global warming also pressurizes human life [3]. Ocean energy in many forms is being investigated as a potential source [4]. Ocean current energy, tidal energy, wave energy, and offshore wind energy are some of them. Tidal energy is still considered a new alternative energy type. In Pakistan, this energy is still immature it may play a key role soon. This pollution-free source of energy is very cost-effective for generating electricity [5]. The relative motion of the earth, the sun, and the moon can be used to generate tidal energy [6]. The distribution of power by using modern technology (IoT-based system) in different ways, can be designated small, medium, and large scales via different renewable or nonrenewable sources. Tidal power has enormous potential due to the

[1]Dept. of Electrical Engineering, Institute of Business Management, Karachi, Sindh, Pakistan
[2]Assistant Professor Dept. of Engineering Management.
[3]Electrical Engineering Department, Institute of Business Management, Karachi, Sindh, Pakistan.
[4]School of Engineering, University of Warwick United Kingdom
Corresponding Author: imran.majid@iobm.edu.pk m.majid.1@warwick.ac.uk

size of oceans and the predictability of tides. The main objectives of the paper are:

1. To demonstrate the concept of tidal energy as a source of green energy for developing economies.

2. To understand measurement parameters above the water surface and below it.

3. To demonstrate the usefulness of this emerging technology for coastal communities (radio beacons, search and rescue nodes, night light, etc.).

With a width of one and a half feet and a height of two feet, it can produce enough power. The vertical design of turbines makes the project more predictable to gain most of the force from all sides and mold the turbine in a single direction, even if the tide comes and hits the turbine from any direction. Thus, the unique vertical design of the turbine is very suitable for the seashore tides.

Pakistan has 990 km long coastline. The tidal power is more predictable and reliable than solar or wind energy both of which are dependent on the sun and air which makes it less predictable. Another point is that water is denser than air, therefore, tidal energy produces more energy compared with wind turbines. Tidal energy is inexpensive to maintain, it doesn't produce direct greenhouse gases or other waste. The tidal energy transducer could also be installed on the river barrages. To install the tidal energy transducers the selection of existing barrages and search of new areas, where barrages can be constructed across tidal rivers bays, and estuaries. The turbines in the barrage converts the power of tides in a similar way a river dam harness the power of a river. The gates of the barrages gates open when the tide rises. At high tide the barrage gates close, creating a pool or tidal lagoon. There are six existing barrages on the Indus river which are: Sukkur Barrage, Kotri Barrage, Guddu Barrage, Taunsa Barrage, Chashma Barrage and Jinnah Barrage. In those barrages the tidal energy transducer could be installed.

It is a project that can easily be operated and installed over the long coastal line of the country. For installation, the best possible areas we have assumed to test the project are Sonmiani Beach, Kalamata beach, and Seaview Karachi. Furthermore, it can easily be implemented over the Indus River in Sindh.

2 Literature Review

Kramer et al. [7] used the Sensor Cloud-based economic project to design water quality monitoring for rural areas. This article describes the whole process of water quality monitoring, embedded design, sensors, and data dissipation procedure. The roles of the government, network operators, and locals in ensuring adequate data dissipation are also discussed. It also looks into the Sensor Cloud Domain. Because automatically improving water quality is not feasible at this time, efficient and enhanced technology, in addition to economic practices, is assumed and suggested to improve water quality and public awareness. Sun et al. [8] discussed an efficient energy management framework to provide satisfactory QOI in IoT sensory environments. In contrast to previous efforts, it is transparent and compatible with lower-level protocols in use, preserving long-term energy efficiency without sacrificing any QOI levels [9]. The new idea of QOI-aware "sensor-to-task relevancy" clearly analyses a sensor's sensing capabilities in the IoT sensory environment, as well as the QOI criteria required by a task. [10]. Under the constraint of service delay, an energy management decision is made dynamically at runtime as the best option for long-term traffic data [11]. Finally, an extensive case study is proposed based on the utilization of sensor networks to monitor water levels. A simulation depicts the performance of the suggested algorithms to demonstrate the ideas and techniques given in this work.

2.1 Underwater Sensors

Heidemann et al. [12] suggest Wireless data transmission in the deep ocean/sea is the emerging technology used for ocean-based observational structures. The use of underwater sensor networks has made it relatively easy to control pollution, monitor the climate, record instruments, and predict natural disasters. The

study of marine life is another achievement of using underwater sensors. Also, the data collected is utilized to search more and survey different missions. Because they cover miles of ocean range, underwater wireless sensing structures are well understood for stand-alone applications. The development of underwater sensor networks is driven by the necessity to sense the underwater world [12]. Fixed or mobile applications, as well as short and long-range applications, may all have quite distinct requirements. As a result, such requirements can result in demanding distinct designs. The types of underwater sensor network deployments vary as needed, such as mobility and density differences in areas. Underwater sensors structures are often static and attached to docks or tied to the seafloor.

2.2 Surface Water Sensors

The framework of water technologies implemented by Maroli et al. in [13] showed that the above surface water sensing system is a dynamic wireless network architecture that combines multiple communication technologies and solutions to let people and other things to interact. This advanced technology paves the way for the creation of unique applications for so-called smart ocean weather inspection. In the case of water management, the utilization of above surface water sensors allows for monitoring weather parameters in the ocean, such as pressure air, temperature, and airspeed. The implementation of an above-water sensing system also provides an enabling facility to keep the constant check at sea- level. These essential above-surface water sensors can be valuable tools in this context because they allow multiple technologies to store and analyze data from various real-time sensors.

2.3 Review of IoT enabling technologies

Internet of Things is assumed to have a strong influence in distinct evolving technologies such as clouds computing, wireless sensor networks security protocols, search engines, big data, web services, embedded systems, and the Internet [14].

Wireless sensor networks (WSN): It is made up of various sensors that are linked together to monitor various types of data [15].

Cloud Computing: It is also known as On-demand computing, is a type of Internet-based computing that allows computers and other devices to process and share data on demand. It can take many different forms, such as IaaS, PaaS, SaaS, DaaS, and so on.

Big Data Analytics: It is the process of evaluating large data sets that contain various types of data. Big data, for example, can be used to uncover hidden patterns, market trends, customer preferences, and other useful business data.

Communication protocols: It serves as the backbone of IoT systems, allowing for connectivity and application integration. As these protocols enable data exchange formats, encoding, and communication data addressing, they make data exchange over the network easier.

Embedded Systems: It's a type of computer system that combines hardware and software to accomplish specific tasks A microprocessor/microcontroller, RAM/ROM, network components, I/O units, and storage devices are all part of the system.

2.4 Methods of tidal energy extraction

Following are the five approaches of tidal energy extraction.

2.4.1 Tidal barrages

Tidal barrages are structures that are commonly built over the mouth of an estuary through which all of the water streams flow through the basin [16]. The tidal barrages are equipped with conduit entryways that allow water to flow into and out of the basin [17].

During elevated tide, water stream into the sound, and the water is held back by closing the floodgate entryways as low tide approaches which can be seen in Fig. 1. Knowing the area's flow extent and working it at the right times of the flow cycle constrains the

flood doors. When the floodgates are allowed to open during low tide, turbines located at the conduit entryways generate electricity [18]. Authors have used this rule to reference a variety of energy extraction methods, including ebb generation, flood generation, ebb and flood generation, pumping, two basin plans, and so on. The advantage of using the barrage technique to generate power over petroleum products is that it reduces greenhouse gas emissions.

Fig. 1. Tidal Barrages

2.4.2 Tidal stream energy

Mendi et al. [19] emphasized that tidal power was centered on harnessing the tidal flow and generating energy through potential storage rather than the tidal stream. Tidal stream innovations have made huge strides toward in the most recent decade. In UK waters identified with flowing stream energy, extensive exploration is underway. The UK has an objective to accomplish 20% of its power necessity through sea assets. Around 40 energy-converting machines are being developed, with prototypes being built in UK labs and waters (Irena, 2014) [20]. There are no standardizations for flowing stream energy because it is still a developing technology [21]. However, an assortment of gadgets is being created to utilize the water stream to separate power. However, the effectiveness of each device must be thoroughly evaluated through extensive testing in order to select the most appropriate device for a specific application.

2.4.3 Tidal Fences

In [22], tidal fences are installed within the fence framework. These fences are made up of individual and vertical turbines and are also called caisson. A turning channel blocks the entire flow of water and just lets it pass through these fences. These tidal fences are also used in vast basins. Like channels between offshore islands and mainland or two islands, these tidal fences can be installed as shown in Fig. 2. As these fences do not require basin flooding, they leave a negligible impact on the environment. These fences are cheaper and easy to install. In barrages, the entire framework is needed to be installed before any electricity production; these fences have vital advantages of being able to produce power as soon as the initial implementations are installed.

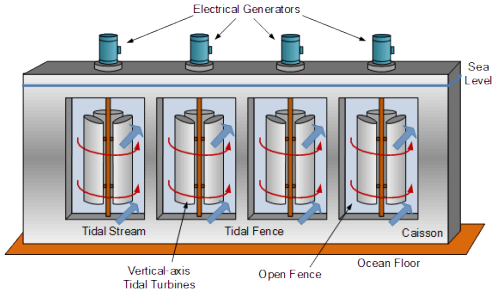

Fig. 2. Tidal fences [23].

2.4.4 Tidal lagoons

In [24], tidal lagoons are considered the modification of barrages. Just like standard barrages, tidal lagoon produces power by conventional hydro-turbine. The difference between tidal lagoons and conventional barrages is that those conventional barrages‟ design used the natural coastal line to decrease the barrages‟ lengths. Nonetheless, tidal lagoons require blocking the river without regarding how deep that is. That's why the cost increases considerably. Wherever there are high-range tides, a lagoon of low cost can easily be installed. These lagoons cause a little visual impact as they appear like a conventional sea wall at lower tides and are below the high tide mark in water [25]. By using demolished structures and loose clusters found in different quarries, these tidal lagoons can be built. Entire debris would be dumped as long as the confined wall is completed. As far as any debris can be used to construct the confined wall, the cost of

building a lagoon can easily be restricted. By using the cheapest materials, the price of installing these structures can be decreased. This beneficial technique of construction created an opportunity of constructing an artificial reef. For fishes and birds, a small and warm water lake can also be built in middle. They can easily swim around without any interruption and cause harm to turbine sluices.

2.5 Tidal energy around the world and Pakistan

The need to decrease co_2 emissions combined with a slow increase in the price of petroleum, has resulted in a significant increase in interest in tidal energy [26]. Today, this energy is increasingly being considered as a viable option for a long-term power source around the world. Extraordinary tides can be found all over the world. The Pentland Firth, Scotland; the Severn Estuary; the Aleutians; Norway's fjords; the Philippines; the Straits of Messina, Italy; the Bosporus, Turkey; the English Channel; Indonesia; and Alaska and British Columbia's waterways are just a few of them.

Tidal energy has many benefits compared to other sources of energy it is a clean, renewable, sustainable resource that is not utilized in its full capacity. It has huge potential to meet the global growing energy requirements in the current challenging period and in the future. Arsalan in [27] studied the GIS based approach to analyze the sustainable use of the estimated tidal energy potential in Pakistan. They further suggested potential sites and from those sites the energy could be distributed to the metropolitan city in an easy way. Pakistan has huge potential for renewable energy production and the severe shortage of electricity due to its heavy reliance on imported fuels [28]. Rahem et al. [28] reviewed the alternative sources of energy and their distribution strategies. Neil et al. [29] studied the impact of tidal energy arrays in the regions of tidal asymmetry and suggested that that energy extracted with respect to tidal asymmetries will have important implications for large-scale sediment dynamics. Rauf et al. [30] has overviewed the energy status of Pakistan and discussed major aspects of energy sector of Pakistan. In their research work they suggested based on the reports from National institute of oceanography reports that 170 km area of creek system of Indus delta has a huge potential of tidal energy.

In 1967, a large hydroelectric plant was commissioned that harnessed the power of the tides to generate electricity. It generated about 540,000 kW of electricity [24]. According to studies, the European regional waters have 106 areas for separating flowing energy, which would produce 48,000 Giga Watts of power per year. Around 50,000 MW of introduced limit is estimated to be reachable just along the coasts of British Columbia. There's also the possibility of extracting around 90,000 MW of electrical energy off Russia's northwestern coast, and around 20,000 MW at the inlet or Mezen stream and the White Sea.

TABLE I. HIGHEST TIDES OF THE OCEAN ON A GLOBAL SCALE [31]

Site	Country	Tidal Elevation (m)
Bay of Fundy	Canada	16.2
Severn Estuary	England	14.5
Port of Ganville	France	14.7
La Rance	France	13.5
Puerto Rio Gallegos	Argentina	13.3
Bay of Mezen (White Sea)	Russia	10
Penzhinskaya Guba (Sea of Okhotsk)	Russia	13.4

Table 1 shows the height of available tides in some of the regions where tidal power stations could be built. In some of these locations, tidal power plants have already been built, while others are still in the planning stages. Table 2 lists the main characteristics of four large-scale tidal power plants that were built after WWII and are still operational [32].

TABLE II. EXISTING LARGE TIDAL POWER PLANTS DISTRIBUTIONS [33].

Site	Country	Bay area (km2)	Avg. tide (m)	Installed power (MW)
La Rance	France	22	8.55	240
Annapolis	Canada	15	6.4	18
Jiangxia	China	1.4	5.08	3.9

3 System Methodology

The architecture of the IoT-based tidal energy transducer is designed such that the entire structure of the prototype occupies roughly an area of 9 square feet with a height of 5 feet. The turbine structure is based on three blades each of 1x2 feet in size. The turbine is supported by an iron rod which supports the entire prototype and the IoT underwater and above-water sensors. Three generators are fixed at the top of the turbine, which is supported by a frame welded to an iron rod. The turbine pulley has a circumference of 25 inches whereas the generator's‟ each pulley has 1 inch of circumference. So, one rotation of the turbine generates 25 rotations of a single turbine. But there are three turbines fixed so each rotates 25 times. It shows, if the speed is increased it will generate more power. Furthermore, a potentiometer is fixed to carry out the voltage and current of all three generators combined. As the tide hits the turbine, it moves in an anti-clockwise rotation. It doesn't matter if the tide is coming forth or going back, since the design of the turbine is vertical; it makes it always rotate in a single direction. The IoT structure is based on Arduino ATMega328p, the microcontroller, and is programmed concerning the sensors attached. All four sensors, which include turbidity sensor, water flow sensor, pH sensor, and the BME280 (temperature, humidity, and air pressure) sensor, are connected to Arduino via a wire, and the microprocessor is supplied 5 Volts from a battery fixed at the top. Sensors sense the data and send it to Arduino then Arduino in which the Wi-Fi Module ESP8266 is connected, regulates the data, and transfers data to the destination source, which could be a cellphone or laptop connected to the internet. The data on the destination source can be seen by using an application (can be downloaded via play-store).

The pH sensor, turbidity sensor, BME280 atmospheric sensor, and water flow sensor are all connected to Arduino, as shown in Fig. 3. Then, to transfer data between the microcontroller and the output source, a Wi-Fi module is connected to Arduino.

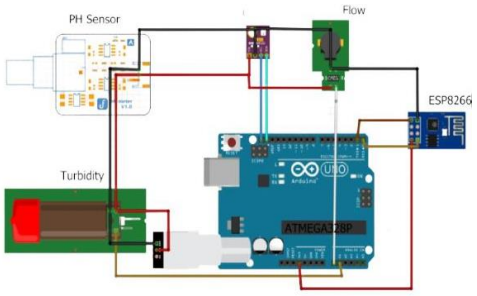

Fig. 3. Arduino connected to IoT sensors

3.1 Architecture of IoT based Tidal Energy Transducers

All four sensors are connected to Arduino, as shown in Fig. 4. Arduino supplies a voltage of 5 v, and it is linked to a cloud where data is stored. This also works as a source between the output device and the microcontroller. Data logger links the cellphone to the Arduino.

3.2 Tidal energy Calculations

The energy due to the tidal stream (kinetic energy) and the energy due to the release of the stored water in the basin make up the total tidal energy (potential energy). It is also true that an increase in tidal variations or tidal stream energy leads to a significant increase in energy extraction.

Following notation are used in this model:

ρ The density of seawater $\left(\frac{kg}{m^3}\right)$

cp power coefficient

A	The cross-section area of the channel (m^2)
V	current velocity $\left(\frac{m}{s}\right)$
∈	turbine efficiency
P	power generated (W)
h	vertical tidal range (m)
Þ	The density of water 1025 $\left(\frac{kg}{m^3}\right)$
g	gravity $\left(\frac{m}{s^2}\right)$

1. Kinetic energy: The kinetic energy of a stream flow passing through a cross-section at a given velocity is given in (1):

$$P = \frac{1}{2}\rho v^3 \quad (1)$$

2. The turbine's power output, also known as its efficiency "∈" depends on the design of the turbine [19, 34]. The power output for a turbine from these kinetic systems can be obtained by (2) as follows:

$$P = \frac{\in v^3}{2} \quad (2)$$

3. Potential energy: The potential energy is mainly dependent on the tidal prism of the basin. Potential energy obtained due to the stored water can be calculated as in (3):

$$E = \frac{\mathrm{A}gh^2}{2} \quad (3)$$

From (3), it can be seen that the potential energy varies with the square of the tidal range. So, a barrage should be placed in such a location where it is possible to achieve maximum storage head.

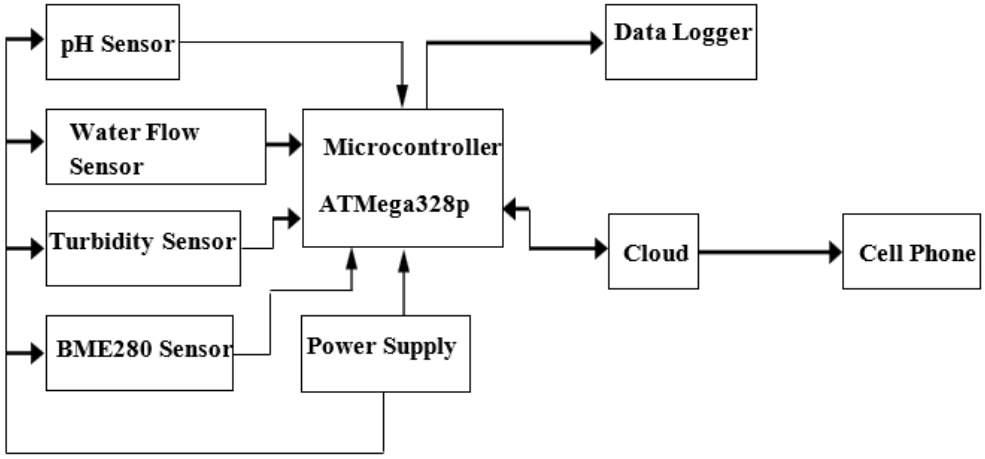

Fig. 4. Microcontroller connected to data logger, sensors and power supply

3.3 Tidal energy generation design

This prototype model enables us to generate electricity using both types of tides, the flood, and the ebb tide. The main advantage of this type of model is that the turbine works in one way does not matter from which side tide is coming. All tides force is utilized to generate another force that would move the turbine in a single direction. Three wings have been installed on an area of 2 square feet to get maximum power. The Tidal turbine design is shown in Fig. 5. The diameter of each Turbine Wing Arc is 3 feet. Two bearings are fixed at the two ends of the turbine to reduce the friction force, which provides smooth rotation with no certain friction [35]. The whole vertical design is supported by a pipe of 2 cm diameter, which works as an axis of turbine around which it rotates. It also strengthens the

entire structure to remain stable during tides striking. This pipe provides a path for the underwater sensors wires so that they can easily be connected to the Arduino that is present in the upper box. The upper box holds the BME280 Atmospheric Sensors, ESP2866 Wi-Fi module, and an ATMega Arduino. Whereas, the lower box holds three different sensors: pH sensor, turbidity sensor, and Water flow sensor, which are connected via wires. Three sensors present in a lower box are connected via wires, which go through the axis pipe of the turbine. Then, these sensors are connected to the microcontroller. The upper box sensors have the same installation as they are connected via wires to the Arduino. The whole structure is based on an iron frame, and the turbine is designed from an iron sheet. Furthermore, it is covered with paint to prevent from getting iron rust as the turbine is in constant contact with water.

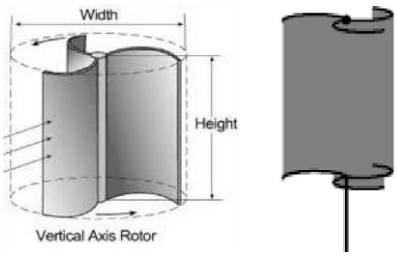

Fig. 5. Tidal turbine design.

The entire design is smooth and friendly for marine life as well. The arc of each turbine wing has a 1-foot length. The lower box is kept into a thin filter so that nothing except water enters the box and harms the sensors. The entire structure heights 4 feet. The lower three feet remain in the sea as the turbine keeps gaining tidal force and underwater sensors keep inspecting seawater. One foot stays out of the water so that the upper water sensors check the required parameters, and the microcontroller stays out of the reach of the water.

3.3.1 Above-water sensor

The BME280 is a combined digital pressure, temperature, and humidity sensor. It has small dimensions, low power consumption, high precision, and stability that allow the implementation in the forecast, environmental monitoring, altitude detection, and IoT application. In this prototype project, the BME280 sensor is connected directly to the microprocessor via wires. Both the microcontroller and the BME280 sensor are connected to the upper box. The python programming of the sensor is installed into the Arduino. It senses the surroundings and then sends data to Arduino, which is connected to a 5v battery. Then, the microcontroller sends the data via the ESP8266 Wi-Fi module. This ESP8266 Wi-Fi module is a self-contained SOC with an integrated TCP/IP protocol stack that can give microcontrollers access to Wi-Fi networks. Each ESP8266 module comes pre-programmed with an AT command set firmware. After processing the data is transmitted through a Wi-Fi module, and is shown at the output application. It can be seen on destination sources such as mobile or laptops. The connection of BME280 sensors is located at the top of the rod so that it can easily inspect the environment without any interruption. Along with that, the Arduino ATMega and Wi-Fi module are also connected via wires. Two DC generators are installed at the upper pulley. These generators are supported by a rubber stripe, which is firmly roped around the generator's pulley and the main pulley to make enough grips for rotation. As the turbine rotates, the generators keep rotating in the anti-clockwise direction. One complete rotation of the turbine makes generators rotate about 25 times. Thus, it engenders more rotations in generators making them produce higher power.

3.3.2 Underwater sensor

The underwater system includes a pH sensor, turbidity sensor MJKDZ Model, water flow sensor YF-5201 Model, and the turbine itself. These three sensors are installed in the lower box just below the turbine. Three of them are installed and attached in a way that they can gain maximum input and witness

most of the seawater inspection. The seafloor is majorly unexplored, so this prototype presents a handful of opportunities to inspect the seafloor. The sensors are programmed with Python language. All sensors are attached at the bottom and connected via wire, which goes through the turbine's axis pipe. The pH scale is a logarithmic scale whose range is from 0-14 with a neutral point being 7. If values are above 7 it indicates a basic or alkaline solution, and if values are below 7, it would indicate an acidic solution. It works on a 5V power supply and is easy to interface with Arduino. The water flow sensor measures the rate of flow of water. This rate of flow of water is measured in cubic meters or liters per hour. This also consumes 5v. The turbidity sensor measures how clear the water is. It indicates the degree to which the water loses its lucidity. The 2 sq feet Turbine is vertically attached to the rod, and it rotates anti-clockwise. The bidirectional attitude of the wave doesn't affect the turbine's speed as it is vertically designed to accumulate the tide the force of any direction.

4 Results and Discussion

The result and discussion section consist of testing, results, and comparisons.

4.1 Testing

1. Implementation of IoT Based Tidal Energy Transducer was carried out at Sea View Karachi as shown in Fig. 6.
2. The whole prototype project was set in the water at a distance of 25 meters into the sea.
3. The entire iron- frame was first fitted into the ground, and then the sensors boxes were attached. All the arrangement of microcontroller and sensors was already installed.
4. First, the turbine was locked, and the stability of the project was checked to see if it was stable at sea. After attaching each required part, the turbine was allowed to rotate.
5. With each rotation, the turbine generated electricity. Other sensors were fitted in upper and lower boxes. The upper box carried BME280, a Wi-Fi module, and an Arduino ATMega. Along with that, the upper box also carried a 12Volts lead battery. This was supposed to provide a power source to the microcontroller and other sensors.
6. After allowing the project to execute its desired function, the results were carried out. The output of power and sensors data can be seen in Table 3.
7. The multimeter fixed at the upper box provided the reading regarding the generation of power whereas the cellphone worked as the destination source for showing outputs of sensors‟ values.
8. The BLYNK APP, which is an android application designed for ultimate outputs of projects on Arduino, showed the data of each sensor.
9. In every 5 seconds, the data was collected, thus each time data varied in very small fractions. pH and BME280 sensor did not show much variance in output. However, turbidity and water-flow sensors‟ results varied in some fractions, since each tide hit the sensors at different speeds and allowed water of different turbidity.
10. Finally, the implementation of the entire project was carried out successfully, and all desired results were noted down.

TABLE III. ENERGY GENERATION OF TURBINES

Experiment No	At home		At sea	
	Efficiency	Power	Efficiency	Power
1	10.83 %	1.3 W	33.3 %	4.0 W
2	21.66%	2.4 W	33.8 %	4.17 W

4.2 Results

After completing the project its inspection, as well as testing, was carried out. The values of various parameters were discovered using the designed tidal energy turbine and Internet of Things (IoT) based sensors, which were installed at the site. The entire prototype was carried into the sea for the test, and it was supported by a thick iron rod. The underwater sensors were installed into a box so that the seawater does not harm the sensors. Above water, sensors were right above the structure tightened by an iron- frame, and there the battery,

as well as the microcontroller, was set. All the sensors were connected to the microcontroller by a thin wire and the Wi-Fi module transferred the data to the cellphone with the help of cloud computing. The entire structure of the prototype was fixed in the sea, and then the experiment was carried out. The test of energy generation of the project was done at the Seaview site of Karachi, and its inspection was also tested at home to check if all the equipment was working accurately.

Fig. 6. IoT based Tidal Energy Transducer at the Arabian Sea

TABLE IV. ENVIRONMENT SENSOR RESULTS OBTAINED FROM PROTOTYPE AND VALIDATED WITH WATER QUALITY MONITORING SYSTEM IN [36].

Exp. No	Results obtained from the project referred in [36]			Results obtained from this project		
	pH Sensor	Turbidity Sensor	Temperature Sensor	pH Sensor	Turbidity Sensor	Temperature Sensor
1	8.4	50%	28 ℃	9.08	60%	27.82 ℃
2	7.9	50%	28 ℃	9.38	74%	27.65 ℃
3	6.5	40%	27 ℃	9.07	32%	28.02 ℃

The experiment of IoT-based inspection of seawater parameters was carried out at sea, as the results are shown in Table 3. Three different readings were taken in different areas. The time of the three experiments was also different as there was a gap of 20 minutes between each experiment. Every time experiment was carried out in real-time and results were noted down at the same time as shown on the output source.

The voltage and current generated were calculated by a millimeter fixed at the upper box. Firstly, the turbine was tested at home with airspeed provided by a fan. The efficiency of the experiment at home was low, as shown in Table 3. Due to the low force of air, the turbine rotated at a lower speed, thus, producing lower power. Again, when the turbine was tested in the sea, the efficiency turned out to be normal. The tidal force created enormous speed in the turbine and thus it produces power of above 4 watts. The expected power was 6 watts as the generators installed have 6 watts power-producing capacity. It was quite hard to achieve the ideal condition where the turbine can move at an ideal speed. However, the outcome of the turbine in seawater was quite normal as per the expectations.

4.3 Results Comparison

A project based on the smart solution for water quality monitoring systems was designed. Using IoT, that project enabled real-time water quality monitoring, and the results are given and compared to this project in Table 4.

5 Conclusion

To seek alternatives of energy resources has always been the need and interest of humans. Since humans have always wandered in their surroundings to acquire cheap and reliable energy resources. Tidal energy is one such source that requires no big human efforts once the stage is set and starting installation is finished. This energy is present on earth in the form of ocean tides in an unimaginable amount. In Pakistan, this prototype project can be utilized to define energy production at a major level leveraging the energy sector of the country. Aside from that, this project will inspect the ocean water and its various parameters such as pH, turbidity, viscosity, and water flow after working on deep-sea surveillance by installing IoT sensors. The humidity of the air in the surrounding area is also measured. In the future, this project can be designed to improve and enhance more surveillance of the deep sea by calculating and inspecting different parameters using advanced sensors, to make the seawater more sustainable for the surroundings including rechargeable batteries and relay beacons. In short, the whole project is a prototype of the energy generation at a small level that can be transformed into a major tidal energy generation plant.

Author contribution

Suresh Kumar: Conceptualization, Methodology, Software Danish: Data curation, Writing- Original draft preparation. Alveena Aslam: Visualization, Investigation. Dr. Irfanullah Khan: Writing- Reviewing and Editing. Dr. Muhammad Imran Majid: Supervision. Software, Validation.

Conflict of interest

The Author(s) declare(s) that there is no conflict of interest.

REFERENCES

[1] S. R. Bull, "Renewable energy today and tomorrow," Proceedings of the IEEE, vol. 89, no. 8, pp. 1216-1226, 2001.

[2] F. Sultana, "Water justice: Why it matters and how to achieve it," Water International, vol. 43, no. 4, pp. 483-493, 2018.

[3] V. R. Ravipudi and H. S. Keesari, "Introduction to Renewable Energy Systems," in Design Optimization of Renewable Energy Systems Using Advanced Optimization Algorithms: Springer, 2022, pp. 1-9.

[4] A. Olabi and M. A. Abdelkareem, "Renewable energy and climate change," Renewable and Sustainable Energy Reviews, vol. 158, p. 112111, 2022.

[5] N. Sifakis and T. Tsoutsos, "Planning zero-emissions ports through the nearly zero energy port concept," Journal of Cleaner Production, vol. 286, p. 125448, 2021.

[6] M. Janssen, "Reconsidering a scientific revolution: The case of Einstein versus Lorentz," Physics in perspective, vol. 4, no. 4, pp. 421-446, 2002.

[7] S. Kramer, C. Jones, G. Klise, J. Roberts, A. West, and Z. Barr, "Environmental permitting and compliance cost reduction strategies for the MHK industry: lessons learned from other industries," Journal of Marine Science and Engineering, vol. 8, no. 8, p. 554, 2020.

[8] Z. Sun, C. H. Liu, C. Bisdikian, J. W. Branch, and B. Yang, "QoI-aware energy management in Internet-of-Things sensory environments," in 2012 9th Annual IEEE Communications Society Conference on Sensor, Mesh and Ad Hoc Communications and Networks (SECON), 2012: IEEE, pp. 19-27.

[9] C. H. Liu and Y. Zhang, Cyber physical systems: architectures, protocols and applications. CRC Press, 2015.

[10] L. Song, K. K. Chai, Y. Chen, J. Loo, S. Jimaa, and Y. Iraqi, "Energy efficient cooperative coalition selection in cluster-based capillary networks for CMIMO IoT systems," Computer Networks, vol. 153, pp. 92-102, 2019.

[11] Z. Sun, C. H. Liu, C. Bisdikia_, J. W. Branch, and B. Yang, "9th Annual IEEE Communications Society Conference on Sensor," Mesh and Ad Hoc Communications and Networks, 2012.

[12] J. Heidemann, M. Stojanovic, and M. Zorzi, "Underwater sensor networks: applications, advances and challenges," Philosophical Transactions of the Royal Society A: Mathematical, Physical and Engineering Sciences, vol. 370, no. 1958, pp. 158-175, 2012.

[13] A. A. Maroli, V. S. Narwane, R. D. Raut, and B. E. Narkhede, "Framework for the implementation of an Internet of Things (IoT)-based water distribution and management system," Clean Technologies and Environmental Policy, vol. 23, no. 1, pp. 271-283, 2021.

[14] A. Al-Fuqaha, M. Guizani, M. Mohammadi, M. Aledhari, and M. Ayyash, "Internet of things: A survey on enabling technologies, protocols, and applications," IEEE communications surveys & tutorials, vol. 17, no. 4, pp. 2347-2376, 2015.

[15] P. S. Pandian, K. P. Safeer, P. Gupta, D. T. I. Shakunthala, B. Sundersheshu, and V. C. Padaki, "Wireless sensor network for wearable physiological monitoring," J. Networks, vol. 3, no. 5, pp. 21-29, 2008.

[16] L. Blunden and A. Bahaj, "Tidal energy resource assessment for tidal stream generators," Proceedings of the Institution of Mechanical Engineers, Part A: Journal of Power and Energy, vol. 221, no. 2, pp. 137-146, 2007.

[17] V. Khare, C. Khare, S. Nema, and P. Baredar, Tidal Energy Systems: design, optimization and control. Elsevier, 2018.

[18] V. Khare, S. Nema, and P. Baredar, Ocean Energy Modeling and Simulation with Big Data: Computational Intelligence for System Optimization and Grid Integration. Butterworth-Heinemann, 2020.

[19] V. Mendi, J. K. Seelam, and S. Rao, "Evaluation of tidal stream energy at major tidal inlets of Goa, India," ISH Journal of Hydraulic Engineering, vol. 28, no. sup1, pp. 403-411, 2022.

[20] [20] P. Higgins and A. Foley, "The evolution of offshore wind power in the United Kingdom," Renewable and sustainable energy reviews, vol. 37, pp. 599-612, 2014.

[21] A. Vantoch-Wood et al., "National policy framework for marine renewable energy within the United Kingdom," MERiFIC Task, vol. 4, no. 1, 2012.

[22] C. Vogel and R. Willden, "Designing multi-rotor tidal turbine fences," International Marine Energy Journal, vol. 1, no. 1 (Aug), pp. 61-70, 2018.

[23] A. Behera, "Energy Harvesting and Storing Materials," in Advanced Materials: Springer, 2022, pp. 507-555.

[24] K. Elliott, H. C. Smith, F. Moore, A. H. van der Weijde, and I. Lazakis, "Environmental interactions of tidal lagoons: A comparison of industry perspectives," Renewable energy, vol. 119, pp. 309-319, 2018.

[25] D. A. Paley, Cooperative control of collective motion for ocean sampling with autonomous vehicles. Princeton University, 2007.

[26] E. S. Fu, Y. Fang, and B. K. Horn, "Power of ocean: Evaluation of blue energy," in 2018 4th International Conference on Universal Village (UV), 2018: IEEE, pp. 1-4.

[27] M. Arsalan, H. Fatima, A. Khalid, I. Zia, and I. Ahmad, "Harnessing the potential of tidal currents in indus delta creeks for making sustainable and green Pakistan," University of Engineering and Technology Taxila. Technical Journal, vol. 21, no. 1, p. 15, 2016.

[28] A. Raheem et al., "Renewable energy deployment to combat energy crisis in Pakistan," Energy, Sustainability and Society, vol. 6, no. 1, pp. 1-13, 2016.

[29] S. P. Neill, "Impact of tidal energy arrays located in regions of tidal asymmetry," in Proc. 2nd Oxford Tidal Energy Workshop, 2013, pp. 19-20.

[30] O. Rauf, S. Wang, P. Yuan, and J. Tan, "An overview of energy status and development in Pakistan," Renewable and Sustainable Energy Reviews, vol. 48, pp. 892-931, 2015.

[31] A. Gorlov, "Tidal Energy, Northeastern University," ed: Boston Massachusetts, USA Academic Press doi, 2001.

[32] K. Murali, V. Sriram, A. Samad, and N. Saha, Proceedings of the Fourth International Conference in Ocean Engineering (ICOE2018): Volume 2. Springer, 2018.

[33] S. J. Kulkarni, "Tidal Energy: A Review," International Journal of Research, vol. 2, no. 1, pp. 55-58, 2015.

[34] X. Zhang, Y. Xiong, S. Xie, and H. Liu, "Optical-fiber-based dynamic measurement system for 3D tip clearance of rotating blades," Optics Express, vol. 27, no. 22, pp. 32075-32095, 2019.

[35] B. Akinnuli, O. Ojo, O. Caleb, and K. Okeyedun, "Design and Simulation of A Vegetable Shredding and Washing Machine."

[36] S. Geetha and S. Gouthami, "Internet of things enabled real time water quality monitoring system," Smart Water, vol. 2, no. 1, pp. 1-19, 2016